MONASH UNIVERSITY
THESIS ACCEPTED IN SATISFACTION OF THE
REQUIREMENTS FOR THE DEGREE OF
DOCTOR OF PHILOSOPHY
ON..... 3 May 2002 .....
..... [redacted] .....
Sec. Research Graduate School Committee

Errata

p. 101, line 13: "possible to quantify" for "possible quantify"
p. 148, last paragraph, line 3: "yet a rat" for "yet it a rat"
p. 150, line 8: "used to show that" for "used to shown that"
p. 151, 2nd paragraph, line 5: "may be the" for "may the"
p. 154, line 3: "episodes of oxidative stress or inflammation" for "episodes of oxidative stress of inflammation"

Addenda

Comment based on the studies performed in Chapters 3 and 4, and interpretation on p. 151:
The studies in Chapters 3 and 4 of this thesis examined the induction of cellular ferritin expression, which occurs mostly in activated microglial cells and macrophages. It should be noted that ferritin immunocytochemistry does not label all microglia and macrophages within the brain, but appears to label a subset of these cells when they have become activated. There may be some phagocytes that do not express ferritin when they become activated, and further examination of these cell types with other markers of inflammation could be used to determine how strong a correlation exists between ferritin labelling and phagocytic activation. It would also have been desirable to examine the induction of ferritin expression after injection of other metal ions or Aβ-metal complexes, however time constraints did not permit the examination of ferritin expression to become a major aim of this thesis.

p. 117, Add as a new paragraph at the end of the chapter:
"It should be noted that the species differences present between rat and human Aβ implies that there may also be a difference between rat and human cells. Thus, while human Aβ was not toxic to rat neurons in the present study, the possibility remains that it may be toxic to human neurons."

p. 140, Add at the end of paragraph 2:
"While injections of saline do not directly cause oxidative damage, oxidative stress may be indirectly caused by the cellular damage and inflammation produced by the injection procedure."

p. 148, Add as a new paragraph at the end of section 8.2:
"The *in vivo* model of intracortical injection used throughout this thesis has overcome many of the problems associated with similar techniques that have been used by other researchers. Nonetheless, it needs to be considered that this model is only capable of directly assessing acute neurotoxicity that occurs in association with a breach of the blood-brain barrier, and deposition of the injected substance. This model does not reproduce the chronic changes that occur during Alzheimer's disease, and the results presented in this thesis should be interpreted in the light of this limitation."

p. 153, line 14, insert after "Alternatively,":
"it could be inferred from the results presented in Chapters 5 and 6 that"

In vivo neurotoxicity of Aβ and metal ions: relevance for Alzheimer's disease.

Glenda M. Bishop.

B.Sc.(Hons).

This thesis is submitted in total fulfilment of the requirements for the degree of **Doctor of Philosophy.**

Department of Psychology, Monash University.

December 2001.

Table of Contents.

List of figures.

List of tables.

Summary.

Brains from patients afflicted with Alzheimer's disease (AD) contain numerous senile plaques that are composed of the amyloid-β peptide (Aβ). These plaques are found in regions of the brain that exhibit widespread neuronal damage. It is generally believed that Aβ causes the neurodegeneration, with many *in vitro* studies demonstrating the toxicity of Aβ to cortical or hippocampal neurons cultured from neonatal rats. In addition to Aβ, senile plaques contain elevated concentrations of iron, copper and zinc, all of which have been demonstrated to be neurotoxic. These three metal ions bind to Aβ and promote the aggregation of the peptide. Metal ions have also been reported to mediate the *in vitro* toxicity of Aβ, and thus may be partially responsible for the neurodegeneration seen in AD. The possibility that metal ions potentiate the neurotoxicity of Aβ has not been examined *in vivo*, so the purpose of this thesis was to compare the neurotoxicity of Aβ and Aβ-metal complexes in the rat cerebral cortex.

To examine the *in vivo* neurotoxicity of Aβ, a model of intracortical injection was developed so that the amount of neuronal loss associated with the injected Aβ deposits could be determined 1-7 days after injection. The naturally occurring human variants, Aβ1-40 and Aβ1-42, were examined, along with equivalent variants of endogenous rodent Aβ peptide. 1.0μl of 1.0mM Aβ was injected into rat cerebral cortex. These deposits were rapidly cleared from the extracellular space, and were no longer present after 7 days. The number of dying neurons associated with the Aβ deposits was less than the number associated with injections of the saline vehicle, indicating that pure Aβ peptides tend to attenuate neuronal loss. This finding suggests that pure Aβ is not responsible for the toxicity of plaques in AD.

To determine whether Aβ-metal complexes are neurotoxic, mixtures of Aβ, iron, copper or zinc were co-injected into rat cerebral cortex. It was found that when 1.0mM iron or zinc were co-injected with Aβ, the Aβ-metal deposits were associated with significantly more neuronal loss than deposits of pure Aβ. However, Aβ-copper deposits were not neurotoxic. This result indicates that some of the metal ions in plaques may indeed be responsible for the neurodegeneration that is associated with senile plaques in AD. An unexpected finding was that Aβ decreased the overall neurotoxicity of iron and copper, but it did not decrease zinc neurotoxicity. Furthermore, the presence of zinc appeared to prevent Aβ from protecting against the toxicity of iron and copper. These findings

indicate that complex interactions occur between Aβ and metal ions, and these interactions can be either neurotoxic or neuroprotective.

Oestrogen replacement therapy decreases the risk of AD in post-menopausal women, and improves cognitive function in women who have AD. Oestrogen may provide neuroprotection through antioxidant actions, and thus differences in the level of plasma oestrogen may decrease the neuronal loss caused by oxidative stress. The different stages of the oestrous cycle in female rats are associated with changes in plasma oestrogen levels. Each stage of the oestrous cycle was compared with respect to the amount of neuronal loss produced by intracortical injections of saline, metal ions and Aβ-metal complexes. The amount of neuronal loss did not differ between any stage of the oestrous cycle. This finding suggests that the protection provided by oestrogen replacement therapy in AD is not related to antioxidative properties.

The thesis has provided novel data on the lack of *in vivo* neurotoxicity of pure Aβ and the potentiation of Aβ neurotoxicity by the metal ions that are normally present in plaques. The increased neurotoxicity of some Aβ-metal complexes implies that the metal ions within plaques may contribute to the neurodegeneration seen in AD brains. Furthermore, the finding that Aβ can protect against redox-active metal ions suggests a hitherto unsuspected role for Aβ in the neutralisation of toxic metal ions. Together these findings have implications for the treatment of AD, since they indicate that for anti-amyloidogenic agents to be successful, they must be combined with chelation therapy.

Declaration.

This thesis does not contain material that has been accepted for the award of any other degree or diploma in any university or other institution, except where acknowledged otherwise. To the best of my knowledge, this thesis contains no material published or written by another person, except where due reference is made in the text.

Signed [redacted] Date 13.12.01

Publications during PhD candidature.

Published and accepted manuscripts.

1. **BISHOP, G.M.** and Robinson, S.R. (2001) Quantitative analysis of cell death and ferritin expression in response to cortical iron: implications for hypoxia-ischemia and stroke, Brain Res. 907:175-187.
2. Robinson, S.R. and **BISHOP, G.M.**, Amyloid β as a bioflocculant: implications for the amyloid hypothesis of Alzheimer's disease, Neurobiol. Aging *in press.*

Manuscripts submitted for publication.

3. **BISHOP, G.M.** and Robinson, S.R., The acute response to deposits of fibrillar Aβ *in vivo*: neuronal loss and ferritin expression. *Under review, Brain Res.*

Manuscripts in preparation.

4. **BISHOP, G.M.** and Robinson, S.R., Human Aβ but not rat Aβ protects rat cortical neurons against iron toxicity.
5. **BISHOP, G.M.** and Robinson, S.R., Metal ions present in plaques potentiate the toxicity of human Aβ1-42 *in vivo.*
6. **BISHOP, G.M.** and Robinson, S.R., Effect of the oestrous cycle on the neurotoxicity of Aβ-metal complexes.
7. **BISHOP, G.M.** Effects of Aβ *in vivo*: a review of models injecting or infusing Aβ into the brains of animals.

Conference proceedings.

Abstracts directly related to the work in the PhD thesis.

1. **BISHOP, G.M.**, O'Dowd, B.S. and Robinson, S.R. (1998) Human β-amyloid peptide injected into rat cerebral cortex is not neurotoxic and does not induce microglial reactivity, Proc. Aust. Neuroscience Soc. 9:200. Annual Meeting of the Australian Neuroscience Society.
2. **BISHOP, G.M.**, O'Dowd, B.S. and Robinson, S.R. (1998) Human β-amyloid peptide is not neurotoxic to rat cerebral cortex, Neurobiol. Aging 19 Suppl. 4S:S127. 6th International Conference on Alzheimer's Disease and Related Disorders.

3. Robinson, S.R., O'Dowd, B.S. and **BISHOP, G.M.** (1998) β-amyloid peptide fails to activate microglial ferritin expression *in vivo*, Neurobiol. Aging 19 Suppl. 4S:S127. 6th International Conference on Alzheimer's Disease and Related Disorders.
4. **BISHOP, G.M.** Humphrey, R.K.B., Robinson, S.R., Smith, M.S.R., and Walsh, D.A. (1998) The use of Fluoro-Jade to identify dying cells, 38th Annual Meeting of the Japanese Teratology Society.
5. **BISHOP, G.M.** and Robinson, S.R. (1999) β-amyloid provides less neuroprotection in old rats, Proc. Aust. Neuroscience Soc. 10:212. Annual Meeting of the Australian Neuroscience Society.
6. **BISHOP, G.M.** and Robinson, S.R. (2000) β-amyloid is more neuroprotective if it contains fibrils, Proc. Aust. Neuroscience Soc. 11:189. Annual Meeting of the Australian Neuroscience Society.
7. **BISHOP, G.M.** and Robinson, S.R. (2000) β-amyloid helps to protect neurons from oxidative stress, Neurobiol. Aging 21 Suppl 1S:S226. The 7th International Conference on Alzheimer's Disease and Related Disorders.
8. **BISHOP, G.M.** and Robinson, S.R. (2001) β-amyloid protects rat cortical neurons from iron and copper toxicity, Proc. Aust. Neuroscience Soc. 12:133. Annual Meeting of the Australian Neuroscience Society.

Abstracts that are not directly related to PhD thesis, but were obtained during candidature.

9. Fox, S.R., **BISHOP, G.M.** and Robinson, S.R. (1999) High levels of microglial iron in the cortices of old primates: implications for the neurotoxicity of β-amyloid, Proc. Aust. Neuroscience Soc. 10:213. Annual Meeting of the Australian Neuroscience Society.
10. Zhang Y.F., Swan, L.E., **BISHOP, G.M.** and Robinson, S.R. (2001) Iron binding capacity of rat retina varies during the oestrous cycle, Proc. Aust. Neuroscience Soc. 12:191. Annual Meeting of the Australian Neuroscience Society.

Reuse of published work.

This thesis contains some text that was originally written for other manuscripts, which were a joint collaboration with my principal supervisor, Stephen Robinson. A number of sections in Chapter 1 have used text that was originally written for manuscript number 2 on the publications page. Most of the text in Chapter 3 was originally written for manuscript number 1, and a large portion of the text in Chapter 4 was originally written for manuscript number 3. In addition, Chapter 2 contains the methodology sections that were written for these publications.

A tiny portion of the data presented in Chapter 4 (obtained from a total of 8 animals) was originally presented in my Honours thesis, which was submitted for the Bachelor of Science (Honours) degree at The University of Queensland in 1997. These animals were included in the current thesis to prevent the unnecessary death of animals that would have been required to repeat the work. Permission to include this data has been granted by the Monash University Research Graduate School Steering Committee.

Acknowledgements.

I would like to express my deepest gratitude to my supervisor Stephen Robinson for his guidance and support throughout my degree. Steve has the most incredible enthusiasm for research, and this has been an enormous help when things would seem too difficult. During the last few years, he has taught me to question everything, and my love of science and my desire to continue to work in research has been strengthened by his positive attitude. We have had quite a journey (all the way down the eastern coast of Australia), but have finally reached the end. Steve has been a wonderful supervisor and a great friend.

Many thanks also go to my associate supervisor, Professor Kim Ng, for his assistance with the statistical analysis and design of my experiments. Kim also provided me with an abundance of personal support after my move to Monash University to help me with the difficulties I experienced. I would also like to thank Laura Swan for her assistance with the iron staining reported in Chapter 7 and for the interesting times that we had while performing this work together. I am also grateful to Gunta Jaudzems for her technical assistance with electronmicroscopy. Thanks also go to Cheryl Roberts, Robyn Clarke, Carina Holmquist and Mel Brown, for their advice on the care and treatment of my animals and for assistance in finding the best way to perform certain procedures.

Special thanks also go to the members of the lab who have provided assistance at various points, but more importantly they provided their poor little ears when I needed to complain because my experiments didn't work: Malia Edwards, Joannah Cane, Nicole Hall, Elena Hartley and Penny Moutsoulas. I am indebted to the generous support given to me by friends within the department as well as others who have shared this experience with me: Raelene de Ross, Katie Bagot, Katherine Johnson, Jamie Freemont, Kellie Hutchinson, Melissa Broe and Toni Raso.

Lastly, I would like to thank my family, who have always believed that I could achieve whatever I wished to do. I am eternally grateful to my father who has given me endless support throughout my university career, but most importantly he instilled in me the belief that "it's not worth doing if you don't do it right". From this I have always achieved the best that I can, and I will always continue to do so with this in mind.

Abbreviations.

Aβ	Amyloid-β
Aβ1-40	40 amino acid variant of Aβ
Aβ1-42	42 amino acid variant of Aβ
ACh	Acetylcholine
AD	Alzheimer's disease
AGE	Advanced glycation end-product
ApoE	Apolipoprotein E
APP	Amyloid precursor protein
APP23	Transgenic mouse line overexpressing mutant APP with the Swedish double mutation
BSA	Bovine serum albumin
C100	C-terminal 100 amino acids of APP
ChAT	Choline acetyltransferase
CSF	Cerebrospinal fluid
DAB	3',3'-diaminobenzidine
DMSO	Dimethyl sulphoxide
DS	Down syndrome
Fe^{2+}	Ferrous iron, valency of II
Fe^{3+}	Ferric iron, valency of III
H&E	Haematoxylin and eosin
HEPES	*N*-2-hydroxyethylpiperazine-*N'*-2-ethanesulphonic acid
IP	Intraperitoneal injection
KPI	Kunitz-type protease inhibitor
LDL	Low-density lipoprotein
MAP-2	Microtubule-associated protein-2
PB	Phosphate buffer
PBS	Phosphate-buffered saline
PDAPP	Transgenic mouse line overexpressing mutant APP with the Indiana mutation
PS	Presenilin
PS-1	Presenilin-1
PS-2	Presenilin-2
ROS	Reactive oxygen species

Tg2576	Transgenic mouse line overexpressing mutant APP with the Swedish double mutation
TUNEL	Terminal deoxynucleotide transferase-mediated dUTP-biotin nick end labelling

I can live with my arthritis,
My dentures fit me fine,
I can see with my bifocals,
But I sure do miss my mind.

- Anonymous

CHAPTER 1:

Introduction.

1.1. Alzheimer's disease.

1.1.1. Psychological and pathological characteristics of Alzheimer s disease.

Alzheimer's disease (AD) is the most common cause of dementia in the aged. A decline in short-term memory and a loss of olfactory discrimination are followed by a progressive worsening of memory, confusion, behavioural disturbances such as depression or aggression, a loss of socially learned behaviours and eventually a loss of the ability to communicate, feed or attend to personal hygiene (see Berg and Morris, 1994; Folstein and Bylsma, 1994). The disease has a protracted course, with the interval between diagnosis and death being around 7-10 years.

The brains of AD sufferers are characterised by enlargement of the cerebral ventricles and a widening of the cortical sulci due to the atrophy and death of cortical neurons. Microscopical examination of the cerebral cortex reveals a high incidence of neurofibrillary tangles that are composed of hyperphosphorylated tau, and a high density of extracellular plaques that are primarily composed of amyloid-β (Aβ) peptide (e.g. Braak and Braak, 1991; Cummings et al., 1996). The plaques are often accompanied by hypertrophic astrocytes and reactive microglia, this gliosis being indicative of a localised inflammatory response (e.g. McGeer and McGeer, 1995). In addition to inflammation, AD brains contain evidence of oxidative stress (e.g. Markesbery, 1997; Munch et al., 1998). These neuropathological features are abundant in the entorhinal cortex, inferior temporal cortex, amygdala and hippocampus. The primary sensory and motor cortical areas and subcortical brain regions are spared, with the exception of certain pathways such as the cholinergic projections from the nucleus basalis and the noradrenergic pathway from the locus ceruleus (see Hof and Morrison, 1994).

There has been much speculation regarding the importance of tangles and plaques in the pathogenesis of AD, however a consensus has never been reached on whether either feature, is the primary causative agent in the disease. It is likely that both features are interrelated and influence the progress of the disease, however greater attention has been given to senile plaques since most of the genetically-inherited forms of AD appear to be involved with the overproduction of Aβ (see section 1.2.4). Thus, this thesis will concentrate on senile plaques and the role of Aβ in neurodegeneration.

1.1.2. Senile plaques.

Two types of senile plaques contain the Aβ peptide. Diffuse plaques are an amorphous aggregation of Aβ and are not associated with neurodegeneration, and thus are not believed to be directly causative in the pathology of AD (Rozemuller et al., 1989). Neuritic plaques, on the other hand, are dense aggregations of Aβ, where the peptide forms β-pleated sheets that radiate from the centre of the plaque (Delaere et al., 1991; Wisniewski et al., 1989b). Neuritic plaques contain a dense core that is surrounded by a less-compacted corona, and the plaques are associated with dystrophic neurites (Delaere et al., 1991; Ohgami et al., 1991; Rozemuller et al., 1989). The spatial distribution and number of neuritic plaques in AD have been correlated with the extent of cognitive loss (e.g. Cummings et al., 1996).

Senile plaques are not only found in the brains of patients suffering from AD, they are also present in the brains of patients suffering from Down syndrome (DS) (Mann et al., 1984; Rumble et al., 1989). There can also be considerable numbers of senile plaques in non-demented aged human brains (Arriagada et al., 1992; Crystal et al., 1988) and in the brains of non-human primates, such as rhesus monkeys, orangutans and squirrel monkeys (Selkoe et al., 1987). They have also been observed in brains from dogs (Nakamura et al., 1997), polar bears (Selkoe et al., 1987) and camels (Nakamura et al., 1995). Plaques rarely form in rodent brains, with neuritic plaques being observed in the brains of three aged rats out of 250 examined (Vaughan and Peters, 1981).

1.1.3. Components of plaques.

The major component of senile plaques is Aβ (Selkoe et al., 1986), however they also contain many other proteins including a variety of complement factors (Rogers et al., 1992; Rozemuller et al., 1990), apolipoprotein E (Namba et al., 1991), and α_1-antichymotrypsin (Abraham et al., 1988). Senile plaques also contain iron, copper and zinc (Lovell et al., 1998), as well as ferritin and transferrin (Connor et al., 1992a; Grundke-Iqbal et al., 1990; Jellinger et al., 1990). Ferritin is also present in the cell bodies and processes of microglial cells that are closely associated with the senile plaques (Connor et al., 1992a; Grundke-Iqbal et al., 1990; Kaneko et al., 1989; Robinson et al., 1995). Advanced glycation end-products (AGEs) are also present in senile plaques (Sasaki et al., 1998; Smith et al., 1994; Takedo et al., 1996). These are

formed when monosaccharides react with the amino groups on proteins, and the sugar side chains become oxidised (see Munch et al., 1997).

Since neuritic plaques are associated with neurodegeneration, it is widely believed that they are toxic (see Wisniewski et al., 1989a). This toxicity could be due to any of the components that are found within neuritic plaques, but Aβ is generally regarded as the most likely factor since it is the major component. Many studies have examined the toxicity of Aβ, and these will be reviewed in section 1.3.

1.2. Aβ Peptide.

1.2.1. Synthesis of Aβ.

Aβ is a 39-43 amino acid peptide that is generated from the larger transmembrane protein, amyloid precursor protein (APP; see Figure 1.1). The APP gene, located on chromosome 21 (Goldgaber et al., 1987; Tanzi et al., 1987), is alternatively spliced to form variants of APP that are 695-770 amino acids in length. The 751 and 770 isoforms of APP contain a Kunitz-type protease inhibitor (KPI) domain (Kitaguchi et al., 1988; Ponte et al., 1988; Tanzi et al., 1988), and these isoforms are mostly produced by astrocytes (Gray and Patel, 1993).

APP is frequently proteolytically cleaved within the Aβ sequence by α-secretase, yielding a 3kDa peptide and a truncated form of APP (Haass et al., 1993; Mattson et al., 1993a; Palmert et al., 1989). KPI-APP is less readily cleaved by α-secretase and instead is preferentially cleaved to form full-length Aβ (Ho et al., 1996). Cleavage of APP by β-secretase yields the C100 peptide, a 100 amino acid C-terminal fragment of APP (Citron et al., 1995; Maruyama et al., 1994). C100 is then cleaved by γ-secretase to produce the peptides Aβ1-40 or Aβ1-42 (Dyrks et al., 1993). β-secretase has been identified as the aspartic protease BACE (Hussain et al., 1999; Vassar et al., 1999), while current evidence indicates that presenilin (PS) may be the catalytic component of γ-secretase (Esler and Wolfe, 2001; Li et al., 2000). Astrocytes demonstrate very little β-secretase activity *in vivo* and it is likely that most of the Aβ in the brain is produced and secreted by neurons (Zhao et al., 1996). It is important to note that production and secretion of Aβ1-40 and Aβ1-42 is a normal process, not a pathogenic one, with relatively high concentrations of Aβ1-40 and Aβ1-42 being present in the cerebrospinal

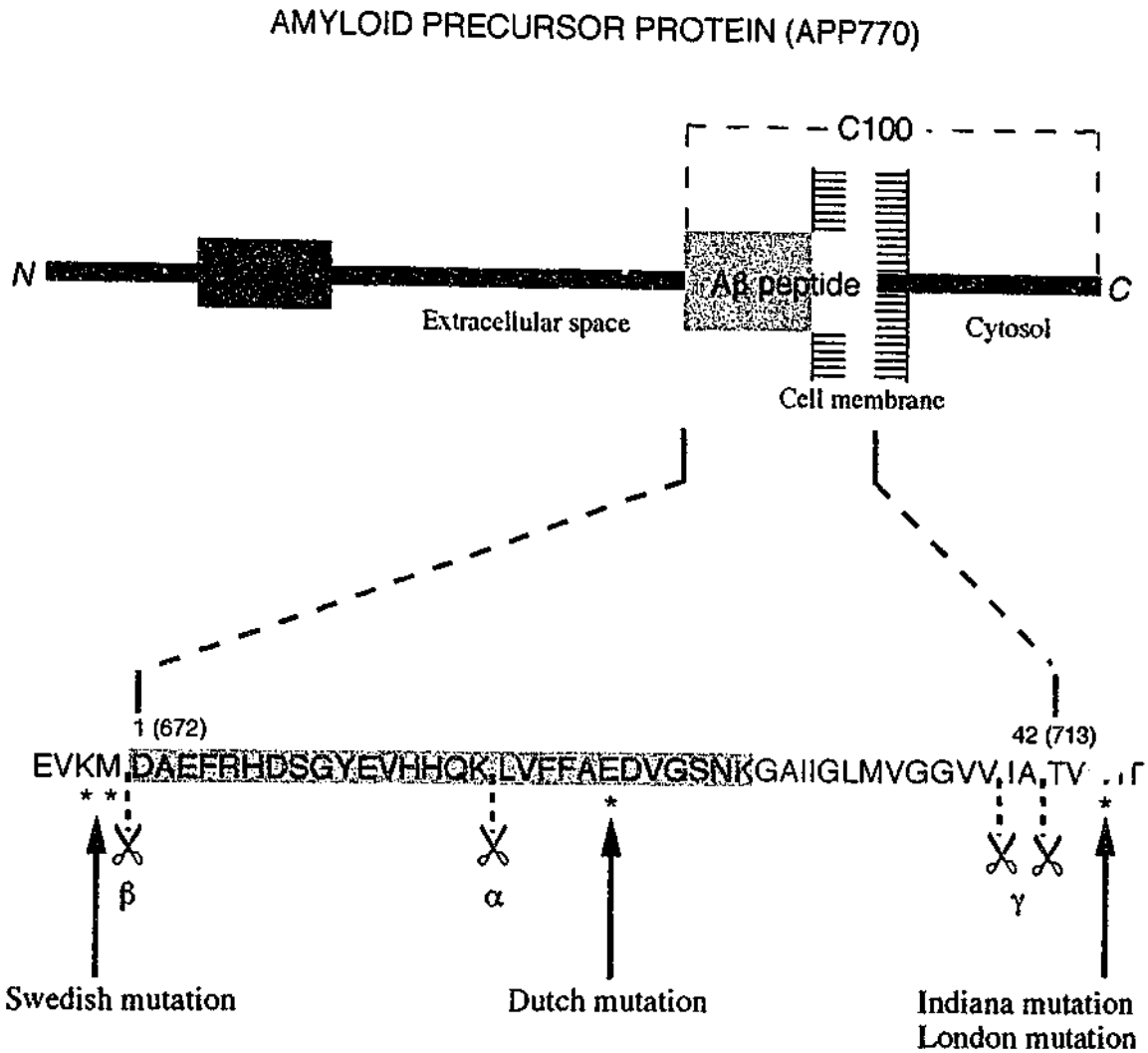

Figure 1.1. Production of Aβ from APP.
The APP770 peptide (black line) spans the cell membrane and contains the Aβ peptide sequence (blue and yellow), and can contain the Kunitz-type protease inhibitor (KPI) domain (green). Cleavage of APP by α-secretase cleavage produces a 3kDa product and a truncated form of APP. Cleavage of APP by β-secretase yields C100, the 100 amino acids at C-terminus of APP. γ-secretase can then cleave C100 to produce the Aβ peptide. Residues 1-28 of Aβ are extracellular (blue) and the final 12-14 residues are intramembranous (yellow). Genetically inherited mutations of APP include the Swedish double mutation (residues 670/671), the Dutch mutation (692), and the Indiana and London mutations (717). Modified from Iversen et al., 1995.

fluid (CSF) of all cognitively normal individuals throughout life (Kunicki et al., 1998; Shoji et al., 1998; Tamaoka et al., 1996).

1.2.2. Variants of the Aβ peptide.

Aβ1-40 and Aβ1-42 differ from each other by only two amino acids that are present at the C-terminus of Aβ1-42 (see Figure 1.2). These two amino acids alter the secondary structure of the peptides, with Aβ1-40 in solution tending to form into a random coil conformation, while dissolved Aβ1-42 tends to form β-pleated sheets similar to those formed by Aβ fibrils in senile plaques (Barrow and Zagorski, 1991; Kirschner et al., 1986). Aβ1-42 has a lower solubility than Aβ1-40 (Barrow and Zagorski, 1991; Burdick et al., 1992; Hilbich et al., 1991; Jarrett et al., 1993), which results in an increased ability of Aβ1-42 to form amyloid fibrils, leading to the widely accepted belief that it is the most toxic of the naturally occurring Aβ variants.

In the CSF, Aβ1-40 is the predominant variant (Shoji et al., 1998), however Aβ1-42 is the predominant species in senile plaques. Aβ1-42 is present in both neuritic and diffuse plaques (Iwatsubo et al., 1994; Murphy et al., 1994), while Aβ1-40 is generally limited to the core region of neuritic plaques, and is not usually present in diffuse plaques (Iwatsubo et al., 1994). The deposition of Aβ1-42 into plaques in AD appears to correlate with a reduction in the amount of Aβ1-42 in the CSF of AD patients (Motter et al., 1995).

The Aβ sequence is highly conserved. Humans share the sequence with non-human primates, cows, dogs, guinea pigs, pigs, polar bears, rabbits, and sheep (Johnstone et al., 1991; Podlisny et al., 1991). Of the species examined, rat and mouse have a different sequence with substitutions in Aβ occurring at residues 5 (Arg → Gly), 10 (Tyr → Phe), and 13 (His → Arg) (Shivers et al., 1988). It is interesting to note that senile plaques have been observed in species with the "human" sequence (Selkoe et al., 1987), but are rarely observed in rats or mice. It has been speculated that the substitutions in rat Aβ may alter the amyloidogenicity of the peptide (i.e. its ability to form fibrils), preventing its deposition into plaques. However, it has been demonstrated that rat Aβ fibrils are morphologically similar to human Aβ fibrils, and may even be more stable and amyloidogenic than equivalent variants of human Aβ (Fraser et al., 1992). Nonetheless, while Aβ1-40 is present in rat CSF, Aβ1-42 is not detectable (Anderson et

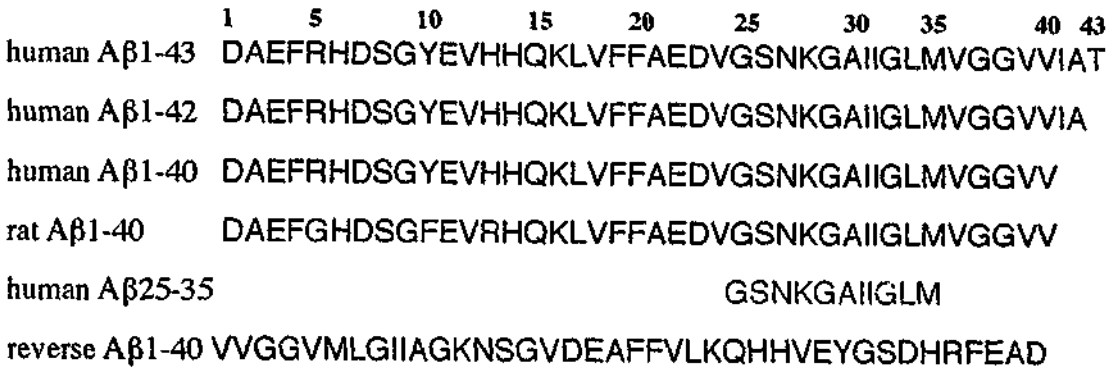

Figure 1.2. Variants of the Aβ peptide.
The Aβ peptide contains 39-43 amino acids. It is normally present as Aβ1-40 or Aβ1-42, which contain 40 or 42 amino acids respectively. Rat Aβ varies from human Aβ by three amino acid substitutions at residues 5, 10, and 13. Truncated forms of Aβ are sometimes used, especially Aβ25-35, which contains only residues 25-35 of full-length Aβ. Reverse Aβ peptide (e.g. Aβ40-1) is often used as a control for Aβ1-40. The reverse peptide contains amino acids in the opposite order. Scrambled peptides contain the same amino acids as the selected peptide, but the amino acids are randomly arranged. The reverse and scrambled peptides are used to ensure that the effects caused by Aβ are not due to the peptide, but to the properties of Aβ itself.

al., 1999), and this lack of the more amyloidogenic A β1-42 may be the reason why Aβ deposits do not form spontaneously in rat or mouse brains.

1.2.3. Physiological role of Aβ.

The normal role of Aβ is not clear, however a number of physiological effects have been reported. Aβ has been reported to stimulate the expression and secretion of APP (Wang et al., 2000), constrict cortical vessels (Paris et al., 1998; Suo et al., 1998), promote blood-brain barrier permeability (Jancso et al., 1998; Strazielle et al., 2000; Su et al., 1999) and induce an inflammatory response (Bergamaschini et al., 1999; Bianca et al., 1999; Hu et al., 1998). These effects could be considered either beneficial or harmful, depending on the circumstance in which they occur. It is important to note however, that the majority of studies have demonstrated Aβ to be toxic. These findings will be discussed in detail in section 1.3.

1.2.4. Genetically-inherited AD and production of Aβ.

Genetically inherited cases of AD are associated with autosomal dominant genetic mutations that have nearly complete penetrance, however they represent only 1-5% of all AD cases (Bird, 1994; Richard and Amouyel, 2001). These mutations in autosomal familial AD appear to be associated with the production and cleavage of Aβ and this linkage has provided some of the strongest evidence in support of the idea that Aβ is the pathogenic agent in AD. Three genes have been implicated: APP, presenilin-1 (PS-1) and presenilin-2 (PS-2). Another genetic factor that influences the development of AD is the apolipoprotein E (ApoE) genotype, however this is only a risk factor and does not guarantee development of the disease.

1.2.4.1. Mutations to APP.

Mutations of the APP gene can occur at a number of different loci and collectively these mutations account for 0.4% of all AD cases (see Richard and Amouyel, 2001). A number of point mutations in the APP gene have been reported, most of which alter only one or two amino acids within the protein (see Figure 1.1). Some of these mutations have been found within the Aβ sequence (Axelman et al., 1994; Hendriks et al., 1992; Kamino et al., 1992), although most are near the γ-secretase cleavage site (Chartier-Harlin et al., 1991; Murrell et al., 1991) and a double mutation has been

reported directly before the β-secretase site (Mullan et al., 1992). The majority of these mutations tend to be associated with increased levels of Aβ1-42 in CSF (Maruyama et al., 1996; Suzuki et al., 1994; Tamaoka et al., 1994), supporting a potential role for this variant in the pathogenesis of AD.

Individuals with DS show an AD-like cognitive decline during their adult life and this decline is accompanied by the appearance of neuritic plaques and neurofibrillary tangles in their hippocampus and cerebral cortex (Mann et al., 1985; Mann et al., 1986). DS patients have an extra copy of chromosome 21, and thus three copies of all genes located on the chromosome. Since the APP gene is located on chromosome 21, DS patients have three copies of the APP gene, and it has been postulated that the overexpression of APP in DS leads to an excessive production of Aβ and an early onset of AD (e.g. Beyreuther et al., 1993). Indeed, it has been shown that overexpression of APP is correlated with excess levels of Aβ (Teller et al., 1996; Tokuda et al., 1997), with elevated levels of soluble Aβ being detected even as early as the foetal stage (Teller et al., 1996).

1.2.4.2. Mutations to PS.

There are two types of PS: PS-1, located on chromosome 14 and PS-2, located on chromosome 1. Mutations to PS-1 cause the majority of familial AD cases and constitute 2-3% of all AD cases, while PS-2 mutations are the least common, accounting for only 0.1% of all AD cases (see Richard and Amouyel, 2001). As mentioned in section 1.2.1, PS is involved in the cleavage of Aβ from its precursor protein. Mutations to PS have been reported to increase the levels of Aβ1-42 in serum and in senile plaques (Borchelt et al., 1996; Scheuner et al., 1996), and this linkage is often regarded as evidence that Aβ deposition is responsible for AD.

1.2.4.3. The ApoE genotype as a risk factor for AD.

The ApoE gene is located on chromosome 19, and the genotype varies in the human population, with the E3 allele being present in about 77% of individuals, while E4 is present in 15% and E2 in around 8% (Zabar and Kawas, 2000). The other ApoE alleles are present in negligible proportions. The ApoE4 genotype is associated with 37% of sporadic late-onset AD cases (see Rubinsztein, 1997), however ApoE4 is a risk factor for both early- and late-onset sporadic AD (Brousseau et al., 1994; Farrer et al., 1997;

Schmechel et al., 1993). Heterozygosity increases the risk 2.7-fold, while homozygosity increases the risk 12.5-fold (Farrer et al., 1997). ApoE4 is also a factor in the age of onset of AD, with affected individuals having an earlier onset if they carry an E4 allele (Chartier-Harlin et al., 1994). In contrast, an E2 allele is protective, and the risk of AD and cognitive decline is decreased (Chartier-Harlin et al., 1994; Farrer et al., 1997). Nonetheless, the possession of an E4 allele is neither sufficient, nor necessary, to cause AD (Plassman and Breitner, 1996).

ApoE interacts with Aβ, at least to the extent that ApoE can be immunocytochemically detected in some senile plaques (Namba et al., 1991; Strittmatter et al., 1993; Wisniewski and Frangione, 1992), and Aβ deposits will not develop in transgenic mice overexpressing mutant APP if their expression of ApoE is knocked out (Bales et al., 1999). By contrast, overexpression of ApoE4 in APP transgenic mice causes a 10-fold increase in fibrillar Aβ deposits (Holtzman et al., 2000). Similarly, humans with an ApoE4 allele display higher numbers of senile plaques (Berr et al., 1994). Thus, ApoE in general, and ApoE4 in particular, seem to facilitate the deposition of Aβ.

1.2.5. The amyloid hypothesis of AD.

Given that neuritic plaque load is reported to correlate with cognitive decline in AD (Cummings et al., 1996), and that the mutations associated with autosomal familial AD increase the amount of Aβ1-42 in the brain, the view has been formed that fibrillar Aβ is neurotoxic and is largely responsible for the pathogenesis in AD. This prevailing view has become known as the 'amyloid hypothesis', and variants of this hypothesis have guided most of the research into AD pathogenesis during the past decade (Hardy and Higgins, 1992; Rozemuller et al., 1989; Selkoe, 2001). The amyloid hypothesis (Figure 1.3) posits that an altered proteolysis of APP leads to a gradual accumulation of Aβ1-42 in the interstitial fluid of the brain. Aβ1-42 oligomerises and deposits into diffuse plaques, providing a focus for the subsequent deposition of Aβ1-40 and other proteins. This accumulation of toxic fibrillar Aβ injures neurites within the plaques and in the surrounding neuropil. This focal injury disrupts neuronal function and homeostasis and eventually causes neuronal death. As increasing numbers of neuritic plaques are formed there is a cascade of neuronal loss that results in dementia. In this view, familial AD is caused by genetic mutations that directly lead to the overproduction of Aβ, while sporadic AD is caused by genetic and/or environmental

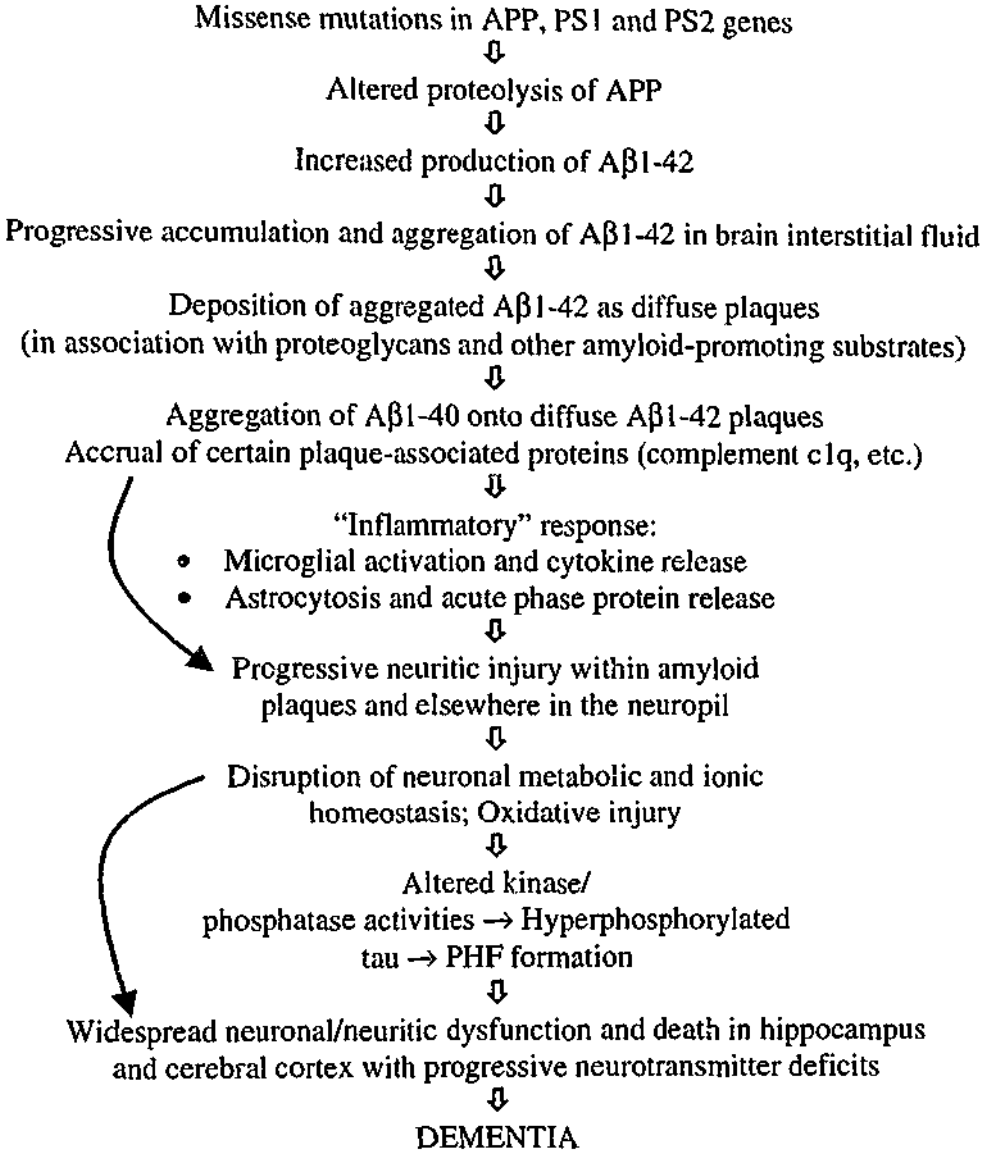

Figure 1.3. The amyloid hypothesis of AD.
A hypothetical sequence of the pathogenetic steps in autosomal familial forms of AD. From Selkoe, 2001.

factors that predispose the brain to an increased production or a reduced rate of clearance of Aβ.

1.2.6. Transgenic models of AD.

The involvement of APP and PS mutant genes in the development of AD has led to the generation of transgenic mouse models that express these mutant genes. According to the amyloid hypothesis, it would be expected that these transgenic mice should develop the clinical and pathological symptoms of AD. These mice provide a valuable model in which the effects of Aβ overexpression can be measured, and the role of genetic mutations in AD pathogenesis can be examined.

1.2.6.1. Transgenic mice expressing mutant APP.

Transgenic mice have been produced that overexpress APP containing the Swedish double mutation (KM670/671NL): the Tg2576 strain (Hsiao et al., 1996) and the APP23 strain (Sturchler-Pierrat et al., 1997). There are also mice expressing the Indiana mutation (V717F): the PDAPP mice (Games et al., 1995); and mice expressing the London mutation (V717I) (Moechars et al., 1999). Each of these strains has a different phenotype, related to the consequences of the mutation (see Figure 1.1), as well as the promoter to which the human APP gene is linked. As they age, these transgenic mice can acquire a massive plaque burden in their cerebral cortices and hippocampal formation, and the plaques are associated with activated microglial cells and hypertrophic astrocytes (Games et al., 1995; Hsiao et al., 1996; Sturchler-Pierrat et al., 1997). These transgenic mice show that human APP mutations do cause plaque deposition and associated gliosis, albeit when the mutant APP is massively overexpressed.

In late stages of AD, the Aβ burden is 1.3-11% of neocortical volume in the inferior temporal and entorhinal cortices (Hyman et al., 1993; Mufson et al., 1999), and the different strains of APP transgenic mice have at least that amount, often more. However, neuronal loss is not seen in the two most widely studied APP transgenic mouse lines, PDAPP and Tg2576. Stereological neuronal counts in the entorhinal cortex in PDAPP mice that were 8,12 or 18 months old found no difference in neuronal number between transgenic and control mice, even though in the oldest mice assessed, the entorhinal cortex had been exposed to Aβ plaques for 6-8 months, and had a plaque

burden of 20-50% (Irizarry et al., 1997b). Similarly, in Tg2576 mice that were 16 months old, stereological neuronal counts in the CA1 region of the hippocampus were not different to the number of neurons in non-transgenic mice (Irizarry et al., 1997a), even though these mice would have had Aβ deposits for approximately 4-5 months. The same regions of the brain are greatly affected in AD, both by the presence of Aβ plaques (Arnold et al., 1991; Hyman et al., 1986) and by a substantial amount of neuronal loss (Vogt et al., 1992; West et al., 1994; West et al., 2000). One strain of transgenic mouse, APP23, does show neuronal loss in the pyramidal layer of the CA1 region (Calhoun et al., 1998), where Aβ burden in the whole of the CA1 region can reach 28%. However there is no neuronal loss in neocortical regions of these mice, despite similar densities of plaques, being up to 26% of neocortical volume (Calhoun et al., 1998). This lack of inter-regional correlation indicates that plaque deposition alone does not cause neuronal loss, and that other factors must have contributed to the loss in CA1. A lack of toxicity of Aβ deposits in APP23 transgenic mice is further indicated by the frequent occurrence of axonal sprouting in the vicinity of Aβ plaques (Phinney et al., 1999). These observations led the researchers to conclude that "cerebral amyloid deposition has neurotropic effects" (Phinney et al., 1999).

While neuronal loss is not normally evident in APP transgenic mice, there have been reports of decreased synaptophysin and MAP-2 immunoreactivity in the molecular layer of the dentate gyrus in PDAPP mice (Dodart et al., 2000; Games et al., 1995). However the same study has found considerable variability between cortical areas with respect to synaptophysin expression, and this variability is not linked in any consistent way to the deposition of Aβ (Dodart et al., 2000). In contrast, Tg2576 mice have no change in synaptophysin immunoreactivity (Irizarry et al., 1997a) but they do display decreased immunoreactivity for somatostatin, substance P and choline acetyltransferase (ChAT) in regions where plaques are present (Tomidokoro et al., 2000). From these findings, it has been suggested that there may be a neuronal dysfunction in the transgenic mice, even though neuronal loss is not present. However, a decreased level of immunoreactivity for these markers is not necessarily indicative of synaptic loss, as these markers are closely related to neurotransmitter metabolism and turnover. The presence of vesicular acetylcholine (ACh) transporter may give a more accurate reflection of synaptic function in cholinergic cells. It is noteworthy therefore that Tg2576 mice have an increased density of this transporter in the frontal and parietal cortices, while the density in the entorhinal cortex is unchanged (Wong et al., 1999), suggestive of normal

functioning of the cholinergic pathways in these mice. Mild disruption of cholinergic pathways has been seen in APP23 mice, where the local cholinergic fibre network appears to be distorted in the vicinity of plaques (Sturchler-Pierrat et al., 1997). However, in mice with the London mutation, there are variable changes in the cholinergic system and it depends on the specific brain region as to whether there is a decrease or an increase in ChAT activity (Bronfman et al., 2000). Thus, in the absence of quantitative electronmicroscopical analyses of synapse densities it is difficult to ascertain whether there is a decrease in synaptic function. At best, it can be concluded that the expression of some neurotransmitters and related enzymes is decreased in some APP transgenic mouse strains.

Dystrophic neurites have been seen in most APP transgenic mice, and many of these neurites contain tubular or filamentous structures that are recognised by antibodies against phosphorylated neurofilaments and phosphorylated tau (Masliah et al., 2001; Sturchler-Pierrat et al., 1997). These structures are different from the paired helical filaments that are seen in AD, and no neurofibrillary-like structures or neuropil threads are observed. It has been proposed that the filamentous structures may resemble the early cytoskeletal pathology that occurs in AD (Masliah et al., 2001). However, such changes are also common in brain injury (King et al., 1997) so it cannot be concluded that this cytoskeletal pathology necessarily results from Aβ deposition.

Behaviourally, the APP transgenic mice display some cognitive changes, however these changes occur prior to Aβ deposition in the mice (Dodart et al., 1999b; Hsiao et al., 1996; Moechars et al., 1999). There does appear to be a progressive decline in cognition (Chen et al., 2000), but there is never a complete loss of memory, as seen in AD patients. Aggression and other abnormal social behaviour have been observed in some strains (Moechars et al., 1999), but these are probably related to the genetic background of the mice used to create the transgenic line (see Guenette and Tanzi, 1999). The other behavioural symptoms seen in AD patients, such as olfactory loss and an inability to feed and groom, have not been reported in any of the APP transgenic strains.

In summary, the APP transgenic mice show that overexpression of human APP mutations can cause Aβ to deposit as plaques. The plaques appear to be involved in the activation of glia and the promotion of dystrophic neurites, but their effect on the cholinergic pathways is minimal. Furthermore, the APP transgenic mice demonstrate

that plaques do not cause neuronal loss or neurofibrillary tangles, and probably do not cause synaptic loss. The mild cognitive impairment seen in these transgenic mice precedes amyloid deposition, and therefore may have a different basis. Indeed, most of the pathological changes observed in APP transgenic mice occur prior to the deposition of Aβ and many researchers have reached the conclusion that the changes are plaque-independent (e.g. Dodart et al., 1999a; Hsia et al., 1999; Moechars et al., 1999). One group has even concluded that the "results strongly argue against a direct acute neurotoxic mechanism of Aβ deposits *in vivo* in the transgenic mouse" (Irizarry et al., 1997b).

1.2.6.2. Transgenic mice expressing PS mutations.

In addition to the APP transgenic mice, other mice have been engineered to overexpress the PS-1 or PS-2 mutations found in some forms of autosomal familial AD. PS transgenics display an increased level of soluble Aβ1-42 (Borchelt et al., 1996; Duff et al., 1996; Oyama et al., 1998), but they do not develop Aβ plaques, tangles or gliosis. This result demonstrates that these particular mutations do not directly cause plaque deposition in mice. On the other hand, the mutations do decrease the activity of antioxidant enzymes within the brains of these transgenic mice (Leutner et al., 2000), and cultured neurons from these mice are more likely to undergo apoptosis when trophic factors are removed (Czech et al., 1998). Thus, while the PS mutations do not cause plaque deposition they do compromise the ability of neurons to withstand injury. This conclusion is consistent with the fact that PS-1 mutant mice display increased levels of neurodegeneration despite their lack of Aβ deposits (Chui et al., 1999).

When mutant PS-1 transgenic mice are crossed with mutant APP transgenic mice, AD-like pathology can be detected in the double transgenics, and it is present at a much earlier age than in APP single transgenics (Borchelt et al., 1997; Holcomb et al., 1998; McGowan et al., 1999). Double transgenic mice display increased microglial and astrocytic reactivity in association with Aβ plaques (Matsuoka et al., 2001). They also exhibit a decrease in the density and size of synaptic boutons expressing the vesicular ACh transporter (Wong et al., 1999). Furthermore, these double transgenic mice display cognitive impairments on standard behavioural tests (Arendash et al., 2001; Holcomb et al., 1998), but it should be noted that these impairments are frequently evident before any pathological changes appear (Holcomb et al., 1998).

Only overexpressed mutant forms of APP have been shown to produce plaques in mice and the PS mutations require the co-overexpression of a mutated APP as well to generate plaques. Thus, even a powerful PS mutation that induces early-onset AD in humans requires assistance in the mouse. Nonetheless, these double transgenics are considered by many researchers to be the best available animal model of AD, but it is sobering to consider that no AD sufferers are known to express mutations in both of these genes. Thus, these double transgenic mice may mimic some of the features of AD, but their physiological relevance is questionable.

1.3. Neurotoxicity of Aβ.

In addition to the transgenic mouse models of AD, a number of other models have been used to study the neurotoxicity of Aβ. These techniques vary from examining the properties of dissolved Aβ in test tubes, adding the peptide to cell cultures, or injecting or infusing Aβ into the brains of living animals. Such studies are discussed below.

1.3.1. *In vitro* toxicity of Aβ.

The *in vitro* models used to study Aβ neurotoxicity generally utilise one of two research paradigms. The most common paradigm is to expose cultured cells to the Aβ, and the other is to put Aβ in a test tube and examine its reaction when mixed with other substances. While several *in vitro* studies have shown Aβ to have neurotrophic actions (Whitson et al., 1990; Whitson et al., 1989; Wujek et al., 1996; Yankner et al., 1990b), the majority have reported that Aβ is neurotoxic to cultured cells (e.g. Pike et al., 1992; Roher et al., 1991). This is the case for both Aβ1-40 and Aβ1-42, while rodent variants of Aβ have been reported to be non-toxic to cultured neurons (Giulian et al., 1996). The basis of Aβ neurotoxicity is not known, but in view of the results obtained with these two paradigms, it has been variously proposed to include the generation of reactive oxygen species (ROS), the disruption of cellular calcium homeostasis, and the recruitment of microglial cells that secrete neurotoxins.

1.3.1.1. Generation of radicals.

Aβ has been reported to spontaneously generate radicals in a test tube at a very fast rate (Butterfield et al., 1994; Hensley et al., 1995; Hensley et al., 1994), with maximal

activity after 6hr. The formation of radicals correlates with the ability of Aβ to decrease glutamine synthetase activity (Aksenov et al., 1995), and to increase intracellular calcium, ROS and carbonyl content (Harris et al., 1995). From these results, it was hypothesised that Aβ radicals interact with cells, producing oxidative stress that leads to neuronal degeneration. This idea is supported by the finding that Aβ is not toxic in the presence of antioxidants such as vitamin E or propyl gallate (Behl et al., 1992), or free radical scavengers (Richardson et al., 1996). Catalase can also prevent Aβ toxicity, indicating that hydrogen peroxide or subsequently generated hydroxyl radicals have a role in the toxicity of the peptide (Behl et al., 1994).

1.3.1.2. Interaction with metal ions.

Iron, copper and zinc are all present in senile plaques at high concentrations (Lovell et al., 1998). All of these metal ions have been demonstrated to mediate the *in vitro* toxicity of Aβ. In fact, it has been reported that Aβ is toxic to cultured neurons only if iron is present in the culture media (Schubert and Chevion, 1995). Contamination of Aβ solutions with iron may also cause toxicity, since pre-treatment of the peptide with deferoxamine decreases the toxicity of Aβ to cultured neurons (Rottkamp et al., 2001). Furthermore, it appears that the spontaneous radical production by Aβ in the test tube may also be attributed to low-level contamination with iron (Dikalov et al., 1999; Monji et al., 2001; Turnbull et al., 2001). The potentiation of Aβ toxicity by high concentrations of copper and zinc is also well established (e.g. Huang et al., 1999b; Lovell et al., 1999; Moreira et al., 2000). Apart from potentiating the generation of ROS, metal ions promote the aggregation of Aβ and cause the peptide to precipitate from solution (Atwood et al., 1998; Mantyh et al., 1993). When Aβ aggregates and forms a β-sheet structure, it is more toxic to cultured neurons (Pike et al., 1993), and thus the interaction of Aβ with metal ions may promote this increased toxicity.

1.3.1.3. Disruption of calcium homeostasis.

Aβ is reported to increase intracellular calcium concentrations and to destabilise calcium homeostasis in cultured neurons (Mattson et al., 1992) by disrupting the regulation of calcium at the plasma membrane (Mattson, 1994). Calcium influx associated with membrane depolarisation caused by excitatory amino acids is augmented by pre-treatment of cell cultures with Aβ (Mattson et al., 1993c). By destabilising calcium homeostasis, Aβ increases neuronal susceptibility to excitotoxic

damage (Koh et al., 1990). However, the excitotoxic actions of Aβ are not specifically mediated by NMDA glutamate receptors (Gray and Patel, 1995), and instead may be mediated via metabotropic glutamate receptors or L-type calcium channels (Iversen et al., 1995). Basic fibroblast growth factor can be used to stabilise intracellular calcium levels and this prevents the potentiation of Aβ excitotoxicity (Mattson et al., 1993b).

The ability of Aβ to form calcium channels in lipid bilayers (Arispe et al., 1993b), along with the ability to disrupt calcium homeostasis, has led to the hypothesis that Aβ exerts toxicity by creating a specific ion channel (Pollard et al., 1995). Hexameric Aβ peptides are thought to insert into the cell membrane, forming a cation-selective channel permeable to calcium (Durell et al., 1994). Aβ ion channels can also conduct monovalent cations such as caesium, lithium, potassium and sodium (Pollard et al., 1993). The conductance of the Aβ ion channel resembles that of L-type calcium channels, however specific blocking agents of these channels cannot prevent ionic flow (Arispe et al., 1993a). It appears that the Aβ-ion channel allows unregulated entry of calcium ions into the cell, and formation of the ion channels may be accelerated by the interaction of Aβ with metal ions which induce the aggregation of Aβ (Kawahara and Kuroda, 2000).

The hypothesis that Aβ toxicity is due to a disruption of calcium homeostasis is related to the hypothesis of radical formation. Oxidative stress disrupts cellular ion homeostasis, and an increase in intracellular calcium concentration leads to ROS production. Mattson and colleagues propose that Aβ indirectly induces lipid peroxidation, resulting in the release of 4-hydroxynoneal which impairs ATPases that are involved in the transport of calcium, sodium and potassium, and ultimately cause an increase in intracellular calcium (Mattson et al., 1997). This produces a cycle whereby ROS are produced, which can further increase intracellular calcium.

1.3.1.4. Release of microglial-derived neurotoxins.

Another hypothesis regarding the mechanism of Aβ toxicity involves mediation by microglial cells. When plaques that have been isolated from human brains are added to cultured neurons, neuronal death does not result (Giulian et al., 1995). However, these researchers have found that if microglia are cultured in a filter-bottom chamber that is placed above the neurons, preventing contact between the microglia and neurons but

allowing diffusion of substances between the chambers, then the addition of plaques to the microglia results in the death of the neurons in the chamber below. In this system, the neurotoxicity appears to be caused by a diffusible agent of less than 1000Da that is secreted by the activated microglial cells (Giulian et al., 1995). This neurotoxin was also found to kill hippocampal neurons when infused into the brains of living rats.

The microglial mediation of plaque neurotoxicity appears to be due to the Aβ within the plaques, since similar results are obtained by exposing microglia to pure Aβ (Giulian et al., 1996; Meda et al., 1995). The neurotoxic agent has not been identified, but the list of potential agents includes TNF-α, ROS and reactive nitrogen intermediates (Bianca et al., 1999; Klegeris and McGeer, 1997; McDonald et al., 1997; Meda et al., 1995; Van Muiswinkel et al., 1999). Residues 10-16 of Aβ are necessary for microglial binding and activation (Giulian et al., 1996), which has important implications for the rodent Aβ variant, since this peptide has two amino acid substitutions within the microglial binding region. These alterations may be why rodent Aβ is not neurotoxic even in the presence of microglial cells (Giulian et al., 1996).

1.3.2. *In vivo* toxicity of Aβ.

More than 60 published studies have assessed the neurotoxicity of Aβ that has been injected or infused into the brains of experimental animals. In these studies, the term 'neurotoxicity' is often loosely used to describe any disruption of neuronal function, whether it is neuronal death, alterations in metabolism or decreased neurotransmitter expression. Thus, when reviewing the studies that have examined the *in vivo* neurotoxicity of Aβ, it is necessary to determine how the toxicity was measured. For instance, some studies have examined alterations in neuronal metabolism, such as changes in the expression of neurotransmitters or the enzymes that are responsible for their synthesis. While such changes indicate a decrease in neuronal function, they do not necessarily indicate an irreversible loss of function that will lead to cell death. This point has been demonstrated by Giovannelli and colleagues, who originally described an impairment of the cholinergic system in response to injections of Aβ (Giovannelli et al., 1995), but later found that this was a temporary impairment and that normal function returned over time (Giovannelli et al., 1998). Other studies have used the numbers of activated astrocytes or microglial cells or the area containing them as an indication of the degree of neurotoxicity, but this is not a good measure of neurotoxicity

since Aβ can directly activate astrocytes and microglia (e.g. Giulian et al., 1996; Pike et al., 1994). Changes in behaviour or cognitive function have also been used as an indicator of neurotoxicity, but the presence of such changes is not always associated with neuronal loss (Nitta et al., 1997).

This review therefore, will be limited to studies that have examined tissue for Aβ-mediated neurodegeneration or neuronal loss. These studies generally use histological stains of neuronal viability or death such as Nissl stains, haematoxylin and eosin, or terminal deoxynucleotide transferase-mediated dUTP-biotin nick end labelling (TUNEL). There are over 30 studies that have assessed Aβ-mediated neurodegeneration as a result of injection or infusion of Aβ into the brains of rats, mice or monkeys. The protocols used in these studies vary considerably and these variations may be responsible for the conflicting results obtained. These methodological differences have been summarised in Table 1.1 according to the appropriateness of each variation, and they will be discussed in detail below.

1.3.2.1. Variations of the protocol used in in vivo *studies.*

The most important variation between different *in vivo* studies is the type of solvent that was used to dissolve the Aβ peptide. Many solvents can dissolve Aβ, but they vary in their physiological relevance and toxicity. The ideal physiological solvent would be CSF from the animal receiving the intracortical injections, but it is not practical to prepare the Aβ in this way. Therefore, the preferable and practical option is a solvent that is known to be non-toxic when added to cells *in vitro*. Such solvents are generally characterised by a buffering capacity and an iso-osmotic concentration of salts. These "physiological" solvents include artificial CSF, PBS, saline and HEPES. Solvents that do not meet these criteria, such as the organic solvents acetonitrile and dimethyl sulphoxide (DMSO), are generally more toxic and in this thesis will be classified as "nonphysiological" solvents. While water is abundant within the brain, it normally contains dissolved salts. For this reason, pure water is also classified as a nonphysiological solvent because by itself it creates cytotoxic changes in osmotic pressure.

The points raised in the previous paragraph are particularly relevant because of the findings of a study performed by Waite and colleagues (1992), which demonstrated the

Table 1.1. Methodological flaws evident in some *in vivo* studies of Aβ neurotoxicity.

Appropriate methodology	Inappropriate methodology
• Use of a "physiological solvent" (e.g. artificial CSF, saline, PBS, HEPES).	• Use of a "nonphysiological solvent" (e.g. water, acetonitrile, DMSO).
• Comparison of Aβ toxicity with that of the injected solvent.	• No comparison with the solvent vehicle.
• Comparison of Aβ toxicity with that of another type of peptide (e.g. rodent Aβ, reverse or scrambled peptides).	• No comparison with other peptides.
• Quantitative analysis of neuronal loss.	• Qualitative or semi-quantitative analysis of neurodegeneration.
• Systematic correction of values obtained to account for variation in the depth of the injection tract.	• No correction for variable depths of injection.
• Injection of naturally occurring Aβ variants (e.g. Aβ1-40 and Aβ1-42).	• Injection of truncated Aβ variants that are not naturally present in the brain (e.g. Aβ25-35).
• Elimination of injection sites that demonstrate mechanical damage or bleeding.	• No criteria for eliminating injection sites that demonstrate mechanical damage or bleeding.

importance of using a physiological solvent when assessing the neurotoxicity of Aβ. They found that Aβ dissolved in acetonitrile and injected into rat hippocampus was neurotoxic, however when dissolved in water Aβ was less toxic, and only a minimal toxic reaction was seen when dissolved in phosphate-buffered saline (PBS) and cyclodextrin. Similarly, when the solvent vehicle alone was injected into the hippocampus, acetonitrile was most toxic, water had some toxicity and PBS was only minimally toxic. This result also shows that the injection procedure itself causes neuronal death and demonstrates the importance of comparing vehicle control injections to Aβ injections. Aβ is highly soluble in acetonitrile, yet it precipitates out of solution when there are salts present, indicating that the type of solvent can alter the structure of Aβ and potentially alter its physiological properties (Waite et al., 1992). It is important to note that acetonitrile can be converted to cyanide in the microsomes of cells (Freeman and Hayes, 1988). Cyanide compromises oxidative metabolism (Goldberg et al., 1987), and thus when Aβ is dissolved in acetonitrile, the compromised metabolism may allow Aβ to be toxic, even though it may not be toxic under physiological conditions. Despite the fact that the toxic effects of nonphysiological solvents have been known for 9 years, many studies have continued to use them. However, there are some situations where organic solvents may be a better choice, such as to maintain constant infusion of Aβ from a mini-osmotic pump. Since Aβ is more soluble in organic solvents than in salt solutions (Waite et al., 1992), the use of an organic solvent will ensure that Aβ remains soluble for the duration of the infusion and will reduce the likelihood of the pump becoming blocked.

Another variation between studies is the type of 'control' that is used for comparison to Aβ. The most appropriate control is the vehicle in which the Aβ is dissolved. However, some studies do not make this comparison but instead compare the neurotoxicity of Aβ to healthy untreated tissue (e.g. Giordano et al., 1994; Kowall et al., 1991). The need for an additional control arises when injecting human Aβ variants into rats or mice, since the endogenous Aβ is structurally different. Thus, it would be of use to compare the effects of human Aβ variants to the effects produced by rodent Aβ variants of equivalent length. Nonetheless, the effects of rodent Aβ are rarely examined, and reverse or scrambled forms of Aβ (see Figure 1.2) have been used in preference

Any of the Aβ variants will provide a control for the peptide's propensity to form large, sticky deposits that displace neurons in the vicinity of the injection site. The volume of the peptide deposit needs to be considered when assaying for cell death, because there will normally be a core of tissue that will not contain healthy neurons due to their displacement by the Aβ deposit (see Figure 1.4). If the protocol assesses neurotoxicity by determining the density of healthy neurons around the injection site (e.g. Giordano et al., 1994; Kowall et al., 1991; Kowall et al., 1992; Maurice et al., 1996), one must be careful not to include the area containing the Aβ deposit in the assessment (Figure 1.4A). Instead it would be best to count the number of neurons around the margin of the Aβ deposit (Figure 1.4B), since there will not be a corresponding peptide deposit at the vehicle injection sites. If however, the study is assessing the number of dying neurons associated with the injection site, perhaps by counting pyknotic profiles, then the total number of dying cells should be counted regardless of whether they are within the Aβ deposit or outside of it (Figure 1.4C). Despite the importance of these considerations, few studies mention the exact part of the injection site that was assessed.

Another major technical problem often encountered is that studies rarely make any adjustments for the depth of the injection. Experience of the present researcher has shown that repeated application of an identical injection protocol can still result in injection tracts of variable depth (see Figure 1.5). When the needle penetrates deeper into the brain, more neurons will be subjected to mechanical damage, and a greater amount of cell death will be seen around these injection sites. This increased neuronal loss is a methodological artefact, and needs to be taken into account when assessing the apparent toxicity of Aβ.

Yet another factor that varies considerably between studies is the variant of Aβ that was examined. The use of different length variants can confer different properties on the peptide, and thus produce different results. For instance, residues 10-16 of Aβ are thought to activate microglial cells (Giulian et al., 1996), however these residues are not present in Aβ25-35. The manufacturer of the Aβ peptide can also be a significant factor, as it has been shown that even though the peptides are claimed to have an identical primary structure, variable toxicity to cultured neurons can occur when the peptides are sourced from different manufacturers (May et al., 1992). The reported neurotoxicity can also be influenced by whether the peptide was freshly prepared or stored for some time

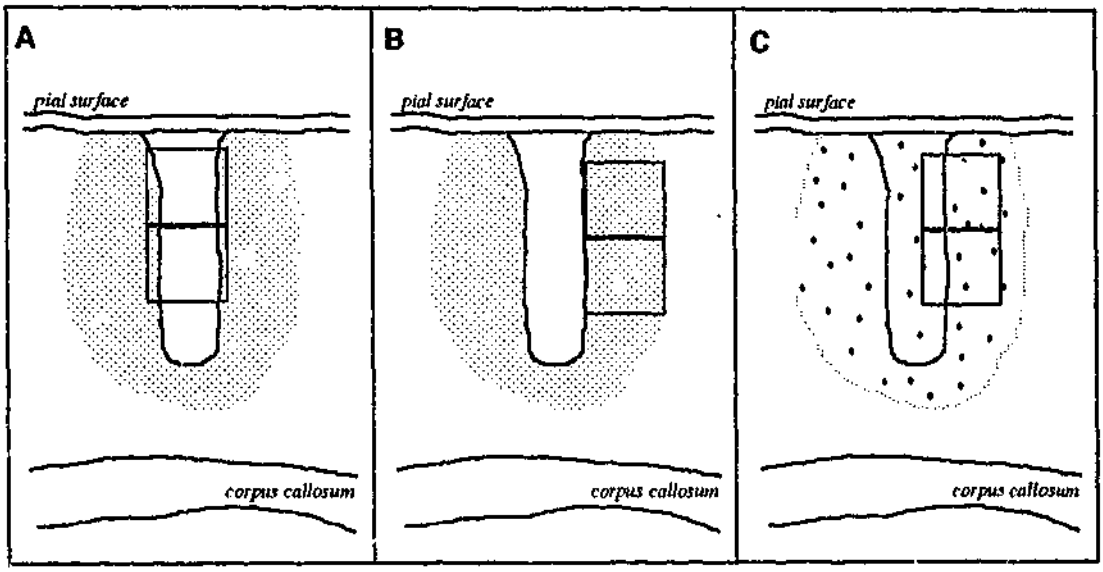

Figure 1.4. The effect of peptide deposits when assessing neuronal death.
An eyepiece graticule in the microscope is used to count cells within a small region (between 0.16 and 0.64mm^2). Normally, 3 to 6 of these regions would be counted for each injection site. When healthy neurons are counted, care must be taken to ensure that regions where Aβ are deposited (the white area in the middle of the injection) are not included in the count because living cells will be displaced by the peptide deposit (**A**). Instead, the healthy neurons should be counted around the Aβ deposit to prevent bias appearing in the results (**B**). However, if the number of dying neurons are being counted, the entire region of the injection site should be analysed to ensure that all dying neurons are included (**C**).

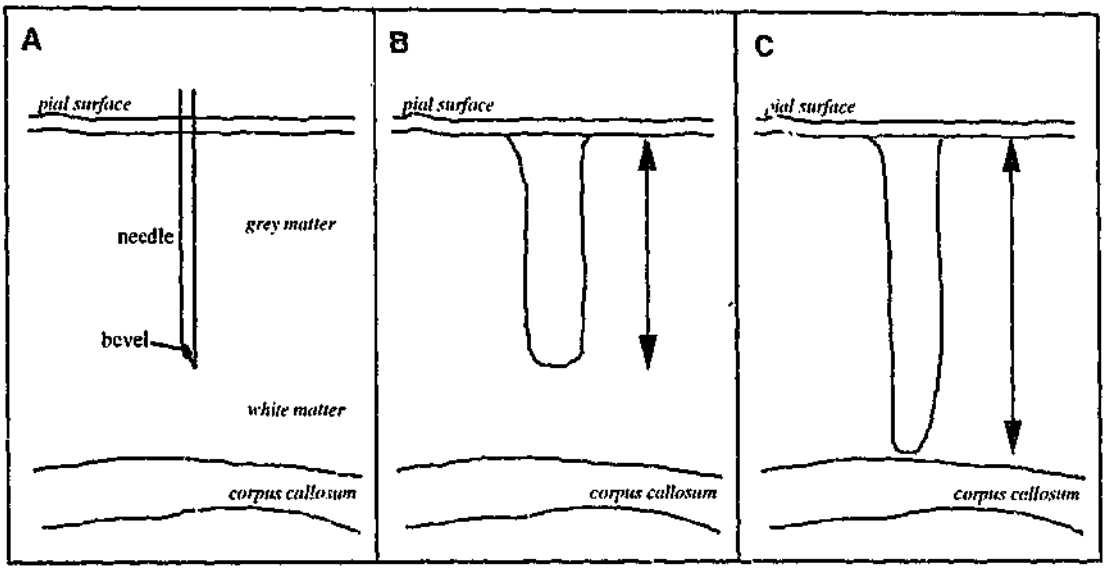

Figure 1.5. Depth of the injection into the cerebral cortex.
Penetration of the needle into the cerebral cortex (**A**) will cause a lesion in the grey matter (**B**). Sometimes the lesion will penetrate deeper into the cortex (**C**) even though the experimenter followed an identical procedure, and a greater number of neurons will be subjected to the injection.

before use. This factor is difficult to take into account because most studies do not state how long the Aβ peptide solution was stored prior to injection.

The region of the brain where Aβ is injected may also produce variable results. For instance, the hippocampus appears to be more sensitive than the neocortex to deposits of Aβ (Calhoun et al., 1998; Frautschy et al., 1991). Some studies have injected Aβ into regions where Aβ deposits do not normally form, such as the vitreous chamber of the eyeball (Jen et al., 1998). While it would be ideal to inject numerous small deposits of Aβ into the regions of the brain that are affected in AD, it is not possible to do this without causing substantial damage to other regions which the needle must pass through (e.g. Emre et al., 1992). Thus, the least amount of damage will be caused by discrete injections into the neocortex, and for this reason many studies have examined the *in vivo* toxicity of Aβ to cortical neurons.

1.3.2.2. Examination of Aβ-induced neurodegeneration.

The studies that have examined Aβ-induced neurodegeneration *in vivo* are summarised in Tables 1.2 and 1.3. They have been further categorised in Table 1.4 into studies that used physiological or nonphysiological solvents to dissolve Aβ (as defined above), and the studies are grouped according to the region of the brain into which the Aβ was injected. When Aβ was dissolved in a physiological solvent, such as saline or PBS, and then injected into the hippocampus or cortex of rats or young monkeys, it was found that Aβ did not kill more neurons than vehicle control injections (Dornan et al., 1993; Games et al., 1992; Geula et al., 1998; Morimoto et al., 1998; Podlisny et al., 1992; Podlisny et al., 1993; Waite et al., 1992; Winkler et al., 1994). There are three other studies that have dissolved Aβ in a physiological solvent that have reported Aβ neurotoxicity. Out of these, it was found that fibrillar Aβ kills cortical neurons when injected into the cortices of old monkeys, but not when injected into the cortices of young monkeys or young or old rats (Geula et al., 1998). It has also been shown that Aβ in PBS is toxic to neurons in the outer nuclear layer of the retina after injection into the vitreous chamber (Jen et al., 1998). Interestingly, plaque cores extracted from brains affected by AD are not toxic to cortical neurons, yet are able to kill hippocampal neurons after micro-injection of the plaque cores dissolved in saline (Frautschy et al., 1991). This difference in regional sensitivity to Aβ resembles that seen in APP23 transgenic mice which display neuronal loss in the CA1 region of the hippocampus, but

Table 1.2. Studies reporting that injection of Aβ kills neurons *in vivo*.

Reference	Animal	Aβ variant	Physiological solvent?	Site of injection
Emre et al., 1992	rat	Aβ1-40	No	Cortex/ Hippocampus
Frautschy et al., 1991	rat young to middle aged	Plaque core	Yes	Hippocampus
Geula et al., 1998	monkey old	Aβ40, Aβ42 (fibrillar)	Yes	Cortex
Giordano et al., 1994	rat young/old	Aβ1-40	No	Cortex
Jen et al., 1998	rat	Aβ1-40, Aβ1-42	Yes	Vitreous chamber (retina)
Kowall et al., 1991	rat	Aβ1-40	No	Cortex or Hippocampus
Kowall et al., 1992	rat, monkey young/old	Aβ1-40, Aβ25-35	No	Cortex
Maurice et al., 1996	mice	Aβ25-35, Aβ1-28	No	Ventricle
Rush et al., 1992	rat	Aβ1-40, Aβ25-35	No	Hippocampus
Sigurdsson et al., 1996	rat	Aβ25-35	No	Amygdala
Sigurdsson et al., 1997a	rat	Aβ25-35	No	Amygdala
Sigurdsson et al., 1997b	rat	Aβ25-35	No	Amygdala
Waite et al., 1992	rat	Aβ1-40, Aβ1-42, rat Aβ1-42	No	Hippocampus

Table 1.3. Studies reporting that injection of Aβ does not kill neurons *in vivo*.

Reference	Animal	Aβ variant	Physiological solvent?	Site of injection
Clemens and Stephenson, 1992	rat young/ middle aged	Aβ1-43, Aβ1-40	No	Striatum, Hippocampus
Dornan et al., 1993	rat	Aβ25-35	Yes	Hippocampus
Frautschy et al., 1991	rat	Plaque core	Yes	Cortex
Games et al., 1992	rat	Aβ1-40, Aβ1-38, Aβ25-35	Yes or No	Cortex or Hippocampus
Geula et al., 1998	rat young/old, monkey young	Aβ40, Aβ42 (fibrillar or soluble)	Yes	Cortex
Giovannelli et al., 1995	rat	Aβ25-35, Aβ1-40	No	Nucleus basalis
Giovannelli et al., 1998	rat	Aβ1-40	No	Nucleus basalis
Morimoto et al., 1998	rat	Aβ25-35, Aβ1-40	Yes or No	Hippocampus
Nelson and Saper, 1996	sheep	Aβ1-40	Doesn't say	Cortex
Podlisny et al., 1992	monkey	Aβ1-40, Aβ25-35	Yes or No	Cortex
Podlisny et al., 1993	monkey	Aβ1-40, Aβ25-35	Yes or No	Cortex
Sigurdsson et al., 1995	rat	Aβ25-35	Yes or No	Ventral pallidum/ Substantia innominata
Smyth et al., 1994	rat	Aβ1-42, Aβ25-35	No	Hippocampus
Soto et al., 1998	rat	Aβ1-42	No	Amygdala
Stein-Behrens et al., 1992	rat	Aβ25-35	Yes or No	Hippocampus
Stephenson and Clemens, 1992	rat	Aβ1-43	No	Striatum, Hippocampus
Waite et al., 1992	rat	Aβ1-40, Aβ1-42, rat Aβ1-42	Yes	Hippocampus
Winkler et al., 1994	rat	Rat Aβ1-42	Yes	Hippocampus or Ventricle

Table 1.4. Summary of the numbers of studies that have assessed neurotoxicity after injection of Aβ into various brain regions.

Site of injection	Aβ injection killed neurons			Aβ injection did not kill neurons		
	Total number of studies	Physiological solvent		Total number of studies	Physiological solvent	
		Yes	No		Yes	No
Cortex	5	1	4	6	5	3
Hippocampus	5	1	4	8	6	5
Ventricles	1	-	1	1	-	1
Amygdala	3	-	3	1	-	1
Retina	1	1	-	-	-	-
Nucleus basalis	-	-	-	2	-	2
Striatum	-	-	-	2	-	2
Ventral pallidum/ Substantia innominata	-	-	-	1	1	1

Note: There may appear to be more studies in this table than are present in Tables 1.2 and 1.3, because some studies injected Aβ into more than one region of the brain. Furthermore, a number of studies examined the effects of both physiological and nonphysiological solvents.

not in the neocortex, even though the Aβ plaque burden in both regions is similar (Calhoun et al., 1998). When Aβ has been dissolved in a nonphysiological solvent and injected into the brain, the results are quite variable, with approximately half of the studies reporting neurodegeneration (see Tables 1.2 and 1.3).

It is important to note that out of 13 studies reporting neurotoxicity, only 3 used physiological solvents and the other 10 (77%) used water, acetonitrile or DMSO. Furthermore, there were 17 studies that did not find neurotoxicity after Aβ injection, and as can be seen in Table 1.3, there were 5 studies that dissolved Aβ in both physiological and nonphysiological solvents, but did not find neurotoxicity for either type of solvent.

Studies using infusion of Aβ have generally used nonphysiological solvents (see Tables 1.5 and 1.6). In contrast to the injection studies, a lack of neurodegeneration was seen in three infusion studies that used nonphysiological solvents (Games et al., 1992; Nitta et al., 1997; Snow et al., 1994), while neuronal death was found in the only infusion study that used a physiological solvent (Frautschy et al., 1998). Constant infusion of Aβ provides the opportunity for the peptide to accumulate over periods of 1 week or more, however this technique does not allow examination of the effects of Aβ after acute time points.

1.4. Studying Aβ-induced neuronal loss in a controlled *in vivo* model.

It is evident that the toxicity of Aβ *in vivo* is not a straightforward issue. However as a generalisation, it appears that Aβ is not toxic to neurons when dissolved in a physiological solvent and injected into the cerebral cortex or hippocampus. The conflicting results of the *in vivo* studies described above demonstrate the need for a well-controlled study that uses a physiological solvent and compares the effects of Aβ injections to those of appropriate control injections. Such a study should count the number of dying neurons around the site of injection, and make appropriate adjustments for depth of injection.

In order to develop a paradigm that took all of the above mentioned factors into account, and to establish the validity of this model, it was decided to examine the effects of a known neurotoxin in such a model prior to the examination of Aβ. Iron is known to

Table 1.5. Studies reporting that infusion of Aβ kills neurons *in vivo*.

Reference	Animal	Aβ variant	Physiological solvent?	Site of injection
Frautschy et al., 1998	rat	Aβ40, Aprotinin, Leupeptin	Yes	Ventricle

Table 1.6. Studies reporting that infusion of Aβ does not kill neurons *in vivo*.

Reference	Animal	Aβ variant	Physiological solvent?	Site of injection
Games et al., 1992	rat	Aβ1-40, Aβ1-38, Aβ25-35	No	Hippocampus
Nitta et al., 1997	rat	Aβ1-40	No	Ventricle
Snow et al., 1994	rat	Aβ1-40, HSPG, HSGAG	No	Hippocampus

be very neurotoxic due to its potentiation of ROS generation in the Haber-Weiss equation (see Halliwell and Gutteridge, 1999), and the neurotoxicity of exogenous iron has previously been demonstrated in the substantia nigra (Ben-Shachar and Youdim, 1991; Rauhala et al., 1998; Sengstock et al., 1992; Sengstock et al., 1993; Sziraki et al., 1998). Thus in Chapter 3, a model of intracortical injection was developed that allowed the spatio-temporal examination of neuronal loss after survival times ranging from 1 to 7 days. Neurotoxicity was examined by using a histological marker that is specific for dying neurons, and then counting labelled cells to obtain a precise determination of neuronal loss. This method overcame the inaccuracy of attempting to count healthy neurons within the limits of the injection site, since it is often difficult to delimit the edge of the injection site from healthy tissue when Nissl stains are used. While developing the model, a thorough study was performed examining the spatio-temporal neuronal loss after injection of iron into rat cerebral cortex. These results have implications for the neurodegeneration that occurs after episodes of hypoxia-ischaemia, and the relevance of the findings has been discussed in Chapter 3.

After it was certain that an appropriate model of intracortical injection had been developed, it was possible to examine the *in vivo* neurotoxicity of the naturally occurring human Aβ variants, Aβ1-40 and Aβ1-42, to determine whether they produce the same amount of neuronal loss, or if one of the variants is more toxic than the other. The volume of the deposits was measured at various survival times and the fibrillar structure of the peptides was determined. The toxicity of human Aβ variants were also compared to the 'endogenous' rodent variant, rat Aβ1-40. This study is described in Chapter 4.

1.4.1. The interaction between Aβ and metal ions.

While it is not clear whether all neuritic plaques contain iron, the fact that iron is elevated in some neuritic plaques suggests that the presence of iron may have some pathological relevance. It is also important to consider differences between human and rodent Aβ variants, since the histidine at residue 13 of the peptide has been implicated in the binding of iron to Aβ (Atwood et al., 1998), and this residue is substituted in rodent Aβ. Thus, the human and rodent Aβ variants may interact differently with iron, and could produce a different degree of neurotoxicity *in vivo*. An investigation of the *in*

vivo neurotoxicity of iron combined with human Aβ, and iron combined with rodent Aβ, is described in Chapter 5.

In addition to iron, there is potential for copper and zinc to alter the *in vivo* neurotoxicity of Aβ (see section 1.3.1.2). Thus, it is pertinent to examine the neuronal loss produced by mixtures of copper and Aβ, and zinc and Aβ. Since iron, copper and zinc appear to be present in plaques simultaneously (Lovell et al., 1998), these metals may interact to influence the toxicity of Aβ. It is therefore necessary to examine the neurotoxicity of a combination of all three metal species with Aβ. The neurotoxicity of Aβ-metal complexes in an *in vivo* model is described in Chapter 6.

1.4.2. The influence of endogenous oestrogen on Aβ neurotoxicity *in vivo*.

In women, menopause causes a decrease in the level of endogenous estrogens. The risk of developing AD is increased after menopause, and oestrogen replacement therapy decreases this risk (Baldereschi et al., 1998; Manly et al., 2000; Waring et al., 1999). Furthermore, oestrogen has been reported to decrease the *in vitro* toxicity of Aβ (Hosoda et al., 2001; Pike, 1999; Thomas et al., 1999) and to decrease the neurotoxicity of iron (Bae et al., 2000; Culmsee et al., 1999; Vedder et al., 1999). The female rat, with an intact reproductive system, provides a model in which oestrogen levels change systematically during the oestrous cycle (Everett, 1989). Thus, the amount of neuronal death associated with injections of Aβ-metal complexes can be compared at different stages of the oestrous cycle. The possibility that endogenous levels of oestrogen alter the toxicity of Aβ-metal complexes is the subject of Chapter 7.

1.5. Summary of the aims.

This thesis reports the results of a series of studies regarding the toxicity of the naturally occurring human Aβ variants to cortical neurons *in vivo*, due to the injection of Aβ peptide into the cerebral cortices of adult rats. The amount of neuronal death produced by human Aβ is compared to that produced by rat Aβ variants. The possibility that Aβ toxicity may be mediated by iron, copper or zinc is examined and compared to the toxicity that was produced by pure deposits of Aβ. Furthermore, the human and rat Aβ variants are compared to determine whether the amino acid sequence difference between the two variants alters the toxicity of an Aβ-iron complex. The last report

examines whether fluctuations in plasma oestrogen levels during the oestrous cycle affect the neurotoxicity of Aβ-metal complexes. Together these studies are intended to further our understanding of the relative contributions of Aβ peptide and metal ions to the pathogenesis of AD.

CHAPTER 2:

Methodology.

2.1. Sourcing and maintenance of animals.

Female Wistar rats aged 9-13 weeks, were obtained from The University of Queensland Central Animal Breeding House, Perth Animal Resources Centre or Monash University Animal Services. Animals were maintained on a 12h:12h light:dark cycle and supplied with standard rat food pellets and water *ad libitum*.

2.1.1. Ethical use of animals in research.

All animal experimentation met the guidelines specified by the "Australian code of practice for the care and use of animals for scientific purposes", as defined by the National Health & Medical Research Council. The studies described in this thesis were performed at three different universities and ethical approval was obtained from each institution. All experimental chapters describe results obtained at Monash University, and this work was approved by the Monash University Psychology Animal Ethics Committee (project approval numbers: PSYC/1998/25A or PSYC/1999/22A). Some of the work described in Chapters 3 and 4 was performed at The University of New South Wales, and this work was approved by the Animal Care and Ethics Committee (registration number: ACEC 1997/145). Eight animals that were used in the work described in Chapter 4 were studied at The University of Queensland, and this work was approved by the University Animal Experimentation Ethics Committee (project approval number: PHYS/PH/489/96/NHMRC or PHYS/PH/192/97/NHMRC).

2.2. Preparation of the substances to be injected.

All of the substances that were injected are listed in Appendix 1.1. All substances were dissolved in sterile saline (0.9% NaCl). Sterile saline was used as the vehicle control for all substances injected.

2.2.1. Iron.

Ferric ammonium citrate (ICN) and ammonium citrate (Sigma) were dissolved to a concentration of 1.0mM on the day of use. Ammonium citrate was used to control for vehicle effects associated with the ferric solution.

2.2.2. Aβ peptides.

Four variants of Aβ were used: two human variants, and two rat variants. Human Aβ1-40 (U.S. Peptide, CA, Lot #10), human Aβ1-42 (U.S. Peptide, CA, Lot #12), rat Aβ1-40 (California Peptide Research, CA, Lot #BB0395), and rat Aβ1-42 (California Peptide Research, CA, Lot#MF0218) were prepared at a concentration of 1.0mM at least one day prior to use. Solutions were stored at 4°C and vortexed at 2400rpm for 2-3sec immediately before use.

2.2.3. Mixtures of iron, copper and zinc.

Solutions of iron (1.0mM ferric ammonium citrate, pH 5.2; ICN), copper (0.4mM cupric acetate, pH 5.4; Sigma) and zinc (1.0mM zinc acetate, pH 5.8; Sigma) were prepared on the day of use. A mixture of all three metal ions (iron+copper+zinc; 1.0:0.4:1.0mM) was prepared by dissolving each of the metal ions at 3-fold the final concentration, and then mixing equal volumes together.

2.2.4. Mixtures of Aβ and metal ions.

For co-injection of Aβ and metal ions, a 2.0mM stock solution of human or rat Aβ1-42 was prepared and stored at 4°C. Immediately prior to mixing with metal ions, the Aβ stock solution was vortexed for 10sec at 2400rpm. The metal ion solution was prepared at twice the desired concentration and added in equal parts to the stock solution of 2.0mM Aβ. This solution was vortexed at 2400rpm for 30sec and stored at 4°C for 18-22hr. Immediately prior to use, the solution was vortexed for 3sec at 2400rpm.

2.3. Surgical and invasive procedures.

2.3.1. Anaesthesia.

Rats used in Chapters 3 and 4 were anaesthetised with intraperitoneal (IP) injections of ketamine:xylazine (80:10mg/kg) or ketamine:xylazine:acepromazine (90:9:0.9mg/kg). Rats used in Chapters 5, 6 and 7 were anaesthetised with 3% halothane in carbogen via a face mask.

2.3.2. Intracortical injection.

Anaesthetised rats were placed in a stereotaxic head holder. Three or four burr holes were drilled in the left and right parietal bones to expose the underlying dura. Burr holes were made in the skull region that was 1.3-7.3mm posterior to bregma, and approximately 3.0-3.5mm lateral to the midline according to the stereotaxic coordinates of Paxinos and Watson (1982). Using stereotaxic guidance, a 26-gauge needle was lowered 1.5mm below the dura, and 1.0µl of either sterile saline or the experimental substance were injected through each burr hole into the gray matter of the parietal cortex, at a rate of 0.2µl per minute. The needle was kept in place for 1min after each injection to reduce backflow of the substance into the subarachnoid space.

2.3.3. Transcardial perfusion.

Rats were euthanased with sodium pentobarbitone (200mg/kg IP), and transcardially perfused with 4% paraformaldehyde in phosphate buffer (PB; 0.1M, pH 7.2). The brains were removed and fixed in paraformaldehyde for 4hr, and stored in PB at 4°C.

2.3.4. Cervical lavage.

A blunted disposable plastic transfer pipette containing a few drops of lukewarm water was inserted into the vagina of the rat. The water was slowly inserted into the vagina and was used to wash off the surface layer of cells. The cells were sucked up into the pipette and then smeared onto a gelatinised microscope slide and allowed to dry. The slide was incubated in a solution of 0.1% methylene blue for 2min and briefly rinsed in distilled water. After air-drying, the smear was coverslipped with Depex and viewed by bright-field microscopy (see section 7.2.2).

2.4. Detection of ferric iron.

2.4.1. Preparation of brain tissue.

The day after the animals were perfused, brains were sectioned coronally at 100µm on a vibratome. The sections were processed immediately.

2.4.2. Modified Perl's stain for the detection of ferric iron.

Sections to be labelled for ferric iron were stained with a modification of the Moos and Mollgard (1993) protocol of Perl's stain. Specific reagents are listed in Appendix 1.2. All solutions were prepared using water that was extensively filtered with multi-stage treatments to remove microbial, ionised, organic and particulate contaminants. Sections were incubated for 30min in 5% potassium ferrocyanide in PB, then incubated for another 30min in 5% potassium ferrocyanide + 1% HCl in PB, then washed for 20min in PB. Intensification of the Perl's reaction was performed with 3',3'-diaminobenzidine-nickel sulphate (DAB-Ni sulphate; 0.05%:0.01%). Sections were incubated for 15min in DAB-Ni sulphate, followed by two 15min incubations in DAB-Ni sulphate + H_2O_2 (0.005%), then washed three times in PB for 20min. The sections were partially dehydrated and mounted onto gelatinised slides, cleared in Histolene and coverslipped with Depex.

2.4.3. Determination of the intensity of iron label.

The amount of iron in the brain was determined on the basis of the intensity of ferric iron label. This was measured from digital micrographs taken with an Olympus DP-50 digital microscope camera attached to an Olympus Provis AX-60 microscope. To ensure consistent imaging conditions, the intensity of the light source was set at '4' and all filters were removed or disabled. The light was focussed so that the field iris diaphragm was sharp, and the aperture iris diaphragm lever was open. The light path was split so that half of the light went to the eyepiece and the other half to the digital camera. The image was viewed with a 10× objective and the magnification changer set at 1.6×. The region of the cortex analysed was located 1.3-3.8 mm posterior to bregma, 2.5-5.0 mm lateral to the midline and 1.0-2.5mm ventral to bregma according to the stereotaxic coordinates of Paxinos and W atson (1982). This is the cortical region where most of the data was obtained for this thesis (see section 2.7.1). Using the software application View Finder 1.0, the image was viewed on the computer screen and focussed. The image was captured at a resolution of 640×480 pixels, with an exposure time of 1/500sec and sensitivity set at 100ASA. The image was captured with the software application Studio Light 1.0 and saved as a JPEG file in 16 million colours at 100% quality. The image was opened in Adobe Photoshop 5.5, where a luminosity histogram was obtained for each captured image and the mean luminosity recorded. Luminosity levels have a range of 256, with '0' being the darkest possible colour

(black) and '256' being the lightest possible colour (white). Thus the lower the luminosity level, the more intense the iron label, and the greater the amount of iron that is present in the cortex.

2.5. Immunocytochemistry

2.5.1. Preparation of brain tissue.

Brains were sectioned coronally at 100µm on a vibratome. Sections were post-fixed in 4% paraformaldehyde for 30min, and then washed three times in PB for 20min each.

2.5.2. Standard immunocytochemistry protocol.

The protocol previously used in the laboratory (Robinson et al., 1995) was modified to develop a faster protocol. Specific reagents are listed in Appendix 1.3. Free-floating tissue sections were incubated for 3hr in a solution of 1% bovine serum albumin (BSA) + 1% Triton-X + 1% ethanolamine in phosphate-buffered saline (PBS; 0.1M, pH 7.4) and then washed in PBS (3 ×20min). Sections were incubated in primary antibody diluted in 1% BSA + 0.5% Triton-X + 0.05% sodium azide in PBS for 18hr at 37°C, and then given three 20min PBS washes. Sections were then incubated at 37°C for 3hr in secondary antibody diluted to a concentration of 1:300 in 1% BSA in PBS. Sections were given three 20min PBS washes, and then incubated for 3hr at 37°C in streptavidin-horseradish peroxidase complex (Amersham; 1:300 in 1% BSA) and washed in PBS, three times for 20min each. Sections were incubated for 10min in DAB-Ni sulphate, for 10min in DAB-Ni sulphate + H_2O_2 (0.005%), and then washed three times in PB for 20min each. Sections were dehydrated, mounted onto gelatinised slides, cleared in Histolene and coverslipped with Depex.

To recognise a specific antigen, an appropriate primary antibody was applied. Each antibody system is outlined below and summarised in Appendix 1.4.

2.5.3. Ferritin immunocytochemistry.

For ferritin immunocytochemistry, the primary antibody was rabbit anti-human L-chain ferritin (ICN), which was diluted to a concentration of 1:2500. The secondary antibody was biotinylated donkey anti-rabbit Ig (Amersham).

2.5.4. Aβ immunocytochemistry.

To perform Aβ immunocytochemistry on injection sites containing human Aβ1-40 or human Aβ1-42, sections were first pre-treated with concentrated formic acid for 5 min, and then given three 20min PBS washes. The sections were processed using the primary antibody mouse anti-human Aβ8-17 (Dako), which was diluted to a concentration of 1:200. The secondary antibody was biotinylated sheep anti-mouse Ig (Amersham).

To perform Aβ immunocytochemistry on injection sites containing rat Aβ1-40, sections were processed using the primary antibody rabbit anti-human Aβ1-40 (Sigma), which was diluted to a concentration of 1:10000. The secondary antibody was biotinylated donkey anti-rabbit Ig (Amersham).

2.5.4.1. Electronmicroscopic analysis of Aβ deposits for the detection of fibrils.

Injection sites containing Aβ peptides were immunolabelled for Aβ peptide, trimmed from the coronal section, and then embedded in Durcupan. Semithin sections were cut longitudinally through the injection sites at 2μm and stained with Toluidine blue (pH 9.0) to localise the Aβ deposits with the light microscope. Ultra-thin sections (70nm) were stained with uranyl acetate and lead citrate, and examined with a Joel 1200EX transmission electron microscope. To examine fibrils within the Aβ deposits, sections were examined using 100 kV intensity at a magnification of 68,000×.

2.5.5. Double-label immunocytochemistry for Aβ peptide and ferritin.

Sections were first pre-treated with concentrated formic acid for 5min, and then processed for ferritin immunocytochemistry as in section 2.5.3, except the primary antibody was used at a concentration of 1:1000. Immunolabelling for Aβ was performed as described above, except streptavidin-horseradish peroxidase complex was substituted for streptavidin-alkaline phosphatase complex (Vector Laboratories; 1:300 in 1% BSA in PBS). Following incubation for 3hr at 37°C, sections were washed twice in PBS and twice in Tris-HCl buffer (0.1M, pH 8.2) for 20min each and then processed with a Vector Red Substrate Kit (Vector Laboratories), giving Aβ deposits a translucent red colour. Sections were given three 20min washes in Tris-HCl buffer, and then were immediately dehydrated, mounted onto gelatinised slides, cleared in histolene and coverslipped with Depex.

2.6. Detection of neurodegeneration.

2.6.1. Preparation of brain tissue.

Brains were sectioned coronally at 100μm on a vibratome. Sections were post-fixed in 4% paraformaldehyde for 30min, and then washed three times in PB for 20min each. Sections were dehydrated with 70% ethanol for 15min, mounted onto gelatinised slides, and allowed to dry.

2.6.2. Fluoro-Jade staining.

The detection of dying neurons was performed by staining sections with Fluoro-Jade using a modification of the technique described by Schmued and coworkers (1997). Specific reagents are listed in Appendix 1.5. Slides were immersed in 100% ethanol for 3min, 70% ethanol for 1min, and distilled water for 1min. Sections were placed in 0.06% potassium permanganate for 15min, and rinsed in distilled water for 1min. Labelling occurred when sections were incubated for 30min in 0.0005% Fluoro-Jade (Histo-Chem, AR) diluted in 0.1% acetic acid. Sections were then given three 2min rinses in distilled water before being rapidly dried on a hotplate, cleared in Histolene and coverslipped with Depex. Stained sections were subsequently examined with a fluorescein (FITC) filter system by epifluorescence microscopy.

2.6.3. Haematoxylin and eosin counterstaining.

Sections to be counterstained with hematoxylin and eosin (H&E) were first stained with Fluoro-Jade and the labelled cells were counted and imaged with confocal microscopy. The coverslips and Depex residues were removed with Histolene, and the slides were immersed in descending concentrations of ethanol (100%, 90%, 70%, 50%) and then dried. Sections were immersed in water for 2min, Mayers hematoxylin for 20min, and rinsed quickly in water. Slides were then immersed in Scotts blue for 90sec, rinsed in water for 3min, and put into 70% ethanol for 1min. Sections were stained with eosin for 3min, then immersed three times in 100% ethanol for 2min each, cleared in Histolene and coverslipped with Depex.

2.7. Microscopic analysis of injection sites.

2.7.1. Exclusion criteria.

Injection sites were excluded from analysis if they: i) showed evidence of mechanical damage; ii) contained appreciable quantities of red blood cells; iii) penetrated the corpus callosum; or iv) were shallower than the length of the bevel on the tip of the needle (Figure 2.1). The injection sites that were analysable were mostly located within the region of the cortex that was 1.3-3.8mm posterior to bregma. Injection sites that were further posterior were often excluded by the criteria, probably due the rostral portion of the parietal bone being slightly thicker than the caudal portion. The thicker parietal bone may have absorbed some of the heat and pressure of the drill and minimised the amount of damage that was produced. Injection sites that were performed in the rostral region of the parietal cortex were also less likely to penetrate into the corpus callosum because the thickness of the cortex is greater in this region than in the caudal portion.

2.7.2. Qualitative observations.

Injection sites labelled for ferric iron, ferritin, H&E or Aβ peptide were examined using bright-field microscopy on an Olympus BH-2 microscope.

2.7.3. Quantitative analysis of ferritin-immunolabelled injection sites.

Ferritin-immunolabelled sections were examined using an Olympus BH-2 light microscope. The injection tract for each substance was visible on at least three serial sections. On each section, all ferritin-labelled cells were counted using an eyepiece graticule and a 20× objective. During each injection, the needle was lowered exactly 1.5mm below the dura into the cortex, however upon examination of the processed tissue, it was evident that the injection tracts had a variable depth. The depth of the injection tract was determined as the distance below the pial surface to which the needle penetrated the cortex. For instance, in the study reported in Chapter 3, saline injection sites had a mean depth of 0.67±0.15mm, ferric ammonium citrate injection sites had a mean depth of 0.84±0.19mm, and ammonium citrate injection sites had a mean depth of 0.76±0.20mm. To overcome the minor variability in injection depth, the number of ferritin-labelled cells (N_f) per mm depth of injection tract was calculated:

$$N_f = \frac{\text{Total number of labelled cells}}{\text{depth of injection tract (mm)}}$$

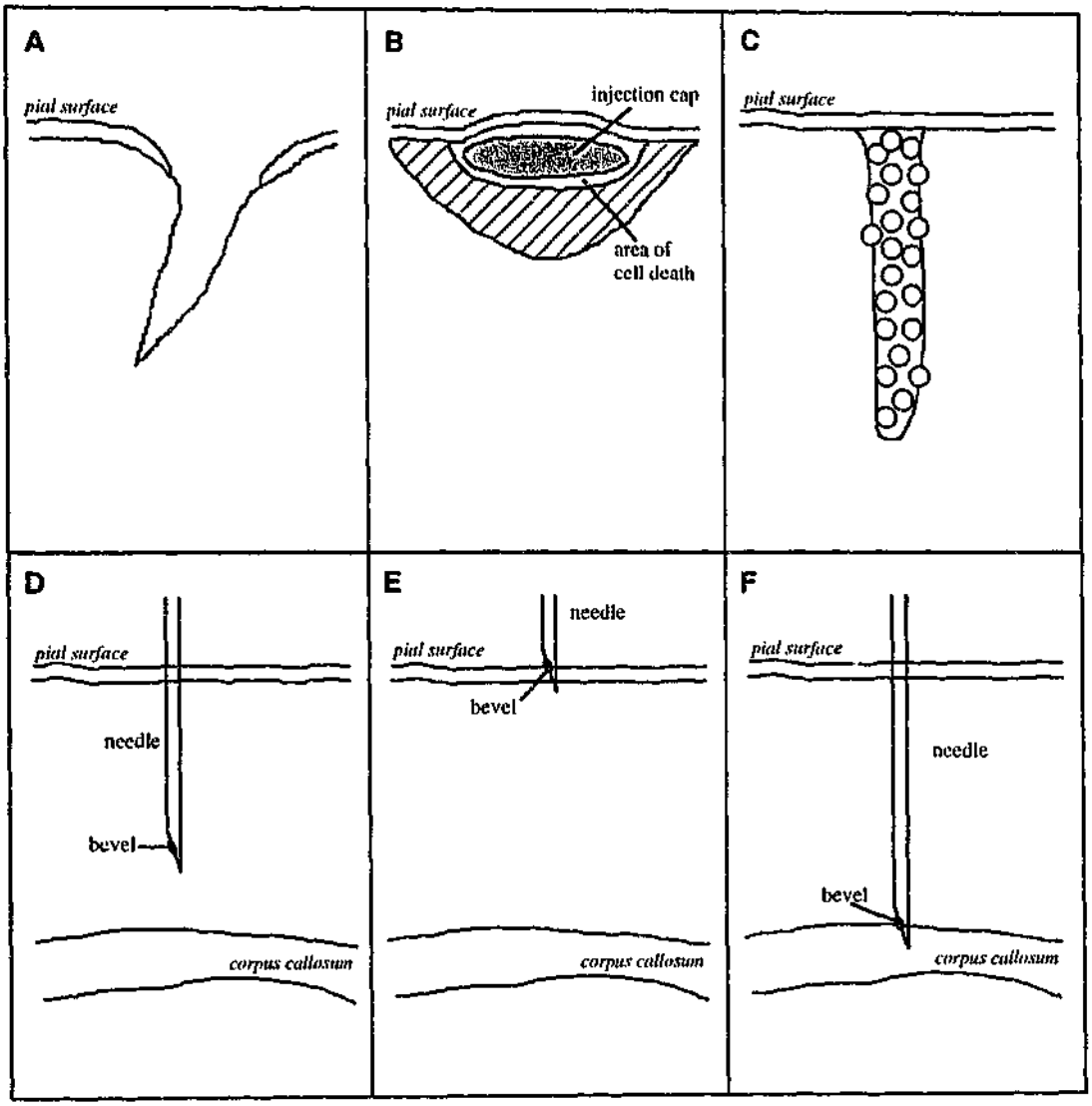

Figure 2.1. Exclusion criteria for analysis of injection sites.
Injection sites were excluded from the analysis if they experienced trauma, eg. tearing caused by the needle (A), damage by the drill (B), or if they contained red blood cells (C). Injection sites were analysed if the needle penetrated below the pial surface and did not penetrate the corpus callosum (D), and were rejected if they were too shallow (E) or too deep (F).

Stereological counting methods are often an accurate way to estimate total cell number from a small sample of the population. However, such techniques are unreliable if the cells of interest have a highly non-uniform or variable distribution, like those around injection sites in the present study. Therefore, every labelled cell around the injection site was counted. This approach avoids the need to estimate cell number, and consequently it is more accurate than stereological methods. For each injection site, the number of ferritin-labelled cells on each serial section was counted, and the section with the highest number of labelled cells was used in the analysis.

2.7.4. Quantitative analysis of Fluoro-Jade-stained injection sites.

2.7.4.1. Chapters 3 and 4.

Sections stained with Fluoro-Jade were examined using an Olympus BH-2 epifluorescence microscope with an FITC filter. The injection tract for each substance was visible on at least three serial sections. The total number of Fluoro-Jade-labelled neurons at each injection site were counted using a 20× objective and an eyepiece graticule. The depth of the injection tract was determined as the depth to which the needle penetrated the cortex. For instance, in the study reported in Chapter 3, saline injection sites had a mean depth of 0.82±0.18mm, ferric ammonium citrate injection sites had a mean depth of 0.90±0.18mm, and ammonium citrate injection sites had a mean depth of 0.82±0.17mm. To overcome the minor variability in injection depth, the number of Fluoro-Jade-labelled cells (N_f) per mm depth of injection tract was calculated:

$$N_f = \frac{\text{Total number of labelled cells}}{\text{depth of injection tract (mm)}}$$

For each injection site, the number of Fluoro-Jade-labelled cells on each serial section was counted, and the section with the highest number of labelled cells was used in the analysis. As described for ferritin-labelled cells in section 2.7.3, this method has a greater accuracy than stereological counting methods because every Fluoro-Jade-labelled cell is counted.

2.7.4.2. Chapters 5, 6 and 7.

The method of analysis of Fluoro-Jade-stained injection sites was refined for studies described in the later chapters of this thesis. While the analysis was similar to that described in section 2.7.4.1, some refinements were made to improve the protocol. A

small and unavoidable amount of mechanical and thermal damage is often seen directly below the pial surface due to drilling of the skull in preparation for the injection. To exclude neuronal loss resulting from drill damage, the most superficial 400µm of tissue at the injection site was excluded from analysis. Thus starting from 400µm below the pial surface, every Fluoro-Jade-labelled neuron in the injection site was counted. Despite the needle having been stereotaxically lowered to the same depth, histological examination revealed variability in the final depth of the injection tract in some brains. To limit excessive variability, injection depths that were outside of the range of 1.3±0.5mm were excluded from the analysis. To control for the variability of injection tract depth, the number of degenerating neurons per mm injection tract was determined (N_f).

$$N_f = \frac{\text{number of Fluoro-Jade-labelled neurons}}{\text{depth of injection tract (mm)}}$$

All sections passing through the injection site were assessed as above, and the section with the greatest number of degenerating neurons per mm injection tract was chosen for each injection site. If there was more than one analysable injection site for the experimental or control substance in a particular animal, the number of degenerating neurons was averaged over these sites. To control for inter-animal variability, the average number of degenerating neurons at experimental injection sites were expressed as a percentage of the average number of degenerating neurons at the contralateral saline injection sites in that animal.

$$\% \text{ Saline} = \frac{N_f \text{ (experimental substance)}}{N_f \text{ (saline)}} \times 100$$

The neuronal loss associated with saline injection sites is the combined result of mechanical damage due to the injection procedure and osmotic or pressure effects caused by the saline solution. Therefore, the saline values represent the baseline against which the toxicity of experimental substances can be compared. Thus, substances that have the same degree of toxicity as saline have a mean of 100%, whereas substances which kill twice as many neurons have a mean of 200% and those that kill half as many neurons have a mean of 50%.

2.7.5. Sections counterstained with H&E.

Dying neurons that were basophilic and shrunken in size in H&E-stained injection sites were counted and the numbers obtained were corrected for depth in the same manner as

for the Fluoro-Jade-stained sections. To ensure that glial cells or healthy neurons were excluded from the counts, control regions lateral to the injection site were also examined for basophilic profiles. The number of profiles within a control region of equivalent volume to the injection site was then subtracted from the total cell count that was found within the injection site. The number of profiles seen at each injection site was then expressed per mm depth of injection tract (as for Fluoro-Jade in section 2.7.4.1).

2.7.6. Quantitative analysis of the volume of Aβ deposits.

Using a drawing tube, the area of the Aβ deposit on each 100μm section passing through the injection site was traced, and the areas on all of the sections through the injection site were summed to calculate the total volume of the deposit.

2.7.7. Photomicrographs.

Digital micrographs were taken using an Olympus Provis AX-60 microscope that was fitted for bright-field and epifluorescence microscopy, and had an Olympus DP-50 digital camera attached. The digital images were imported into Adobe Photoshop 5.5 where they were adjusted for colour balance and contrast. The pictures were then typeset in Adobe Illustrator 9.0 where they were prepared as complete figures, and were printed on an Epson Stylus Photo 870 colour printer with a resolution of 1440dpi. In Figure 3.4, Fluoro-Jade images were taken on a confocal microscope, and then treated as the other photomicrographs.

2.8. Statistical analysis.

2.8.1. Chapters 3 and 4.

Statistical analysis was performed on data pooled from five injection sites for each substance, with these sites being obtained from at least three different animals. For statistical purposes, the numbers of cells at an injection site were assumed to be independent of those at other injection sites. Independent samples t-tests were performed, and statistical significance was determined at $\alpha \leq 0.05$.

2.8.2. Chapters 5 and 6.

Eight animals that passed the exclusion criteria were obtained for each experimental substance, with half of the animals receiving injections of saline vehicle in the left hemisphere, and the other half in the right hemisphere. Box-plot analysis was used to ensure that extreme outliers were not present in any of the groups. To determine if the number of degenerating neurons at an experimental injection site differed from the saline vehicle, a 2-tailed paired-samples t-test was performed, with the statistical significance determined as $\alpha=0.05$. To compare the neurotoxicity of different experimental substances, 2-tailed independent-samples t-tests were performed, with the statistical significance set at $\alpha=0.05$.

CHAPTER 3:

Quantitative analysis of neuronal loss and ferritin expression in response to intracortical injection of iron.

3.1. Introduction.

The reactivity of iron in most living tissues is harnessed for cellular energy production and also contributes to the activity of many proteins and mitochondrial enzymes. However, when iron is unbound in the presence of oxygen, it catalyses the generation of toxic hydroxyl radicals (Halliwell and Gutteridge, 1999), presenting a significant problem for the brain, which has a higher iron content than most organs (Hallgren and Sourander, 1958), and whose function depends on the integrity of neuronal membranes that are rich in oxidisable lipids.

The neurotoxicity of unbound iron has been widely established. The addition of iron to cultures of primary neurons causes peroxidative injury and neurodegeneration (Hutter-Paier et al., 1998; Kim et al., 1999; Pike et al., 1997; White et al., 1999; Zhang et al., 1993), but iron is less toxic to cultured glial cells (Swaiman and Machen, 1990). Indeed, oligodendrocytes respond to iron by synthesizing ferritin, an intracellular iron storage protein, and this presumably helps these cells to sequester iron and protects them from peroxidation (Qi et al., 1995). Similar findings have been made *in vivo*. Thus, injection of ferrous iron into the cerebral cortices of rats causes lipid peroxidation within 15 minutes and neuronal death five days later (Willmore and Rubin, 1982). Iron injections into the substantia nigra cause neurodegeneration, disruption of dopamine metabolism and lipid peroxidation (Ben-Shachar and Youdim, 1991; Rauhala et al., 1998; Sengstock et al., 1992; Sengstock et al., 1993; Sziraki et al., 1998). The effects of iron on glial cells *in vivo* do not appear to have been described.

To limit its neurotoxicity, iron is normally bound and inactivated by transport proteins (eg. transferrin) and intracellular storage proteins (eg. ferritin). However, certain pathological conditions result in the presence of unbound iron in the brain. One such condition is intracerebral haemorrhage in which red blood cells, rich in haemoglobin, are released into the neuropil. The heme from these cells is cleaved to biliverdin by heme oxygenase in astrocytes and microglia, releasing iron (e.g. Turner et al., 1998). The iron released from heme is highly toxic to neurons but not to glia (Regan and Panter, 1993). An *in vitro* study has demonstrated that hemin induces ferritin expression in oligodendrocytes (Qi et al., 1995), while *in vivo* studies have shown that whole blood and haemoglobin induce both ferritin expression and iron accumulation in microglia (e.g. Koeppen et al., 1995).

Most of the non-heme iron in the brain is bound to ferritin as Fe^{3+}, and can only be released after being reduced to Fe^{2+}. The reduction and release of iron from ferritin can be accomplished by superoxide, acidic pH, ascorbate and catecholamines (Allen et al., 1994; Biemond et al., 1988), all of which are abundant in the extracellular fluid of the brain, particularly during hypoxia-ischaemia. The effects of hypoxia-ischaemia on neurons and glia resemble those seen with iron. Thus, hypoxia induces the expression of ferritin in cultured oligodendrocytes (Qi et al., 1995), while *in vivo* models of hypoxic-ischaemic injury in cerebral cortex and hippocampus have shown that neuronal death in the affected area is accompanied by an increased expression of iron and ferritin in microglial cells (Ishimaru et al., 1996; Kondo et al., 1995; Palmer et al., 1999).

The studies mentioned above indicate that iron released from ferritin, transferrin or haemoglobin may contribute to the neurodegeneration that occurs in brain tissues after reperfusion or return to normoxia (Oubidar et al., 1994; Qi et al., 1995). This notion gains support from evidence that the administration of iron chelators, such as desferrioxamine, can reduce hypoxic-ischaemic damage (Karwatowska-Prokopczuk et al., 1992; Paller and Hedlund, 1994; Palmer et al., 1994).

Despite the relevance of unbound iron to brain injury, remarkably little quantitative data is available concerning the spatio-temporal patterns of neuronal death or of ferritin expression that result from exposure of the cerebral cortex to pathologically relevant concentrations of iron. Such data is needed, since it could provide a clearer delineation of the therapeutic window that is available for the treatment of iron-induced brain injury, and it would provide valuable benchmark data against which potential neuroprotective agents could be compared.

The present study has obtained such data after injecting small quantities of ferric iron into the parietal cortices of rats. The mean concentration of iron in serum is approximately 9-30μM, and this is largely due to the iron that is bound to transferrin. In whole human blood, however, the mean concentration of iron is approximately 8.5mM (0.5mg/ml, Triggs and Willmore, 1984), due to the presence of iron contained within hemoglobin. The concentration of non-heme iron in the human parietal cortex is approximately 0.65mM (3.81mg/100g fresh weight, Hallgren and Sourander, 1958), and this is almost identical to that seen in rat parietal cortex (approximately 4mg/100g fresh weight, Focht et al., 1997). Assuming that a significant proportion of the iron from these

two sources will be unbound following hypoxia-ischaemia, a concentration within this range was used (1mM iron). Neuronal loss at the site of injection was quantitatively assessed using the marker Fluoro-Jade. To determine the extent to which exogenous iron stimulates ferritin expression *in vivo*, immunocytochemistry was used to reveal cells containing ferritin. The distribution of bound ferric iron was revealed by a modified Perl's stain.

3.2. Materials and methods.

3.2.1. Animals.

Female Wistar rats aged 9-13 weeks, n=58, were obtained from The University of Queensland Central Animal Breeding House, Perth Animal Resources Centre or Monash University Animal Services.

3.2.2. Substances injected.

Ferric ammonium citrate (ICN) and ammonium citrate (Sigma) were prepared as described in 2.2.1. Sterile saline was also injected as the vehicle control.

3.2.3. Intracortical injection of iron.

Rats were anaesthetised as described in section 2.3.1, and given intracortical injections as described in section 2.3.2. Rats were euthanased after 1, 3, 5, or 7 days, and perfused as described in section 2.3.3. Injection sites were labelled with a modified Perl's stain for the detection of ferric iron, were processed for free-floating immunocytochemistry to reveal ferritin-labelled cells, or were stained with Fluoro-Jade (to detect degenerating neurons) and then counterstained with hematoxylin and eosin (H&E).

3.2.4. Modified Perl's stain for the detection of ferric iron.

Sections to be labelled for ferric iron were stained immediately after sectioning as described in section 2.4.2.

3.2.5. Ferritin immunocytochemistry for the detection of activated microglia and macrophages.

Sections to be labelled for ferritin were processed as described in section 2.5.3.

3.2.6. Fluoro-Jade staining for the detection of neurodegeneration.

The detection of degenerating neurons was performed by staining sections with Fluoro-Jade as described in section 2.6.2.

3.2.7. Hematoxylin and eosin counterstaining of Fluoro-Jade-stained tissue.

Sections were first stained with Fluoro-Jade and the labelled cells were counted and imaged with confocal microscopy. Sections were then processed as described in section 2.6.3.

3.2.8. Microscopic analysis.

Ferritin-immunolabelled sections were examined as described in section 2.7.3.

Sections stained with Fluoro-Jade were analysed as described in section 2.7.2.1.

Injection sites that were stained with Fluoro-Jade were counterstained with H&E and were then examined using light microscopy. The H&E-stained injection sites were compared to confocal images of Fluoro-Jade staining that had been prepared prior to counterstaining. Landmarks such as blood vessels were used to determine the precise location of the labelled cells between the two images. Dying neurons that were basophilic and shrunken in size in H&E-stained injection sites were counted as described in section 2.7.5.

3.2.9. Statistical analysis.

Statistical analysis was performed as described in section 2.8.1. When comparing ferric ammonium citrate injections to control injections, 1-tailed independent samples t-tests were performed since it was predicted that ferric ammonium citrate would induce more ferritin-labelled cells and more Fluoro-Jade-labelled cells than either ammonium citrate or saline.

3.3. Results.

The quantitative data and statistical analysis presented in this chapter are summarised in Appendix 2.

3.3.1. Detection of intracellular ferric iron.

A modified Perl's stain was used to detect ferric iron in tissue sections. In normal cortex this technique lightly labels a subpopulation of neurons and provides intense labelling of occasional ramified microglial cells. At 1 day post-injection, the only iron-rich cells associated with saline and ammonium citrate injection tracts were a small number of red blood cells (Figure 3.1A). In contrast, ferric ammonium citrate injection sites had lightly-stained iron-containing cells along the injection tract and in the area surrounding it (Figure 3.1B,C). By 3 days post-injection, ferric ammonium citrate injection sites had many iron-rich cells near the injection tract and also in the pial surface directly above the injection tract (Figure 3.1E). These cells had an amoeboid profile that is characteristic of activated microglia or macrophages (Figure 3.1F). Diffuse extracellular labelling was also seen at the site of injection, but was not visible elsewhere in the section. Saline and ammonium citrate injection sites contained some iron-rich cells at 3 days after injection, but they were less numerous and were confined to the immediate vicinity of the needle tract (Figure 3.1D). At both 5 and 7 days post-injection, iron-rich cells were present around injection sites in a similar manner to that seen after 3 days, except that the extent of iron labelling was greater at the later survival times (Figure 3.1G,H). The morphology of the iron-rich cells was less reactive, with many cells expressing processes (Figure 3.1I). Small particulate deposits of extracellular iron were frequent at these later survival times, and were dispersed through the neuropil (Figure 3.1I, inset).

3.3.2. Detection of ferritin-labelled cells around injection sites.

In grey matter of normal cortex, ferritin immunocytochemistry labels occasional ramified microglial cells, but other cell types are unlabelled. However, 1 day after injection, small ferritin-labelled cells that may be neutrophils, were seen at the injection sites for all substances. A diffuse extracellular labelling of ferritin at the injection sites was also seen at 1 day. The morphology of the labelled cells changed after 3 days survival, with many amoeboid cells being present (Figure 3.2F). The morphology of

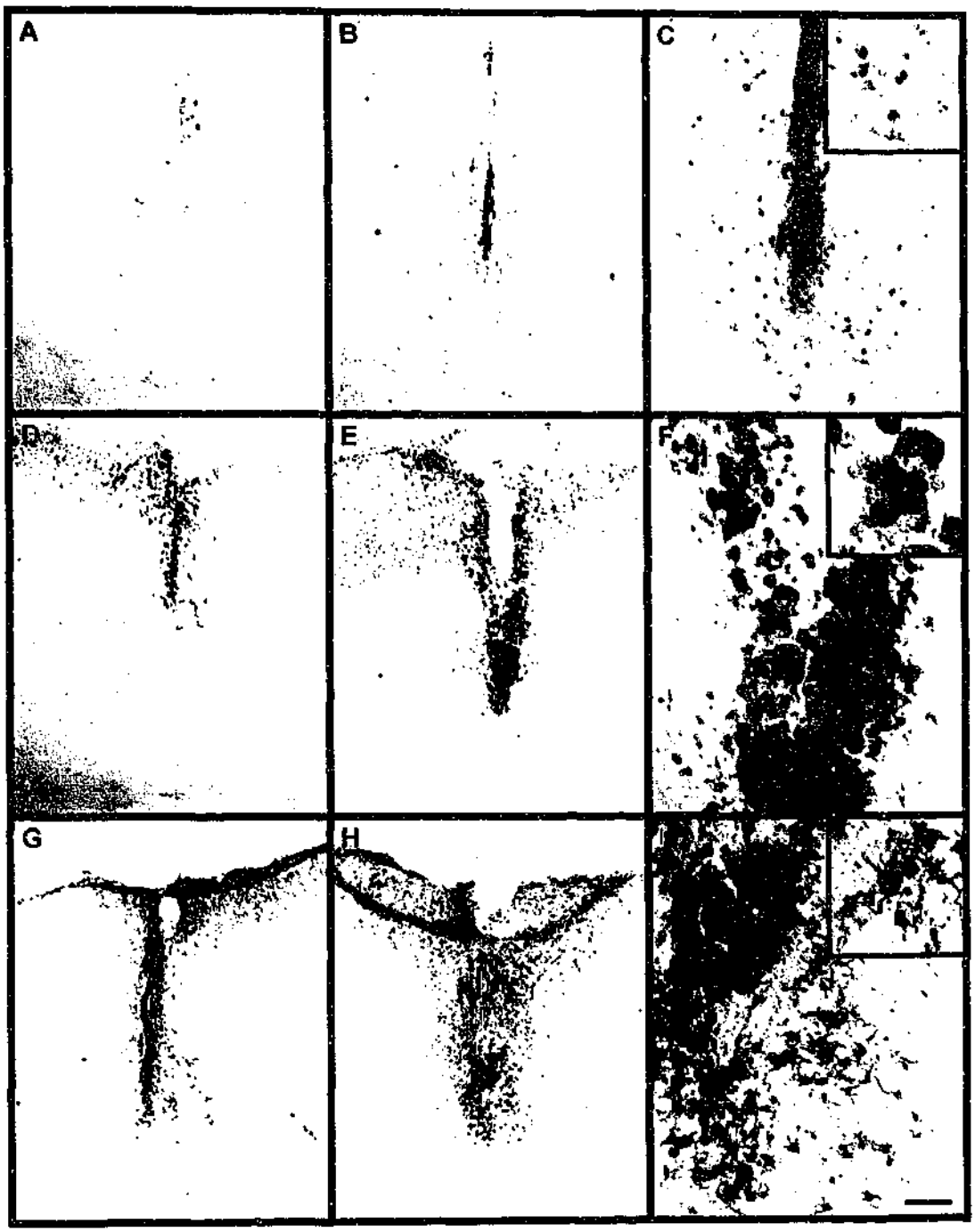

Figure 3.1. Detection of ferric iron at injection sites containing ferric ammonium citrate.

Transverse sections through parietal cortices of rats showing injection sites that have been stained with a modified Perl's technique to demonstrate bound ferric iron. Ammonium citrate injection after 1 (A), 3 (D) or 7 days (G), and ferric ammonium citrate injection sites 1 (B,C), 3 (E,F) or 7 days (H,I) after injection. After 1 day, labelled cells are only present around ferric ammonium citrate injection sites (B), but after 3 days there are labelled cells around injection sites of all substances (D,E). Iron-containing cells are highly amoeboid around ferric ammonium citrate injections, after both 1 (C, inset) and 3 days, but they are much larger 3 days after injection (F, inset). After 7 days, iron-containing cells are still present around the injection sites of all substances (G,H), however some of the cells have a less reactive morphology and small particulate deposits are evident in the neuropil (I, inset). Scale bar = 200μM (A,B,D,E,G,H); 50μM (C,F,I); 25μM (inset C,F,I).

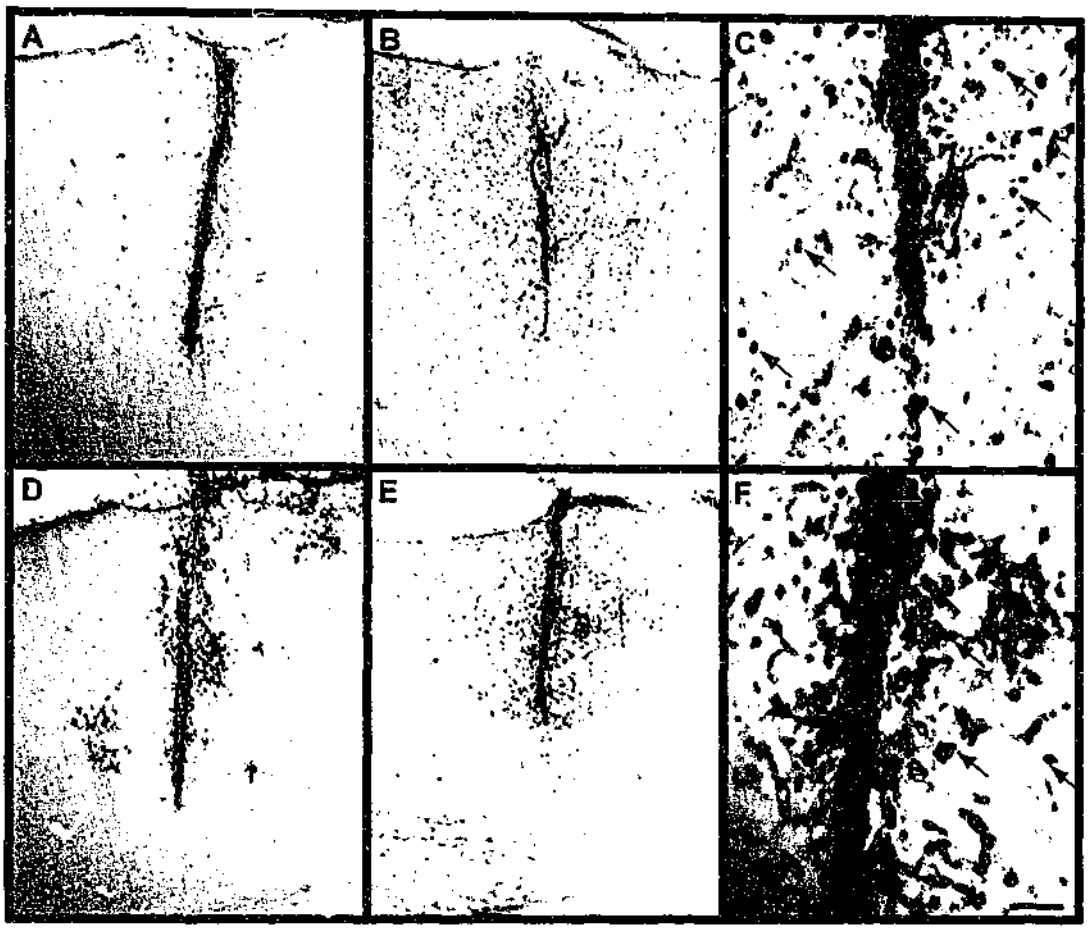

Figure 3.2. Ferritin immunolabelling of injection sites containing ferric ammonium citrate.
Ammonium citrate injection sites 1 (A) or 3 days (D) after injection, and ferric ammonium citrate injection sites after 1 (B,C) or 3 days (E,F) survival. There is a restricted labelling of ferritin-positive cells around ammonium citrate (A) injections 1 day after injection, yet ferric ammonium citrate injections induce greater numbers of ferritin-labelled cells (B). Ferritin labelling increases around control injections (D) after 3 days, but not around ferric ammonium citrate injections (E). Most ferritin-labelled cells have an amoeboid morphology characteristic of phagocytic microglia (C,F; arrows). Scale bar = 200μM (A,B,D,E); 50μM (C,F).

these cells resembled activated microglia and macrophages (Grundke-Iqbal et al., 1990). Foamy macrophages and oligodendrocytes were sometimes seen at injection sites. Five and seven days after injection, most labelled cells had branched dendritic processes typical of ramified microglia. Counts of labelled cells at each time point revealed a relatively small degree of variability for each substance injected, as indicated by the error bars in Figure 3.3A.

One day after the injection of saline, an average of 79±9 (mean±SE) ferritin-rich cells were associated with each injection site, with a similar number (71±24) being seen around ammonium citrate injection sites (Figure 3.3A). By contrast, the number produced by injection of ferric ammonium citrate (565±78) was 8-fold greater than around ammonium citrate injection sites. By three days post-injection, the number of ferritin-labelled cells had increased almost 4-fold around the saline injection sites to give an average of 306±36. Ammonium citrate injections showed a similar increase, producing 360±29 labelled cells. The number of ferritin-labelled cells at ferric ammonium citrate injection sites did not increase greatly between one and three days, so that by three days post-injection they had a mean of 638±104 labelled cells, twice as many as at ammonium citrate or saline injection sites. For the three substances examined, the mean number of ferritin-positive cells remained stable between three and seven days post-injection (Figure 3.3A). The number of ferritin-labelled cells around saline and ammonium citrate injections did not differ at 7 days after injection, however there were significantly more labelled cells around ferric ammonium citrate injection sites than around saline injection sites ($t(8)=2.148$, $p=0.032$, 1-tailed t-test). Only the 7 days survival time was examined statistically, since the other time points exhibited an even greater difference between ferric ammonium citrate injection sites and saline or ammonium citrate injection sites (see Figure 3.3A).

3.3.3. Fluoro-Jade labelling as a marker of neurodegeneration.

When sections were viewed at low magnification (Figure 3.4A), Fluoro-Jade labelling was visible as small white dots in and around the injection tracts. When examined at high magnification (Figure 3.4B) each of these "dots" corresponded to a neuronal soma, usually in conjunction with its apical dendrite. Background labelling of tissue was low, and the neurodegeneration associated with the injection tract was visually distinct from the surrounding neuropil. The injection sites normally spanned most of the cortical

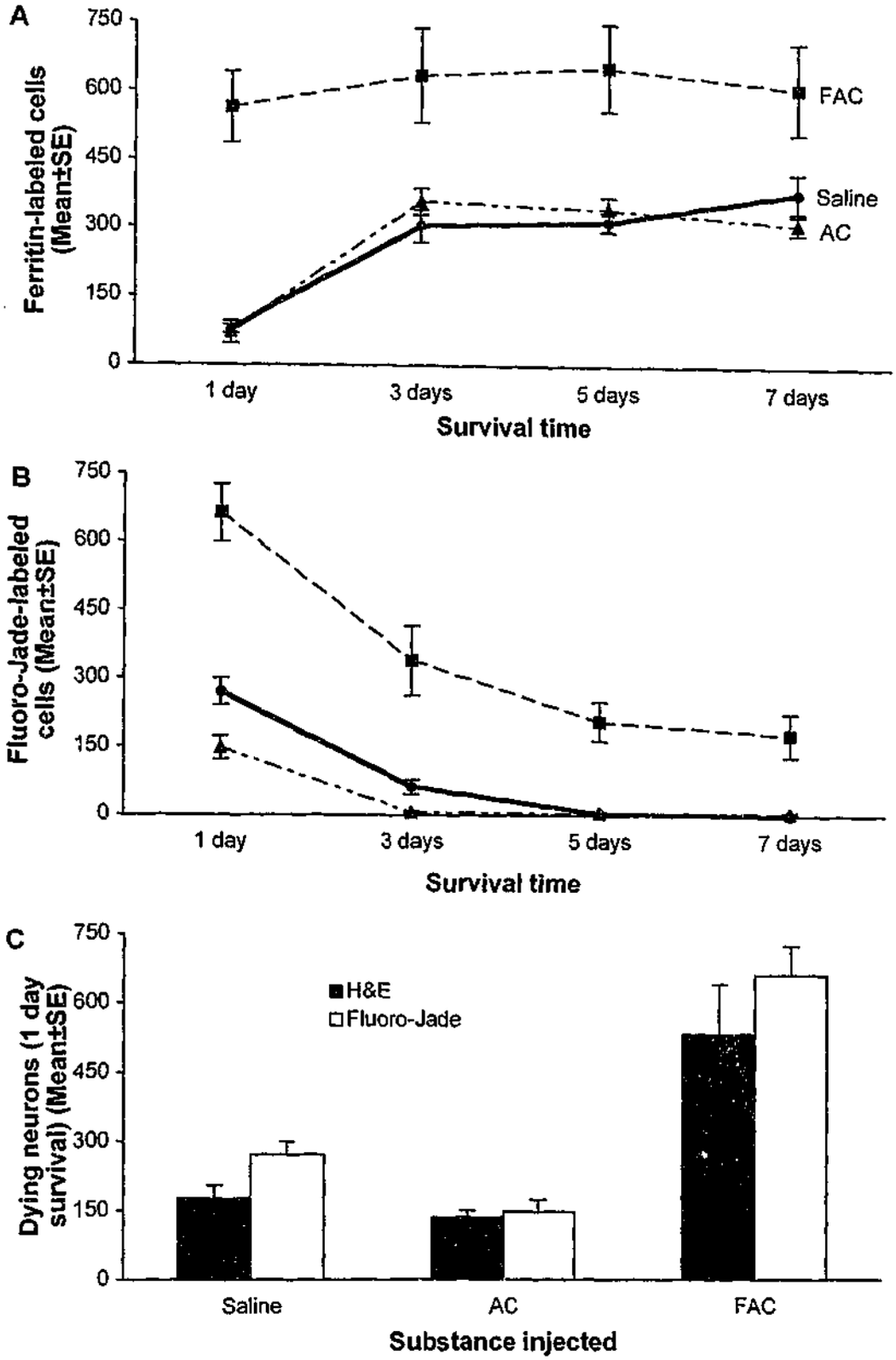

Figure 3.3. Quantitative analysis of ferric ammonium citrate injection sites. The mean number of ferritin-immunolabelled cells for each injected substance (A); and the mean number of degenerating neurons as detected by Fluoro-Jade labelling (B). Comparison between Fluoro-Jade labelling and H&E counterstaining for the detection of neurodegeneration around injection sites 1 day after injection (C). Error bars represent the standard error of the mean. FAC=ferric ammonium citrate; AC=ammonium citrate.

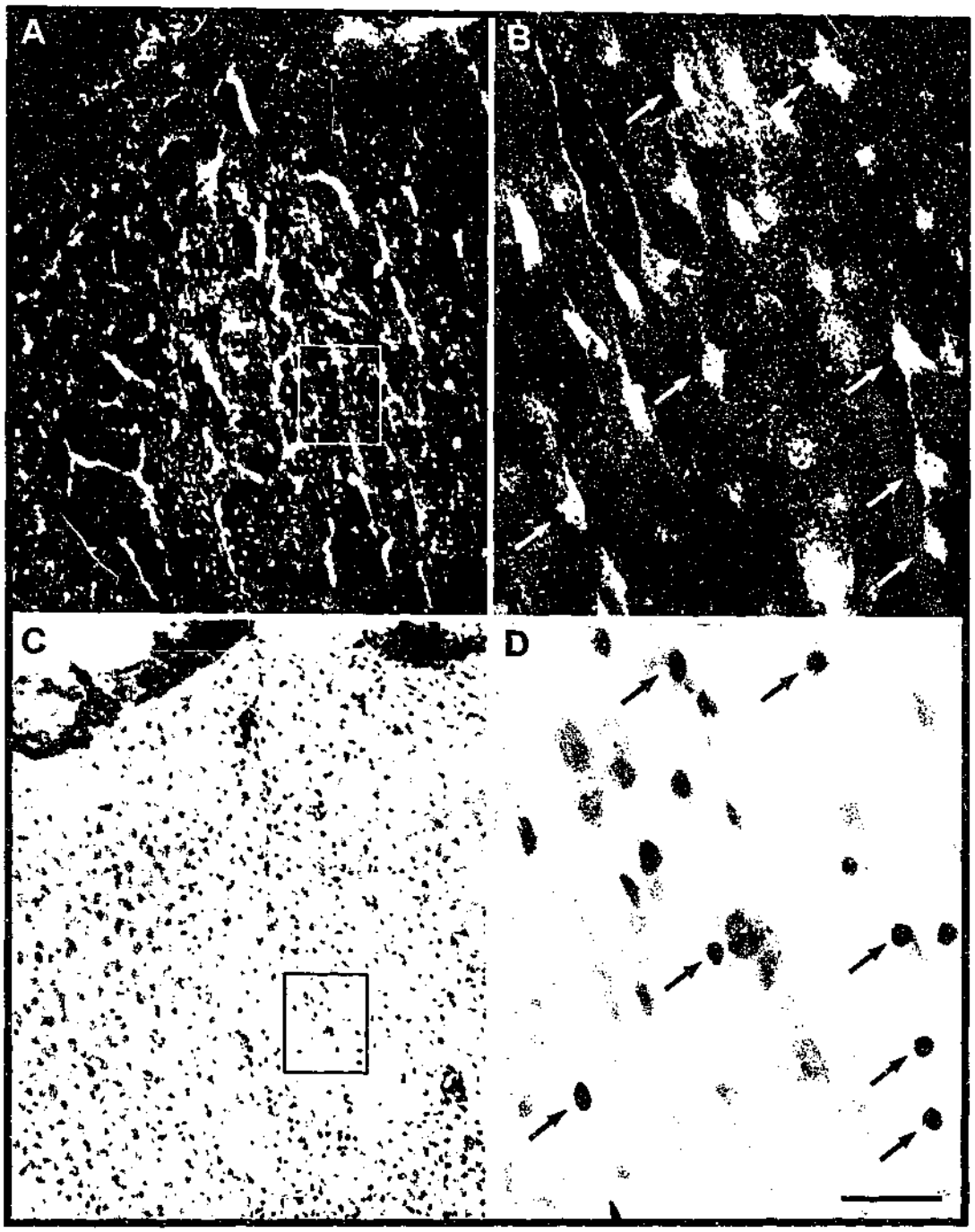

Figure 3.4. Comparison of Fluoro-Jade labelling and H&E counterstaining. Neurodegeneration around an injection site 1 day after injection of saline as detected by Fluoro-Jade labelling (A,B) or H&E counterstaining (C,D). Panels B and D are enlargements of the boxed regions in panels A and C. Degenerating neurons stained by Fluoro-Jade (B; arrows) correspond to the dying and injured neurons that stain intensely with H&E (D; arrows). Scale bar = 150μM (A,C); 25μM (B,D).

layers of the gray matter, and both large and small neurons were seen around each injection tract, their size depending mostly on their location within a cortical layer. Fluoro-Jade-labelled neurons at some injection sites were repeatedly counted by the same investigator and they were also counted 'blind' by two other investigators. The resulting estimates were compared and found to be within +/-5% of the mean.

To assess whether Fluoro-Jade reliably labels degenerating neurons, injection sites were photographed on a confocal microscope then counterstained with H&E. This counterstaining revealed dying neurons near the injection tracts, but it also showed healthy neurons in and around the injection tracts. When photomicrographs of the H&E stained injection sites were compared with the corresponding confocal images, it was evident that the Fluoro-Jade had labelled neurons which are either degenerating or injured (Figure 3.4). Healthy neurons that stained lightly with H&E were not labelled with Fluoro-Jade, confirming the selectivity of this marker.

3.3.4. Quantification of Fluoro-Jade-labelled neurons around injection sites.

Fluoro-Jade-labelled neurons were observed in the vicinity of saline and ammonium citrate injection tracts (Figure 3.5A,B,D,E), but they were more restricted in distribution and less numerous than those associated with injections of ferric ammonium citrate (Figure 3.5C,F). Counts of labelled cells at each time point revealed a relatively small degree of variability for each substance injected, as indicated by the error bars in Figure 3.3B.

After 1 day survival, 271±29 Fluoro-Jade-labelled neurons were observed around saline injection sites, while ammonium citrate injection sites had around half this number (148±26; $t(8)=3.217$, $p=0.012$, 2-tailed t-test). Ferric ammonium citrate injections produced 664±64 degenerating neurons, which is 2.5-fold more than at saline injection sites and 4.5-fold more than at ammonium citrate injection sites (Figure 3.3B). By 3 days survival, the number of Fluoro-Jade-labelled neurons had declined by 50% around all injection sites, and their numbers continued to decline between 3 and 7 days. At 3 days post-injection, ammonium citrate injection sites had 10-fold fewer degenerating neurons than saline injection sites ($t(8)=3.367$, $p=0.010$, 2-tailed t-test), and by 5 days the number of degenerating neurons had declined to almost zero around both ammonium citrate and saline injection sites. Ferric ammonium citrate injections

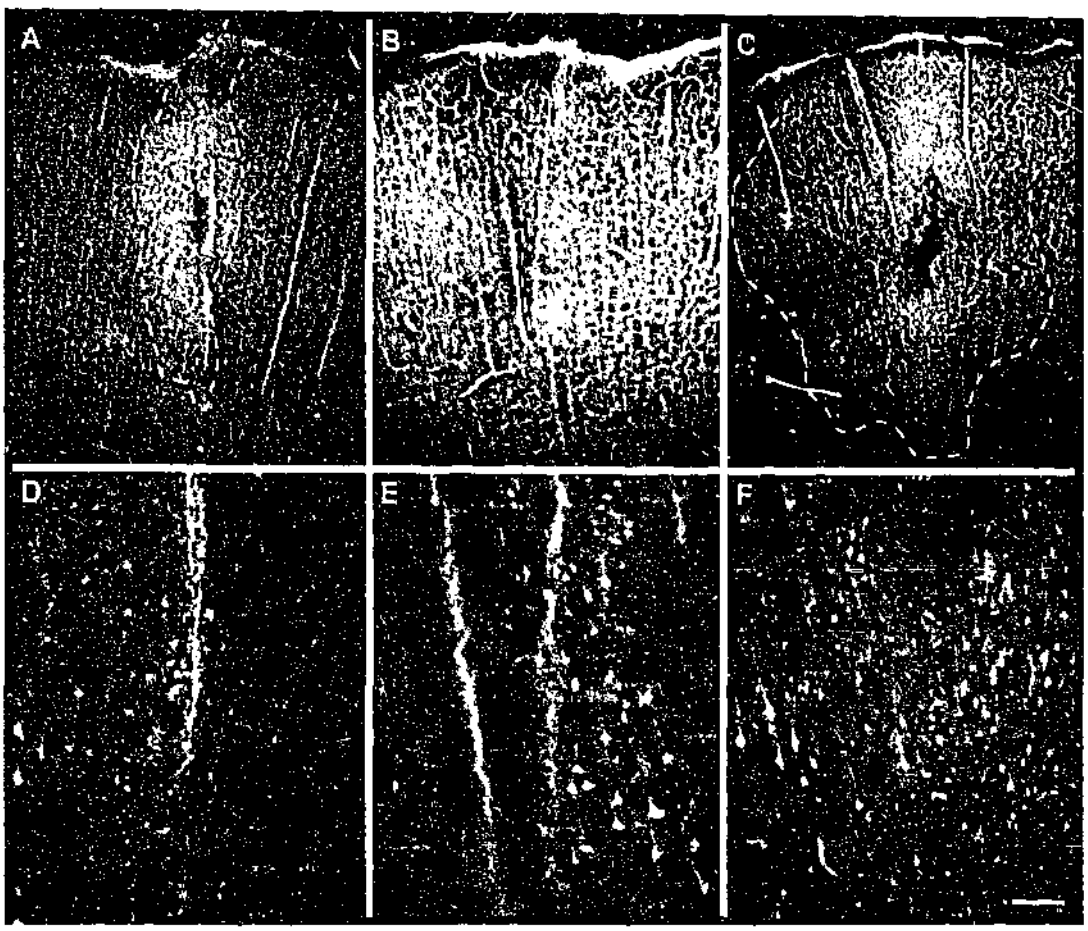

Figure 3.5. Fluoro-Jade staining showing degenerating neurons around ferric ammonium citrate injection sites.
1 day after injection of saline (A,D), ammonium citrate (B,E) or ferric ammonium citrate (C,F). The extent of labelling around the injection sites is indicated by a dashed line. Ammonium citrate injections (B) produce fewer degenerating neurons than saline injections (A). Ferric ammonium citrate injections (C) produce many labelled cells that extend a considerable distance from the needle tract. The labelled neurons are present at a lower density around control injections (D,E) than around ferric ammonium citrate injections (F). Scale bar = 200μM (A-C); 50μM (D-F).

produced more degenerating neurons than saline or ammonium citrate, and the rate of decline with ferric ammonium citrate was much more gradual, with approximately 177 Fluoro-Jade-labelled cells remaining at 7 days, which represents 27% of the number present on day 1.

3.3.5. Quantification of degenerating neurons around injection sites in H&E-stained sections.

To assess whether Fluoro-Jade is an accurate marker of degenerating neurons, the numbers of basophilic and shrunken neurons around injection sites with a 1 day survival were determined (Figure 3.3C). An average of 175±29 dying neurons were observed around saline injection sites, with fewer being present around ammonium citrate injection sites (135±15). Ferric ammonium citrate injections produced 3-fold more dying cells than saline injections, and 3.9-fold more than ammonium citrate injections. There were no significant differences between the number of Fluoro-Jade-labelled cells and the number of H&E-stained profiles for each injection site ($t(14)=2.060$, $p=0.059$, paired-samples t-test). At later survival times, basophilic profiles were present in diminished numbers around injection sites, and their number and distribution appeared to correlate well with that of Fluoro-Jade labelled cells.

It was noted that ammonium citrate injections produced a large amount of mitotic cell division near the injection tract and at the pial surface. This response differed from saline injection sites, where few mitotic figures were seen and these were restricted to the pial surface. Ferric ammonium citrate injection sites produced more mitotic figures than saline injection sites, but fewer than seen around ammonium citrate injections (data not shown).

3.4. Discussion.

Hypoxia-ischaemia and intracerebral haemorrhage are complex events involving a myriad of factors that have the potential to cause neuronal loss, including acidic pH, glutamate excitotoxicity, edema, potassium efflux and inflammation. In the absence of quantitative data concerning the neurotoxicity of iron *in vivo*, it has been difficult to assess whether iron-mediated peroxidation is likely to be a major contributor to the brain injury that results from hypoxia-ischaemia or intracerebral haemorrhage. The present study is the first to obtain quantitative data concerning the spatio-temporal

patterns of neuronal death and ferritin expression that result from exposure of the cerebral cortex to pathologically relevant concentrations of iron, in the absence of other confounding variables. By injecting only 1µl of ferric ammonium citrate over a 5 minute period, negligible compression damage to tissue was produced, and by inclusion of saline and ammonium citrate injection sites non-specific toxicity associated with the injection technique was controlled for. Furthermore, by correcting the data for differences in the depths of individual injection sites, a source of experimental error was reduced that is often overlooked in studies of this type.

3.4.1. Neuroprotection by ammonium citrate.

The fact that ammonium citrate injections produced significantly fewer dying neurons than saline injections suggests that ammonium citrate is neuroprotective. This neuroprotection may be due to the increased availability of citrate to fuel the tricarboxylic acid cycle of injured neurons or their supporting astrocytes. In addition, it may reduce the excitotoxicity of glutamate released from injured neurons by providing ammonia for the amidation of glutamate to glutamine in astrocytes (Hertz et al., 1999). While these possibilities deserve further investigation, this finding also suggests that ferric ammonium citrate may be less toxic than iron that has been directly dissolved in the extracellular fluid of the brain. It is possible therefore that the estimate of neuronal loss caused by ferric ammonium citrate may underestimate the loss caused by an equivalent amount of iron released under pathological conditions. Another finding that deserves comment is the observation that ammonium citrate stimulates cell division. It has been shown that ammonia can induce proliferation of colonic epithelial cells (Ichikawa and Sakata, 1998) and gastric mucosal cells (Tsujii et al., 1995), but the present study appears to be the first to report the stimulation of mitotic division in the central nervous system after directly adding ammonium compounds. Nonetheless it has been suggested that indirectly elevating brain ammonia levels, via methionine sulfoximine inhibition of glutamine synthetase, may result in mitotic division of astrocytes (Brumback and Lapham, 1989). Investigations are underway to identify the progeny of these cells.

3.4.2. Neurotoxicity of ferric ammonium citrate.

This study found that unbound iron causes an extensive amount of cell loss within 24 hours, and that this loss continues at a reduced rate for at least seven days. Ferritin

expression in microglia was also elevated by iron, but unlike cell death, the number of ferritin-rich cells remained constant over the 7 day period of the study. It was surprising to find that ferritin expression was only modestly elevated in the iron-injected group, and furthermore, that the numbers of ferritin-rich cells in the three experimental groups were not proportional to the extent of neuronal death. The sequestration of iron by macrophages and microglia did not reach appreciable levels until three days after the injection of ferric ammonium citrate. Taken together, these observations suggest that once released into the extracellular fluid, iron may remain there for several days before it can be bound to intracellular ferritin and inactivated. These findings have a number of important implications, which are discussed below.

These results clearly demonstrate that a pathologically relevant concentration of unbound iron can cause a substantial amount of neuronal loss. On average, the number of Fluoro-Jade-labelled neurons that are present in a 100μm thick section through an injection site 1-day after injection was 664 cells. Since the average depth of the injection tract was 0.97mm, and the region containing dying neurons approximates a sphere (see Figure 3.5C), the total number of Fluoro-Jade-labelled neurons that are present 1 day after iron injection will be approximately 4284. This represents a very substantial amount of cell death when viewed in a clinical context. The amount of iron in a 1μl injection of 1mM ferric ammonium citrate is equivalent to that present in just 0.15μl of human blood; by extrapolation, an intracerebral hemorrhage involving only 10ml of blood will contain sufficient iron to kill 2.9×10^8 cortical neurons. This estimate may be conservative because the ferric form of iron is a 5-fold weaker pro-oxidant than the ferrous form (Rauhala and Chiueh, 2000), but as most of the iron in brain is stored as the ferric form (in ferritin), injection of ferric iron is likely to be more physiologically relevant.

Even if the concentration of iron released from intracellular stores following hypoxia-ischaemia is lower than that injected in this study, the resultant neuronal loss may still be extensive, since ischaemic episodes often have a widespread distribution. Areas of the brain with a high iron content (e.g. basal ganglia, hippocampus, Benkovic and Connor, 1993; Connor et al., 1992b; Hallgren and Sourander, 1958) are likely to be more prone to iron-induced peroxidation following ischaemia. It should also be noted that several neurological disorders, including Parkinson's disease and AD, are associated with high levels of redox-active iron (Jenner and Olanow, 1998; Sayre et al.,

2000; Smith et al., 1997). Indeed, the concentrations of iron in neuritic plaques in AD has been estimated to be 1.0mM (Lovell et al., 1998), which is identical to that injected in the present study. The extensive neuronal loss caused by this concentration of injected iron adds weight to the notion that iron-mediated peroxidation contributes significantly to the pathogenesis of such disorders.

3.4.3. Time course of iron toxicity.

The present data does not allow determination with certainty of whether cells that were labelled with Fluoro-Jade at 7 days post-injection were injured on day 1 and took 7 days to die, or were injured at a later time by the continued presence of iron. The latter interpretation seems more likely in view of the relatively slow accumulation of iron in cells near the injection sites. Furthermore, even at three days post-injection, some iron-labelling near the injection tracts was associated with the membranes of neurons, rather than being sequestered within microglia and macrophages (Figure 3.1). These observations indicate that the glial response to iron *in vivo* is much slower than that reported in *in vitro* models. For example, Swaimen and Machen (Swaiman and Machen, 1985) demonstrated that iron added to mixed cultures is rapidly taken up into glial cells and incorporated into ferritin within 4 hours. Qi and colleagues (Qi et al., 1995) demonstrated a similar rapid response in cultured oligodendrocytes, where ferritin synthesis occurred within 6 hours after addition of ferric ammonium citrate or hemin to either rat or human oligodendrocyte cultures. In contrast, a slower response was found by other *in vivo* studies. For example, Koeppen and coworkers (Koeppen et al., 1995) showed that injection of whole blood into the thalamus initiates ferritin expression in microglia after 1-2 days, and that iron sequestration began at 2 days post-injection and did not peak until five days. The reason for the slower response *in vivo* is not clear, but it may be associated with a difference in the initial activation state, with cultured glial cells already being in a higher state of activation prior to the addition of iron. Regardless of the reasons, the delayed sequestration of iron *in vivo* is very significant, because it indicates that when released extracellularly, unbound iron may continue to damage neural tissue for several days.

The usefulness of iron chelators in the treatment of reperfusion injury that follows ischaemia is well established (Halliwell, 1989). For example, administration of deferoxamine 5 minutes after hypoxia-ischaemia in neonatal rats reduces brain injury

(Palmer et al., 1994), while bipyridyl, which chelates ferrous iron, given 15 minutes prior and 60 minutes after thrombotic infarction attenuates brain edema (Oubidar et al., 1994). This study found that a single injection of iron resulted in a protracted period of cell death, with substantial numbers of dying cells and basophilic profiles being present at 7 days post-injection, and with some cell death continuing until at least 14 days (unpublished observations). The long duration of cell death has important implications for the treatment of brain injury resulting from cerebral hemorrhage and hypoxia-ischemia, for it suggests that therapeutic intervention with iron chelators and anti-oxidants may be beneficial for several weeks after an incident. This situation contrasts favorably with the narrow window of therapeutic efficacy for NMDA antagonists in the treatment of excitotoxic injury after ischaemic damage (Margaill et al., 1996; Rod and Auer, 1989; Steinberg et al., 1995).

3.4.4. Conclusions.

In conclusion, this data shows that pathologically relevant concentrations of iron, even in the absence of other confounding variables, can cause substantial neurotoxicity over a protracted period. The long duration of this period suggests that benefit may be gained from targeting iron-induced peroxidation in the weeks following a cerebral haemorrhage or an hypoxic-ischaemic episode. Furthermore, the relatively small degree of individual variability obtained in this study with regard to ferritin expression and Fluoro-Jade labelling suggests that this animal model may prove useful in the evaluation of new therapeutic regimes for treatment of haemorrhage or hypoxia-ischaemia.

CHAPTER 4:

Quantitative analysis of neuronal loss after intracortical injection of Aβ peptide.

4.1. Introduction.

As mentioned in Chapter 1, Aβ is generally believed to cause the neurodegeneration seen in AD brains since many *in vitro* studies have demonstrated that the peptide is toxic to cortical or hippocampal neurons cultured from neonatal rats (e.g. Pike et al., 1992; Roher et al., 1991). *In vitro* studies have shown that Aβ kills cultured neurons within 24hr (Harris et al., 1995; Pike et al., 1993; Yankner et al., 1990a), so in *in vivo* studies it is important to be able to examine the toxicity of Aβ shortly after it has been deposited. Transgenic mice that overexpress amyloid precursor protein have an elevated level of soluble Aβ in their brains, leading to a continuous deposition of the peptide into plaques (Games et al., 1995; Hsiao et al., 1996; Sturchler-Pierrat et al., 1997). These mice have provided valuable *in vivo* models of Aβ deposition, showing that Aβ plaques gradually increase in size as the mice age (Johnson-Wood et al., 1997). A limitation of transgenic mice is that Aβ can be deposited months prior to histological examination of the tissue. Since it is not known precisely when the peptide was deposited within individual plaques, it is not possible in these mice to determine with any certainty the acute toxicity of deposited Aβ.

One approach that allows better spatiotemporal definition of Aβ toxicity is the continuous infusion of Aβ via an intracerebrally implanted catheter. Using this method, 4-week infusion of Aβ into the cerebral ventricles has been shown to result in neuronal death (Frautschy et al., 1998). Infusion of Aβ can allow a shorter interval between Aβ exposure and histological examination of the tissue, but since the peptide is continually deposited during the infusion period, it is difficult to accurately determine short-term toxicity. In another experimental approach, Aβ peptide can be directly injected into the cerebral cortices of rodents and primates. This has allowed insights into the neurotoxicity of Aβ after precisely defined exposure times. Several groups have shown that an area of neurodegeneration and gliosis, as detected by Nissl staining, is evident at the site of Aβ injection (Geula et al., 1998; Podlisny et al., 1992), within 2 days of injection (Games et al., 1992). These studies did not count the number of dying cells around the Aβ deposits, so the degree of toxicity exhibited by Aβ is not known with certainty. As cultured neurons die within 24hr of Aβ exposure, there is a need to examine whether neurons die after an equivalent time *in vivo*. In this study therefore, Aβ was injected into rat cerebral cortex dying neurons were counted at 1, 3, 5, and 7

days post-injection. This procedure has allowed examination of the extent to which the acute neurotoxicity of Aβ leads to neuronal death *in vivo*.

Aβ plaques in AD and transgenic mice are also associated with an inflammatory response. *In vitro* studies have shown that Aβ can promote an inflammatory response (Bradt et al., 1998; Paris et al., 1999), particularly in microglial cells (Combs et al., 2000; Meda et al., 1995). One feature of the inflammatory response seen in AD is the expression of ferritin in activated microglia. Ferritin-rich microglia are closely associated with plaques in AD (Batton et al., 1997; Grundke-Iqbal et al., 1990; Kaneko et al., 1989; Robinson et al., 1995), and it has been shown that ferritin-rich cells are concentrated in the centre of plaques (Batton et al., 1997). It is not known why ferritin-rich microglia are so closely associated with plaques in AD. They may have a role in the phagocytosis of Aβ and its removal from the plaque (Grundke-Iqbal et al., 1990); alternatively, they may be involved in the deposition of Aβ into plaques (Batton et al., 1997; Fukumoto et al., 1996; Robinson et al., 1995; Wisniewski et al., 1989b). *In vivo* models of Aβ injection provide an opportunity to gain insights into the relationship between ferritin-rich cells and Aβ, and to determine the spatiotemporal induction of ferritin-rich cells by Aβ deposits. If these cells are present in AD primarily because they phagocytose Aβ, their numbers should be substantially increased after injection of Aβ into the rat cortex. Alternatively, if ferritin-rich cells are mainly involved in the deposition of Aβ in AD, they might be expected to show little or no response to injected deposits of Aβ. The nature of the relationship between ferritin expression and Aβ deposition has not been examined before in *in vivo* models.

Another advantage provided by intracortical injection models is the opportunity to determine the rate of clearance of Aβ deposits from the brain. In the human brain, the aggregation and subsequent deposition of Aβ is presumably counterbalanced by the clearance of the peptide from the brain (Hyman et al., 1993; Saido, 1998). This dynamic relationship may be disrupted in AD, resulting in a decreased rate of clearance of the peptide, and an accretion of Aβ into plaques. This relationship makes it impossible determine the rate of clearance of Aβ from the AD brain. Similarly in transgenic mice that overexpress mutated human APP, there is a continual overproduction of Aβ which prevents determination of the rate of clearance of Aβ deposits. In this study, aged Aβ peptide was injected into the parietal cortices of rats and immunocytochemical labelling

for Aβ peptide has been used to assess the volume of the deposit after various survival times. From this data, it is possible to estimate the rate of clearance of a known quantity of Aβ from the cortex. To ensure examination of the effects of Aβ in its aggregated form, which is the conformation that is most toxic to cultured neurons (Pike et al., 1991), the fibrillar composition of the deposits was determined with electronmicroscopy. Since injected Aβ is rapidly removed from the rat brain, some researchers have attempted to decrease the rate of degradation and removal of Aβ by co-infusing the peptide with protease inhibitors (Frautschy et al., 1998). This allows the peptide to be present for longer periods, and may increase its toxicity. Here the effects of pure Aβ peptide were examined, since protease inhibitors are not present in AD plaques, nor have they been used in cell culture where Aβ exerts toxic effects within 24hr (Harris et al., 1995; Pike et al., 1993; Yankner et al., 1990a).

4.2. Materials and Methods.

4.2.1. Animals.

Female Wistar (n=70) rats aged 9-13 weeks were obtained from The University of Queensland Central Animal Breeding House, Perth Animal Resources Centre or Monash University Animal Services.

4.2.2. Substances injected.

Three Aβ variants were used in this study: human Aβ1-40 (U.S. Peptide, CA, Lot #10), human Aβ1-42 (U.S. Peptide, CA, Lot #12), and rat Aβ1-40 (Californian Peptide Research, CA, Lot #BB0395). They were prepared as described in section 2.2.2. Sterile saline was used as the vehicle control.

4.2.3. Intracortical injection of Aβ peptide.

Rats were anaesthetised as described in section 2.3.1.1 and received 1.0μl injections as described in section 2.3.2. Rats were euthanased after 1, 3, 5, or 7 days, and perfused as described in section 2.3.3. Injection sites were processed for free-floating immunocytochemistry to reveal Aβ peptide or ferritin-labelled cells, or were stained with Fluoro-Jade to detect degenerating neurons.

4.2.4. Aβ immunocytochemistry for the detection of Aβ peptide deposits.

Injection sites containing Aβ were processed to visualise deposits of the Aβ peptide as described in section 2.5.4. Electronmicroscopic analysis was performed to detect fibrils within the Aβ deposits as described in section 2.5.4.1.

4.2.5. Fluoro-Jade staining for the detection of degenerating neurons.

The detection of degenerating neurons with Fluoro-Jade was performed as described in section 2.6.2.

4.2.6. Ferritin immunocytochemistry for the detection of activated microglia and macrophages.

Ferritin immunocytochemical labelling was performed as described in section 2.5.3.

4.2.7. Double-label immunocytochemistry for Aβ peptide and ferritin.

Sections through injection sites of human Aβ1-40 or human Aβ1-42 were processed to visualise both Aβ peptide and ferritin-rich reactive microglia at the injection site. Sections were processed as described in section 2.5.5.

Brain tissue was obtained from six patients with advanced AD (aged 62-85 years; mean post-mortem interval=17.6hr) as described in a previous study from this laboratory (Robinson, 2000). Two of the patients had been studied by the Department of Geriatric Medicine at Concord Hospital (Sydney) and had fulfilled the 'Consortium to Establish a Registry of Alzheimer's Disease' (CERAD) criteria for probable AD (Morris et al., 1989), and tissue from the other four brains were obtained from the Brisbane Brain Bank. Blocks of entorhinal cortex were sectioned at 50μm and double-immunolabelled for Aβ and ferritin as described in section 2.5.5, except they were pretreated with formic acid for 10min. In addition, primary antisera concentrations differed such that rabbit anti-human L-chain ferritin was diluted at 1:25000, and mouse anti-human Aβ8-17 primary antisera was diluted at 1:50.

4.2.8. Microscopic analysis.

Aβ deposits were detected by light microscopy, and the volume of the deposit was determined as described in section 2.7.6.

Fluoro-Jade-labelled cells were detected using an FITC filter on a fluorescence microscope and were counted as described in section 2.7.4.1.

Sections immunolabelled for ferritin were analysed as described in section 2.7.3.

4.2.9. Statistical analysis.

Statistical analysis was performed as described in section 2.8.1. Independent samples t-tests (2-tailed) were performed, and statistical significance was determined at $\alpha=0.05$.

4.3. Results.

The quantitative data and statistical analysis presented in this chapter are summarised in Appendix 3.

4.3.1. Detection of Aβ peptide deposits.

Aβ immunolabelling was used to detect deposits of Aβ at the site of injection. At 1 day after injection, human Aβ1-40 and human Aβ1-42 were deposited in large, dense extracellular clumps toward the middle of the injection tract (Figure 4.1A,B), but by 3 days these clumps were smaller and more granular (Figure 4.1D,E), with some of these granules appearing to be located within cells (Figure 4.2A,B). Directly above the injection tract, small, lightly labelled cells were visible on the pial surface (Figure 4.2D,E). These cells were evident a small distance away from the centre of the injection tract. After 5 days, a difference was evident between the human variants. Human Aβ1-42 peptide was present in a very small extracellular deposit toward the upper part of the injection tract, while human Aβ1-40 was no longer visible at any point along the injection tract. Above the injection sites of both peptides small, labelled cells were evident on the pial surface. By 7 days post-injection, neither of the human Aβ variants were deposited along the injection tract (Figure 4.1G,H), although labelled cells were still visible on the pia above the injection tract, similar to that seen after 5 days. At no time was labelled peptide visible in regions adjacent to the injection site in either the

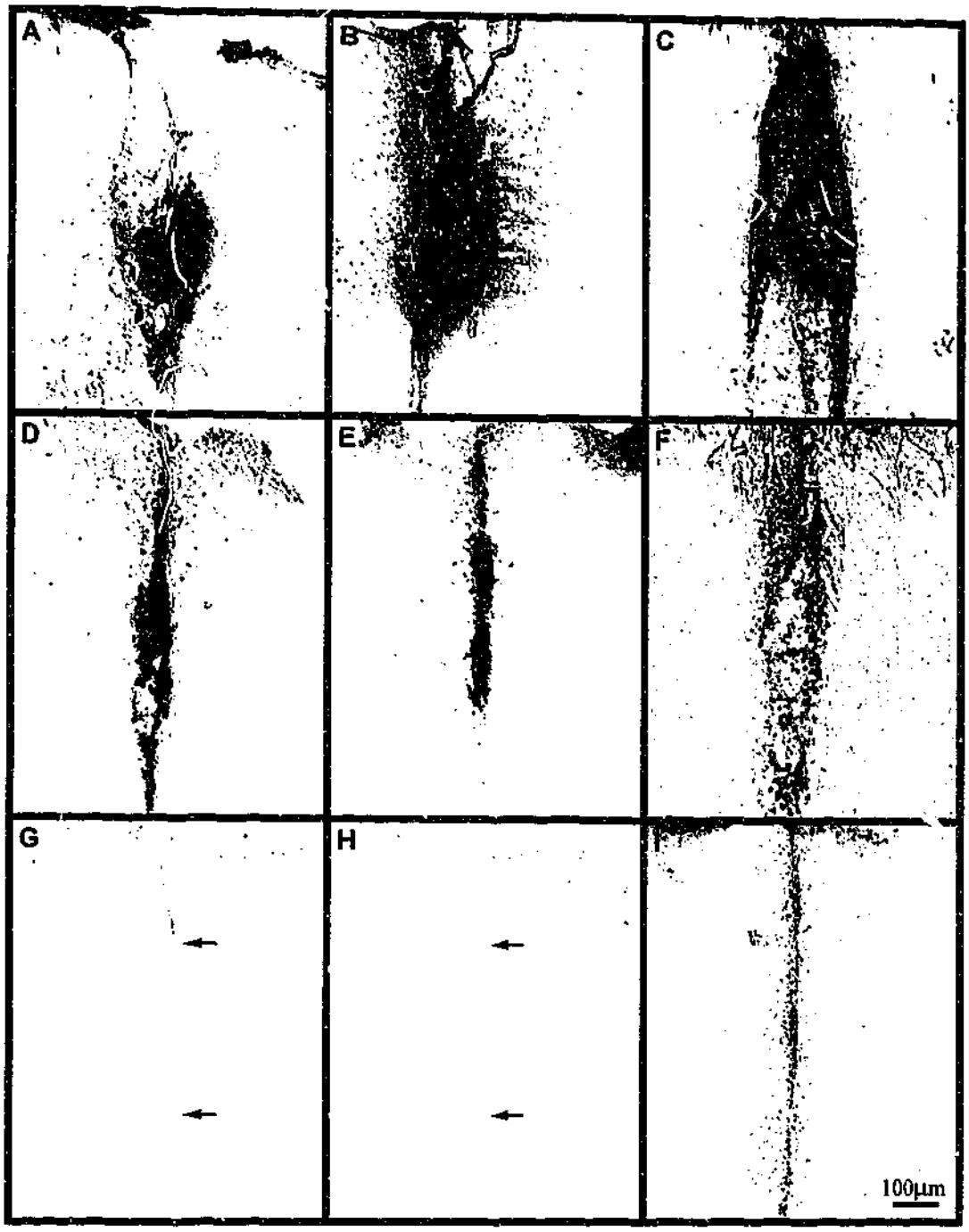

Figure 4.1. Immunolabelling of injection sites for Aβ.
After 1 (A-C), 3 (D-F), or 7 (G-I) days. Injection sites of human Aβ1-40 (A,D,G), human Aβ1-42 (B,E,H) or rat Aβ1-40 (C,F,I). Aβ is present in very large extracellular deposits at 1 day post-injection for all of the Aβ variants (A-C). At 3 days, human Aβ is still present in clumps that are mostly extracellular (D,E), although they are considerably smaller than deposits after 1 day. Rat Aβ deposits are more particulate in nature (F). After 7 days, human peptides are no longer visible along the injection tract (G,H; arrows point to injection tract), however rat Aβ1-40 still has a small amount of peptide visible along the length of the injection tract (I).

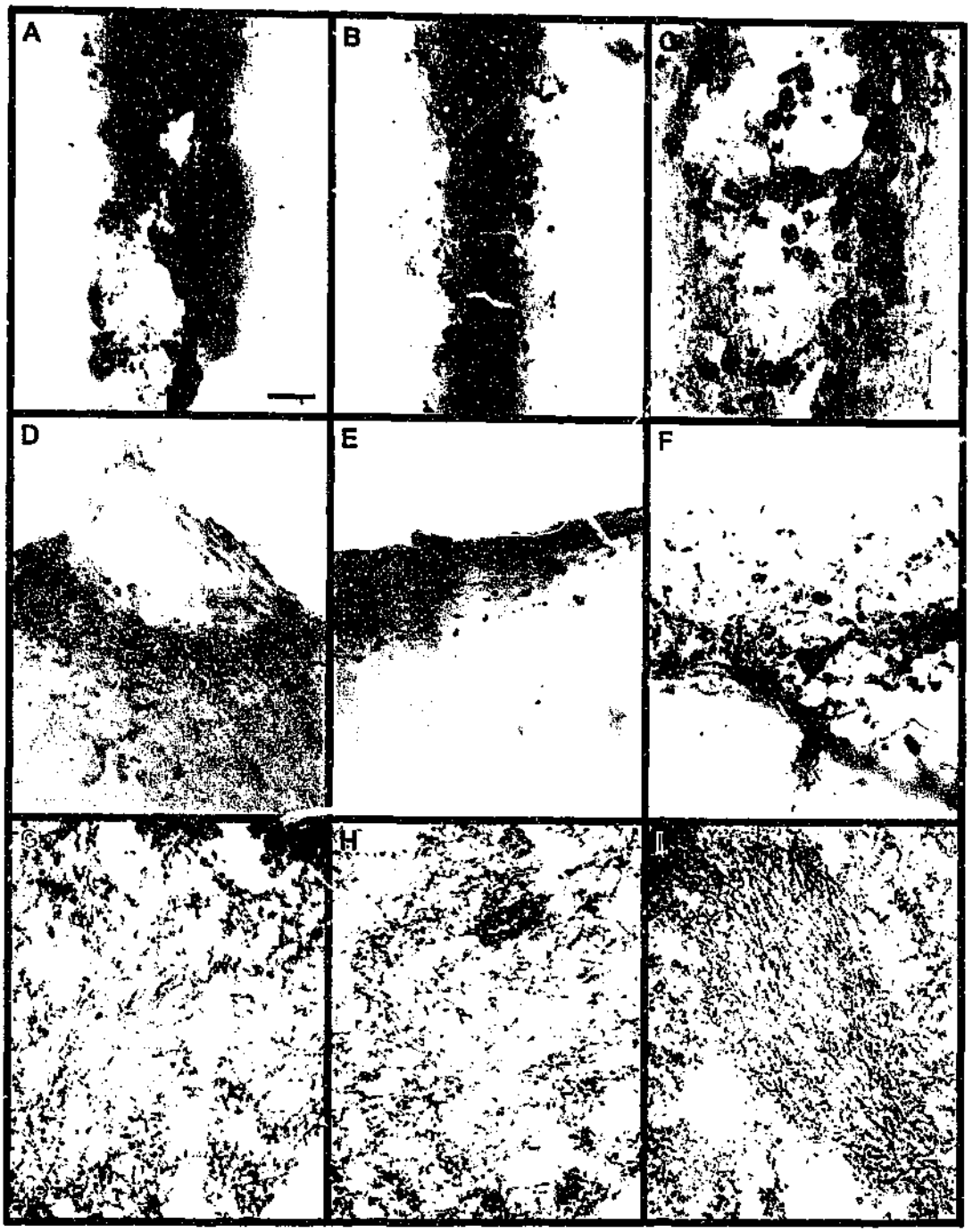

Figure 4.2. Deposits of Aβ 3 days post-injection.
Aβ immunolabelling of injection sites containing human Aβ1-40 (A,D,G), human Aβ1-42 (B,E,H) or rat Aβ1-40 (C,F,I). High magnification micrographs of peptide deposits along the injection tract show that the human Aβ variants are mostly present extracellularly in large clumps, with some diffuse staining around the deposits (A,B), while rat Aβ1-40 appears to mostly be within cells (C). Cellular labelling in the pia above the injection tracts shows that the two human Aβ variants are present intracellularly (D,E), which is quite different to that seen along the injection tract. In contrast, rat Aβ1-40 is mostly present intracellularly (F) as it was along the injection tract (C). Electronmicroscopic examination of deposits of human Aβ1-40 (G), human Aβ1-42 (H), and rat Aβ1-40 (I). Fibrils are present for all of the injected variants, however they are present at greater density around injections of rat Aβ peptide (I). Scale bar = 25μm (A-F), 15nm (G-I).

grey or the white matter, nor was it seen within blood vessels or in the perivascular space.

Deposits of rat Aβ1-40 had a markedly different appearance from deposits of human Aβ. At 1 day post-injection, the deposits along the injection tract were mostly extracellular, with only a few labelled cells present (Figure 4.1C). After 3 days, rat Aβ1-40 had a particulate appearance (Figure 4.1F), with most of these tiny deposits appearing to be within cells (Figure 4.2C). There was extensive cellular labelling in the pia above the injection site that resembled the particulate deposition seen along the injection tract (Figure 4.2F). In contrast to the human Aβ variants, cells containing rat Aβ1-40 on the pial surface were evident a greater distance away from the centre of the injection tract. At both 5 and 7 days the peptide seemed to be entirely contained within cells, and the density of the deposits had decreased (Figure 4.1I). The labelled cells in the pia were still evident, but were displaced further from the injection tract than they were after 3 days survival.

4.3.2. Quantification of the volume of Aβ deposits.

The volume of the Aβ deposit at each injection site was determined and is graphed in Figure 4.3A. The largest deposits were present at 1 day after injection, and the volume steadily decreased over time. Deposits of rat Aβ1-40 occupied 23±3 $\times 10^6 \mu m^3$ after 1 day. By 3 days, only half of the deposit remained (12±3 $\times 10^6 \mu m^3$). Human Aβ1-40 deposits occupied 14±5 $\times 10^6 \mu m^3$ at 1 day post-injection, and similarly decreased by half at 3 days post-injection (8±1 $\times 10^6 \mu m^3$). Deposits of human Aβ1-42 were of a similar volume to human Aβ1-40 at 1 and 3 days survival, however at 5 days post-injection human Aβ1-42 deposits had a mean volume of 3±1 $\times 10^5 \mu m^3$, while human Aβ1-40 was no longer present. In contrast, rat Aβ1-40 was still present along the injection tract at 5 and 7 days, but the volume of the deposit had decreased.

4.3.3. Electronmicroscopic detection of fibrils in Aβ deposits.

Injection sites containing Aβ peptides were examined electronmicroscopically at 3 days post-injection. All three of the injected Aβ peptide variants contained large numbers of fibrils within the immunolabelled deposits. Fibrils in deposits of human Aβ1-40 and human Aβ1-42 appeared to be very similar (Figure 4.2G,H), both in appearance and in

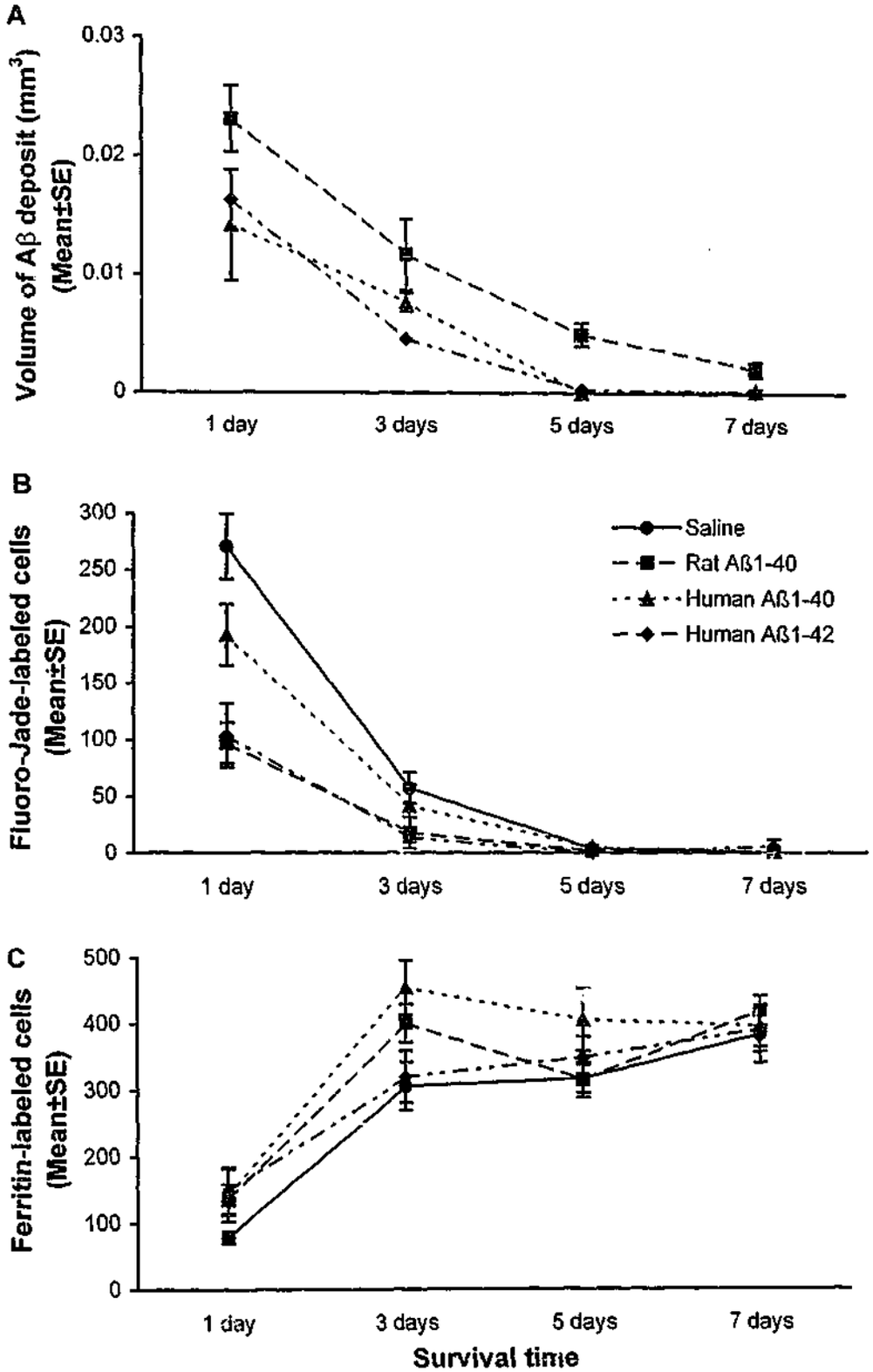

Figure 4.3. Quantitative analysis of injection sites containing Aβ peptide.

Mean volume of Aβ deposits (mm^3) after injection into rat cortex (A). Mean number of Fluoro-Jade-labelled cells after injections of Aβ into rat cortex (B). Mean number of ferritin-immunolabelled cells after injections of Aβ into rat cortex (C). Error bars represent the standard error of the mean.

fibril density. In contrast, rat Aβ1-40 had a much denser arrangement of fibrils than human variants, and the fibrils were more strongly aligned with each other (Figure 4.2I).

4.3.4. Detection of degenerating neurons around injection sites.

Fluoro-Jade stained injection sites 1 day after injection are shown in Figure 4.4(A,B). Fluoro-Jade-labelled cells were located near the injection tracts, and the labelled cells around the Aβ injection sites were more closely confined to the vicinity of the needle tract than the labelled cells associated with saline injections.

After 1 day survival, 271±29 (mean±SE) Fluoro-Jade-labelled neurons were observed around saline injection sites, and there were only slightly less (193±27) around human Aβ1-40 injection sites (Figure 4.3B). Compared with saline, rat Aβ1-40 injection sites 1 day post-injection contained significantly fewer Fluoro-Jade-labelled degenerating neurons (97±18; $t(8)=5.172$, $p=0.001$), and had only half the number that were present around human Aβ1-40 injection sites ($t(8)=2.947$, $p=0.019$) (Figure 4.3B). Human Aβ1-42 injection sites were also associated with significantly fewer dying neurons than saline injection sites (104±28; $t(8)=4.151$, $p=0.003$; Figure 4.4A,B), but they were not significantly different from human Aβ1-40 ($t(8)=2.261$, $p=0.054$) (Figure 4.3B). By 3 days post-injection, the numbers of Fluoro-Jade-labelled cells had significantly decreased for all substances injected. Despite this decrease, human Aβ1-42 injection sites still contained significantly fewer degenerating neurons than saline injection sites after 3 days ($t(4.82)=2.984$, $p=0.032$). At both 5 and 7 days there were few, or no, Fluoro-Jade-labelled cells at any injection site.

4.3.5. Detection of ferritin-labelled cells around injection sites.

Ferritin-immunolabelling detects phagocytic cells, particularly activated microglia and macrophages, as well as a few oligodendrocytes (Connor et al., 1992a; Grundke-Iqbal et al., 1990; Kaneko et al., 1989). The present study found that in grey matter of normal cortex, ferritin immunocytochemistry labels occasional ramified microglial cells, but other cell types are unlabelled. However, 1 day after injection, saline injection sites contained small, labelled cells that may be neutrophils, as well as some larger, amoeboid cells (Figure 4.5A). Ferritin labelling around Aβ injections were similar, however large cells with an amoeboid morphology appeared to be more frequent

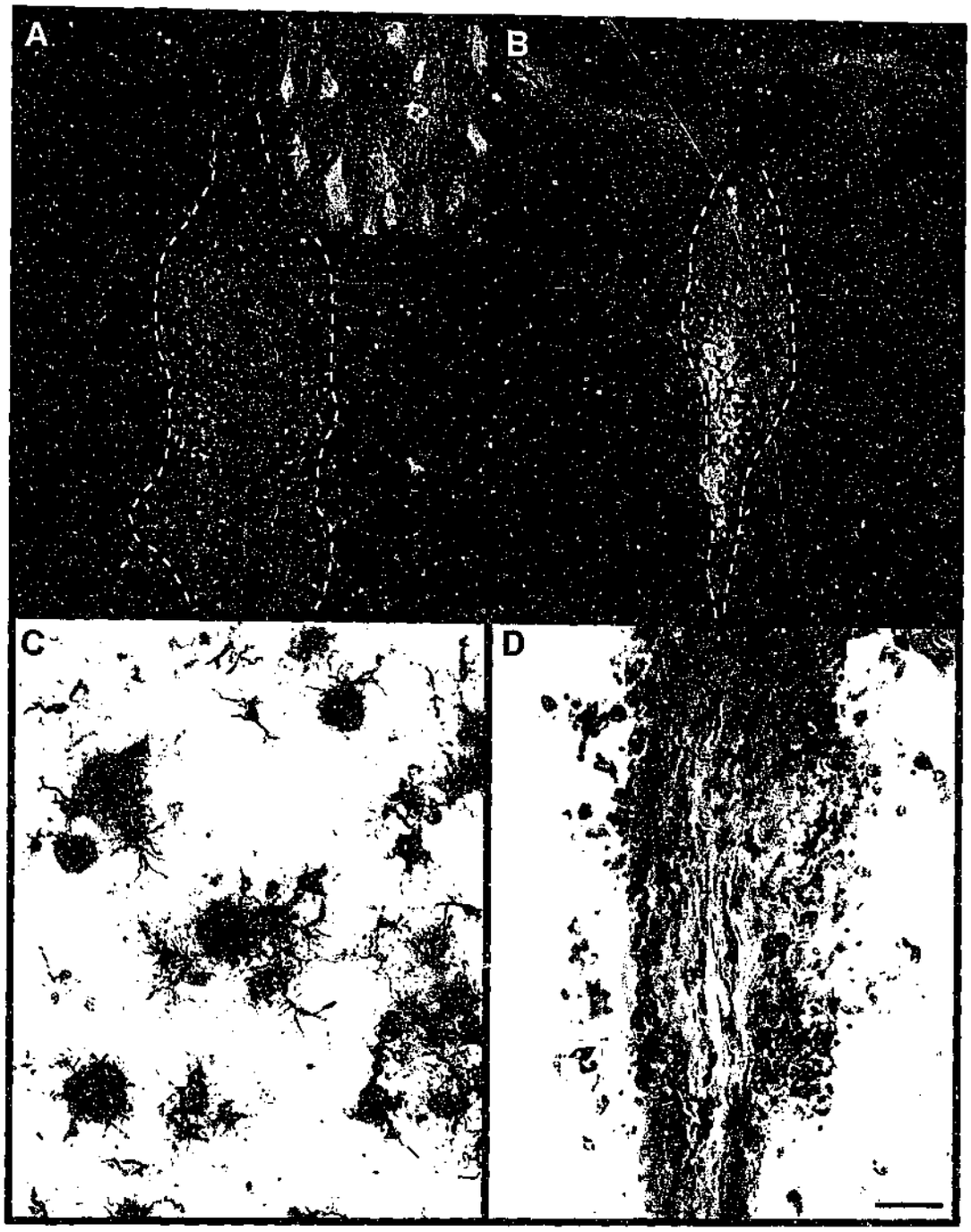

Figure 4.4. Injection sites containing Aβ that have been stained with Fluoro-Jade or double-immunolabelled for ferritin and Aβ.
Injection sites stained by Fluoro-Jade 1 day after injection (A,B). Fluoro-Jade stains degenerating neuronal cell bodies and their primary dendrites (inset A); synaptic labelling is also evident. Saline injection sites (A) have greater numbers of Fluoro-Jade-labelled degenerating neurons than human Aβ1-42 injection sites (B). Dashed lines show the extent of the injection site. Double-immunolabelling for Aβ and ferritin (C,D). Entorhinal cortex from a patient with AD (C) has numerous Aβ plaques (red) that have been surrounded and infiltrated by ferritin-rich cells (brown). An injection site containing human Aβ1-40 3 days post-injection (D) has a large deposit of Aβ (red) that has been surrounded and infiltrated by ferritin-rich cells (brown). Scale bar = 100μm (A,B); 50μm (C,D); 45μm (inset A).

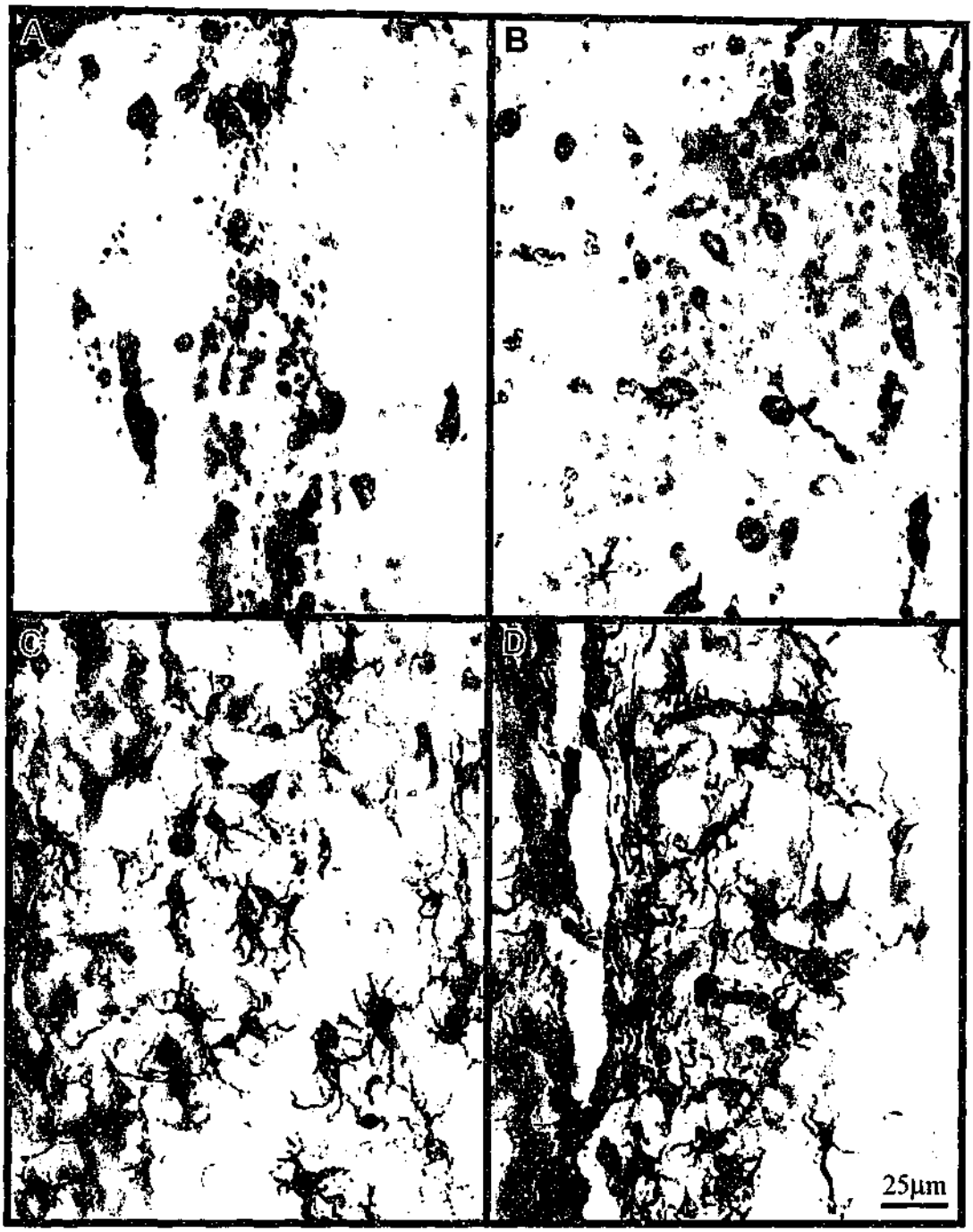

Figure 4.5. Ferritin immunolabelling of injection sites containing Aβ peptide. After 1 day, saline injection sites contain small ferritin-rich cells and a few larger amoeboid cells (A), while human Aβ1-40 injection sites contain a greater number of the large amoeboid cells (B). At 7 days post-injection, both saline (C) and human Aβ1-40 (D) injection sites contain ferritin-labelled cells that have a more ramified morphology.

(Figure 4.5B). After 3 days, at the injection sites of all substances, most of the cells were highly reactive with an amoeboid morphology, although occasionally cells with a more ramified morphology were present. Ferritin-rich foamy cells, presumably macrophages with many filled vacuoles, were quite numerous. At later survival times, a greater proportion of ferritin-labelled cells around all injection sites had a ramified morphology, suggesting decreased activation (Figure 4.5C,D). Ferritin-labelled cells were not present in areas adjacent to the injection tract. Ferritin-labelled cells were also present in the pia above the injection tract of all substances at all survival times.

There were on average 79±9 (mean±SE) ferritin-labelled cells around saline injection sites after 1-day survival (Figure 4.3C). Human Aβ1-40 injection sites had 144±41 labelled cells, and human Aβ1-42 and rat Aβ1-40 had similar numbers, although due to variability between injection sites, the numbers were not statistically different from saline injection sites ($t(4.38)=1.565$, $p=0.186$; $t(4.55)=1.987$, $p=0.109$; $t(8)=2.274$, $p=0.053$; respectively) (Figure 4.3C). At 3 days post-injection, the number of ferritin-labelled cells around injection sites was greater than after 1 day for all of the substances injected. There were 306±36 ferritin-labelled cells around saline injection sites, however human Aβ1-40 injection sites had 1.5-fold more cells (455±41) than saline injection sites ($t(8)=2.726$, $p=0.026$). Both rat Aβ1-40 and human Aβ1-42 had a similar number of labelled cells as saline injection sites. Human Aβ1-42 injection sites had 30% fewer ferritin-labelled cells than human Aβ1-40 injection sites ($t(8)=2.378$, $p=0.045$). The number of ferritin-labelled cells remained relatively stable between 3 and 7 days for all of the substances injected (Figure 4.3C). Moreover, there was little variance between the numbers of ferritin-rich cells around saline and Aβ injection sites at the later survival times.

4.3.6. Double-immunolabelling for Aβ and ferritin.

Double-immunolabelling of entorhinal cortex from patients with AD for Aβ peptide and ferritin showed numerous Aβ plaques in most of the cortical layers. Plaques were of different sizes, but were mostly circular in profile. Ferritin-rich cells were seen clustering in and around the Aβ plaques (Figure 4.4C). Double-immunolabelling of sections from rat cortex revealed a similar picture. Thus at injection sites of human Aβ, ferritin-rich cells were present both within and around the Aβ deposit (Figure 4.4D), and mimicked features of the AD brain. However an important difference was seen with

respect to the morphology of ferritin-rich cells. In rat cortex the cells had a predominantly circular profile and an amoeboid morphology, and were generally larger in diameter, suggesting the presence of a greater number of macrophages. In human cortex the ferritin-rich cells tended to be more ramified and smaller in diameter, suggesting the presence of microglial cells that are in a less activated state.

4.4. Discussion.

In AD, Aβ plaques are associated with neurodegeneration and they contain ferritin-rich cells, such as activated microglia and macrophages. *In vitro* studies have reported that Aβ is neurotoxic and promotes an inflammatory response in microglia. Aβ is generally regarded as the cause of the neurodegeneration in AD, so here the toxicity of Aβ *in vivo* has been investigated. By injecting deposits of fibrillar Aβ into rat cerebral cortex, it is possible quantify the neuronal loss caused by Aβ deposits at precise survival times, and also to count the numbers of ferritin-rich cells associated with these deposits.

4.4.1. Deposition of injected Aβ deposits.

In this study, 1µl of a 1mM solution of Aβ peptide was injected. It has been calculated that 1µg of peptide is equivalent to 10,000 plaque cores (Selkoe et al., 1986), yet here 4µg of peptide was injected, and thus approximately 40,000 plaque cores. While this amount is huge, it is comparable to the amount injected in many other *in vivo* studies, and is less than that used by some others (e.g. Games et al., 1992; Kowall et al., 1992). Using antisera directed against Aβ peptide it was confirmed that the Aβ is always deposited in, or close to, the injection tract. One day after injection, the peptide was present in large clumps that bear a striking resemblance to plaques in the AD brain.

One day after injection, the deposits were considerably smaller than the 1µl volume that was injected. It is likely that some of the Aβ diffused out of the injection site along the needle tract during the injection procedure, and this is indicated by the presence of deposits of Aβ in the pial surface on the first day. Another factor is the clearance by phagocytes that probably occurred during the first 24hr. The most significant factor in reducing the volume of the deposit was probably the tendency of Aβ to aggregate and precipitate from solution (Barrow and Zagorski, 1991; Fraser et al., 1991). This property probably concentrated the peptide along the injection tract.

Another difference between the Aβ variants is related to the presence of fibrils. Electronmicroscopic examination revealed that fibrils were present in deposits of all three variants, and the fibrillar organization of the two human variants were very similar to each other. However, rat Aβ appeared to have a much denser and more organised arrangement of fibrils. Although such differences have not been noted before in an *in vivo* model, *in vitro* evidence suggests that rat Aβ is more amyloidogenic than human Aβ peptides (Fraser et al., 1992). However, it should be noted that due to the different requirements of the primary antisera used for immunocytochemistry, injection sites containing the human Aβ variants were treated with formic acid prior to Aβ staining, whereas rat Aβ was not. This difference in sample preparation may have altered the fibrillar organization of the deposits by dissociating the fibrils.

4.4.2. Clearance of Aβ deposits.

Human Aβ was cleared more quickly than rat Aβ. The reason for this difference is unclear. Perhaps human Aβ is cleared at a faster rate because it is recognised as foreign, whereas rat Aβ may appear to be 'endogenous' to phagocytes, and is removed at a slower rate. Alternatively, if rodent Aβ deposits are more fibrillar than human Aβ deposits, they may be more difficult for phagocytes to degrade, and so the peptide may be present within cells for longer. Regardless of this small difference, it should be noted that all of the Aβ peptides were removed from the cortex very rapidly, initially at a rate equivalent to 5000-10000 plaque cores per day. This indicates that Aβ peptide is rapidly removed from the extracellular space, and suggests that Aβ deposits in the human brain would normally be cleared very soon after formation. Thus in order for extensive plaque formation to occur in AD, there would need to be a massive rate of deposition of Aβ or a reduction in the rate of clearance of Aβ by phagocytic cells.

Cells containing Aβ were present in the pia above the injection tract within 1 day. These cells may have been transporting Aβ to the subarachnoid space, so that it could be removed from the brain via the cerebrospinal fluid. Indeed, Aβ injected into the ventricles of rats is rapidly cleared from the cerebrospinal fluid into the blood (Ghersi-Egea et al., 1996). This mode of clearance of Aβ into the pia may help to explain the high concentration of Aβ in the leptomeninges of AD brain tissue (Shinkai et al., 1997). Aβ is also reported to be removed from the brain via periarterial interstitial fluid

drainage pathways (Weller et al., 1998). In this study however, Aβ did not accumulate around the walls of any blood vessels.

4.4.3. Activation of ferritin-rich cells.

The rapid clearance of Aβ from the site of injection indicates that large numbers of phagocytic cells respond to the presence of the peptide. However, with the exception of human Aβ1-40 after 3 days, it was found that injected deposits of Aβ were not associated with significantly greater numbers of ferritin-rich cells than sites injected with the saline vehicle. This was the case irrespective of the species of the variant, the length of the peptide, or the survival time. The unexpected similarity between injection sites containing Aβ and saline indicates that Aβ does not induce the expression of ferritin. This situation is in contrast to that seen after injection of 1.0mM iron, which induces 8-fold more ferritin-rich cells than vehicle control injection sites after 1 day, and 2-fold more at 3 to 7 days post-injection (see Chapter 3).

The presence of similar numbers of ferritin-rich cells at saline and Aβ injection sites suggests that these cells are responding mainly to the small amount of mechanical damage induced by the injection technique. The failure of Aβ to induce a significant increase in ferritin expression implies that the ferritin-rich microglial cells that are usually present in and around Aβ plaques in AD (Batton et al., 1997; Grundke-Iqbal et al., 1990; Kaneko et al., 1989; Robinson et al., 1995), may not be responding directly to the Aβ within the plaques in order to phagocytose it. Instead they may have a role in depositing the Aβ, as has been suggested previously (Batton et al., 1997; Robinson et al., 1995; Wisniewski et al., 1989b), or they may be responding to another factor that is bound to the plaques.

The deposits of Aβ were rapidly cleared from the cortex, even in the absence of increased numbers of ferritin-rich cells. Aβ-containing cells were detected in the pia above the injection sites, and some of the Aβ along the injection tract also appeared to be in cells, so it is clear that some type of phagocytic cells remove the Aβ. The identity of these phagocytes is unknown, but they may be neutrophils, which are not normally resident in the brain. The penetration of the needle into the cortex will breach the blood-brain barrier, and so neutrophils will be able to infiltrate the injection site. This possibility is supported by the fact that the cells in the pia that contained Aβ were much

smaller than most of the ferritin-rich cells; neutrophils are considerably smaller than microglia and macrophages (Cheepsunthorn et al., 2001; Gong et al., 2000).

4.4.4. Lack of neuronal loss by Aβ *in vivo*.

The amount of neuronal loss caused by Aβ injections was at no time greater than the neuronal loss produced by injection of the saline vehicle solution, even though the injected Aβ equated to tens of thousands of plaque cores. Thus, the quantitative counts of dying neurons support previous *in vivo* studies that have used semi-quantitative methods to analyse neurodegeneration and have reported that Aβ injection into rat cortex does not cause neurotoxicity (Games et al., 1992; Geula et al., 1998). It was clear in this study that Aβ did not kill more neurons than saline. Indeed, Aβ appeared to decrease the neuronal loss caused by the saline vehicle. Of the variants examined, both rat Aβ1-40 and human Aβ1-42 injection sites on days 1 and 3 were associated with significantly fewer degenerating neurons than saline injection sites. This unanticipated finding indicates that pure Aβ peptide attenuates the neuronal loss induced by mechanical damage resulting from the injection technique. To the best of my knowledge, this is the first demonstration of a neuroprotective effect of Aβ *in vivo*. The greater sensitivity afforded by the quantitation of degenerating neurons labelled by Fluoro-Jade allowed us to detect this protective effect.

The deposition of Aβ into plaques has been widely considered to be the cause of neurodegeneration in AD (e.g. Selkoe, 2001), but these results suggest that factors other than Aβ may be responsible for the neurodegeneration associated with plaques. One possible factor may be iron, which is present in plaques at a high concentration of 1.0mM (Lovell et al., 1998). In Chapter 3, it was shown that 1.0μl injections of 1.0mM iron (as ferric ammonium citrate) into rat cortex induce a 4.5-fold more neuronal loss than control injections of ammonium citrate at 1-day survival. This is significant because recent studies have shown that the *in vitro* toxicity that is normally associated with Aβ is probably due to low-level contamination with metals such as iron (Rottkamp et al., 2001; Turnbull et al., 2001). Thus if 1.0mM iron were co-injected with Aβ, a greater amount of neuronal loss might be expected to occur compared with that produced by injections of saline. Such a combination may have been inadvertently produced by Geula and colleagues, who reported that Aβ injections caused neurodegeneration only in aged monkey cortex (Geula et al., 1998). The levels of

endogenous iron are massively increased in the cortices of aged monkeys (Fox et al., 1999), and from this it can be speculated that this iron may have interacted with the injected Aβ to make it neurotoxic.

4.4.5. Conclusion.

This study has quantitatively assessed the *in vivo* neurotoxicity of injected Aβ peptide, and has found that pure Aβ does not kill rat cortical neurons, but instead attenuates neuronal death. It was also found that Aβ deposits do not induce ferritin expression in cells. Both of these findings were not expected, given that Aβ plaques in AD are associated with neurodegeneration and ferritin-rich cells. These findings suggest that neurodegeneration and induction of ferritin expression in AD may occur prior to, or independently of, plaque deposition. Alternatively, other agents in plaques, such as high concentrations of metal ions, may be the ultimate causes of neurodegeneration and ferritin expression. This idea has been examined in the study reported in Chapter 5.

CHAPTER 5:

Quantitative analysis of neuronal loss after intracortical injection of Aβ-iron complexes.

5.1. Introduction.

While many *in vitro* studies have shown that Aβ kills cortical or hippocampal neurons cultured from neonatal rat brains (e.g. Harris et al., 1995; Pike et al., 1993; Yankner et al., 1990a), several *in vivo* studies have shown that injection of Aβ into the cerebral cortex or hippocampus does not appear to produce neuronal loss (Games et al., 1992; Holcomb et al., 2000; Podlisny et al., 1992). Moreover, in Chapter 4 it was shown that intracortical injections of Aβ cause less neuronal loss than control injections of saline vehicle, and it was suggested that other substances within Aβ plaques may be responsible for the toxicity associated with the plaques in AD. For instance, plaques contain high concentrations of iron, copper and zinc (Lovell et al., 1998), all of which are potentially neurotoxic (Armstrong et al., 2001; Hutter-Paier et al., 1998), and therefore could contribute to the neurodegeneration associated with plaques.

It has been established that iron metabolism is disrupted in AD. Iron is present within plaques (Lovell et al., 1998; Smith et al., 1997), and there are alterations in the distribution of proteins involved in the storage and transport of iron (Batton et al., 1997; Connor et al., 1992b; Pinero et al., 2000; Smith et al., 1998). Lovell and coworkers (Lovell et al., 1998) have reported that there is twice as much iron in the AD neuropil than is present in non-demented brains, and that iron is concentrated 1.3-fold further in plaques. While copper is also elevated in AD, the concentration of iron in plaques (52.5μg/g; 1mM) is 2.5-fold higher than that of copper (25.0μg/g; 0.4mM) (Lovell et al., 1998). Pure iron has a similar redox potential to copper (Cotton et al., 1995), so the higher concentration of iron in plaques makes iron a key suspect in the search for contributors to Aβ neurotoxicity in AD (c.f. Huang et al., 1999a; Huang et al., 1999b).

As mentioned in section 1.3.1.2, there is an abundance of evidence implicating iron in the neurotoxicity of Aβ. For example, the presence of iron in culture media is required for Aβ to be neurotoxic *in vitro* (Schubert and Chevion, 1995), and pre-treatment of Aβ with iron chelators decreases its toxicity (Rottkamp et al., 2001). The production of radical adducts by Aβ is thought to be be related to low-level contamination with iron (Turnbull et al., 2001), which is significant because in post-mortem tissue from AD patients, the iron within plaques is redox-active (Sayre et al., 2000). Iron accelerates the formation of AGEs on Aβ (Loske et al., 2000), and AGEs are cytotoxic via the production of free radicals (Loske et al., 1998). Finally, it has been reported that when

iron is mixed with Aβ and added to rat brain homogenates, reactive oxygen species are produced (Bondy et al., 1998). The mechanism by which Aβ exerts its toxicity is likely mediated through histidine residues implicated in the binding of transition metals to Aβ (Atwood et al., 1998; Balakrishnan et al., 1998; Liu et al., 1999). Taken together, these data indicate that combining Aβ with iron increases the toxicity of the peptide *in vitro*. In Chapter 3 it was shown that injections of 1.0mM ferric iron into rat cerebral cortex kill 2.5-fold more neurons than control injections of the saline vehicle. Since there is approximately 1mM iron in plaques (Lovell et al., 1998) and this concentration of iron is neurotoxic, an Aβ-iron complex may be toxic *in vivo*.

Rat Aβ1-42 differs from human Aβ1-42 by three amino acids, one of which is the substitution of histidine for arginine at residue 13 (Shivers et al., 1988). This sequence difference may alter the ability of rat Aβ to bind and interact with iron. If rat Aβ does in fact have a different binding affinity for iron, co-injection of iron with rat Aβ may result in a different level of neurotoxicity than co-injection with human Aβ.

In this study rat cerebral cortex was injected with human or rat Aβ1-42, with an Aβ-iron complex or with iron alone. Tissue was examined 24hr after injection, since the maximal amount of neuronal death produced by Aβ or iron occurs after the first day (see Chapters 3 and 4). In Chapter 4 it was shown that this methodology produces fibrillar deposits of Aβ. The number of Fluoro-Jade-labelled dying neurons associated with each experimental injection site were counted and compared to the number at saline injection sites within the same animal. Aβ immunocytochemistry was used to visualise injected Aβ deposits, and a modified Perl's stain detected ferric iron at the site of injection. In addition, the protocol of intracortical injection used in Chapters 3 and 4 has been refined to increase the statistical power of the comparisons made between the experimental substances injected.

5.2. Materials and Methods.

5.2.1. Animals.

Female Wistar rats aged 12-13 weeks (n=45) were obtained from Monash University Animals Services.

5.2.2. Substances injected.

All substances injected were dissolved in sterile saline (pH 4.5), and are outlined in Table 5.1. Human Aβ1-42 (U.S. Peptide, CA, Lot #12) and rat Aβ1-42 (California Peptide Research, CA, Lot #MF0218) were prepared as described in section 2.2.2. Iron (ferric ammonium citrate; ICN) was prepared as described in section 2.2.1. Mixtures of human Aβ and iron, or rat Aβ and iron, were prepared as described in section 2.2.4. Sterile saline was used as a vehicle control.

5.2.3. Intracortical injection of iron and Aβ.

Rats were anaesthetised as described in section 2.3.1.2 and received 1.0µl injections as described in section 2.3.2. Each rat received three injections of sterile saline in one hemisphere and three injections of the experimental substance in the contralateral hemisphere. After 24 hours, rats were euthanased and perfused as described in section 2.3.3. Injection sites were alternately processed for free-floating immunocytochemistry to reveal Aβ peptide or were labelled with a modified Perl's stain for the detection of ferric iron. To detect dying neurons, injection sites were stained with Fluoro-Jade.

5.2.4. Aβ immunocytochemistry for the detection of Aβ deposits.

Injection sites were processed to visualise deposits of the Aβ peptide as described in section 2.5.4.

5.2.5. Modified Perl's stain for the detection of ferric iron.

Injection sites to be labelled for ferric iron were stained immediately after sectioning as described in section 2.4.2.

5.2.6. Fluoro-Jade staining for the detection of neurodegeneration.

The detection of dying neurons with Fluoro-Jade was performed as described in section 2.6.2.

5.2.7. Microscopic analysis.

Fluoro-Jade-labelled neurons were counted as described in section 2.7.4.2.

Table 5.1. Concentration of Aβ or iron injected for each experimental group.

Experimental Group	Human Aβ1-42	Rat Aβ1-42	Ferric ammonium citrate
Human Aβ	1.0mM	-	-
Human Aβ + iron	1.0mM	-	1.0mM
Rat Aβ	-	1.0mM	-
Rat Aβ + iron	-	1.0mM	1.0mM
Iron	-	-	1.0mM

5.2.8. Statistical analysis.

Eight animals that passed the exclusion criteria were obtained for each experimental substance, with half of the animals receiving injections of saline vehicle in the left hemisphere, and the other half in the right hemisphere. Box-plot analysis was used to ensure that extreme outliers were not present in any of the groups. Statistical analysis was performed as described in section 2.8.2.

5.3. Results.

The quantitative data and statistical analysis presented in this chapter are summarised in Appendix 4.

5.3.1. Deposition of Aβ at the site of injection.

Alternate sections passing through injection sites were immunolabelled for Aβ peptide to visualise injected Aβ deposits. Large extracellular deposits of Aβ were present along the injection tracts containing human Aβ or rat Aβ (Figure 5.1A,D). Co-injection of human Aβ or rat Aβ with iron also resulted in extracellular deposits of Aβ along the injection tracts (Figure 5.1B,E); these deposits were smaller, and appeared to be more dense than injections of pure Aβ peptide. Very little Aβ labelling was present at injection sites containing sterile saline (Figure 5.1G). Iron injections produced more Aβ labelling than saline injections, however the immunolabelling was very diffuse, and was only present in the surrounding neuropil and neurons (Figure 5.1H). No extracellular deposits of Aβ are evident at iron injection sites (Figure 5.1H).

5.3.2. Deposition of iron at the site of injection.

Alternate sections through injection sites that were adjacent to those immunolabelled for Aβ peptide were processed with a modified Perl's stain for the detection of ferric iron. Co-injection of human Aβ or rat Aβ produced large deposits of iron along the injection tract (Figure 5.1C,F) that were almost identical in appearance to the Aβ deposits detected by immunocytochemistry (Figure 5.1B,E). Iron injection sites had small, round, iron-containing cells along the injection tracts and in the adjacent regions (Figure 5.1I). Injections of saline, human Aβ and rat Aβ contained very little iron along the

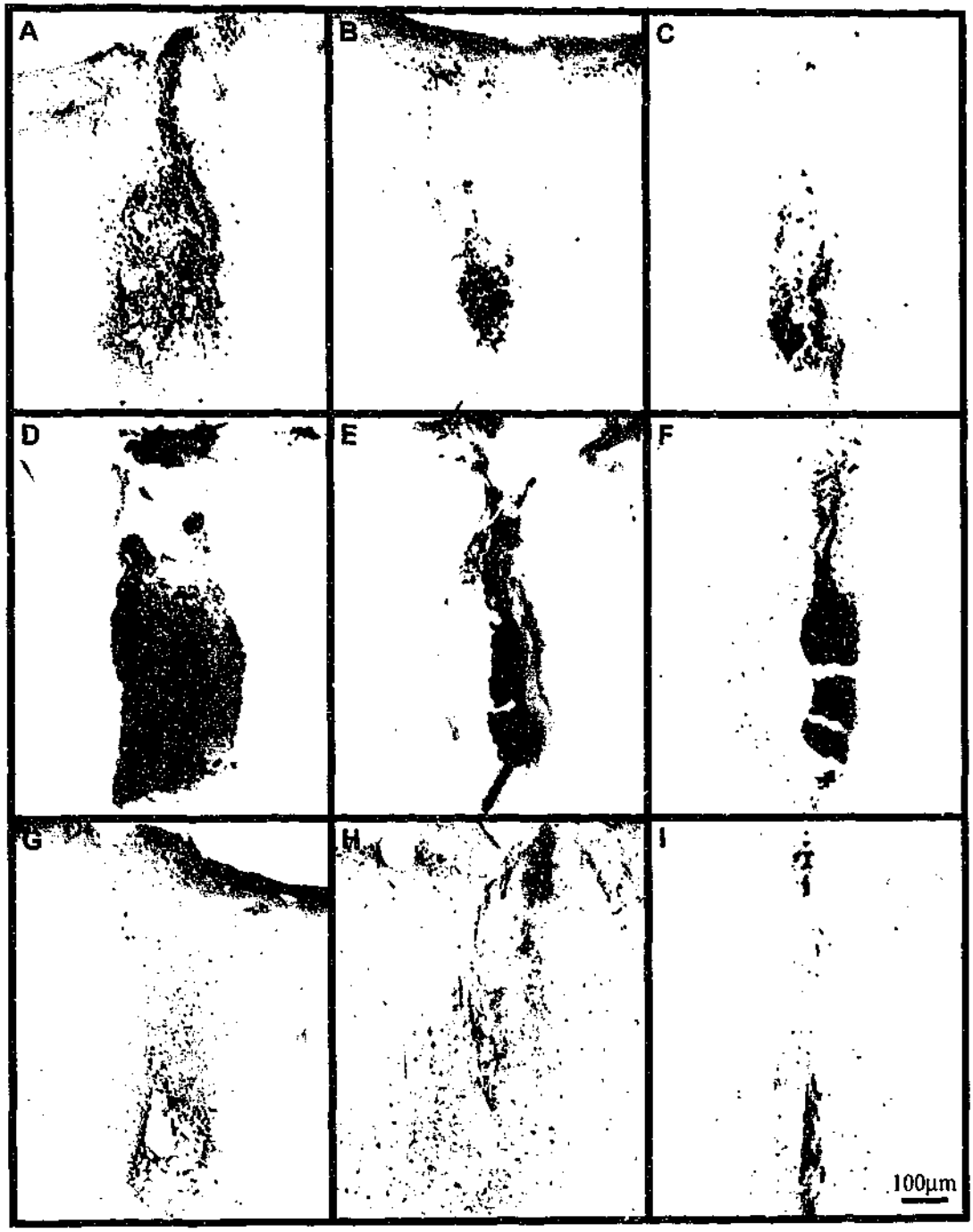

Figure 5.1. Detection of Aβ peptide or ferric iron at the site of injection. Aβ-immunolabelled injection sites containing human Aβ (A), human Aβ + iron (B), rat Aβ (D), rat Aβ + iron (E), saline (G) or iron (H). Modified Perl's staining to detect ferric iron at injection sites containing human Aβ + iron (C), rat Aβ + iron (F), or iron (I). Injection sites containing human Aβ (A) or rat Aβ (D) have large extracellular Aβ deposits, with some of the peptide appearing in cells. When Aβ is mixed with iron, the Aβ deposits are smaller and appear more dense (B,E). Staining of adjacent sections for ferric iron shows that iron is present within the deposit (C,F). Saline injection sites do not contain Aβ deposits, but do have a small amount of Aβ immunolabelling in the neuropil (G). A similar picture is seen at iron injection sites, although Aβ immunolabelling is also present within some neurons (H). Ferric iron is present at iron injection sites, mostly within small round cells (I). Some injection sites in this figure appear to have cavitations (E,F,G,I), that may appear to be caused by the substance that was injected. However, the 'hole' in the tissue is due to processing techniques that use harsh acid treatments, and are not due to the substance that was injected.

injection tract, and most of that present was associated with red blood cells (data not shown).

5.3.3. Quantitative analysis of Fluoro-Jade-labelled cells.

The number of Fluoro-Jade-labelled degenerating neurons at each experimental injection site was expressed as a percentage of the number of Fluoro-Jade-labelled neurons around control saline injection sites. More than 80,000 neurons were counted from a total of 40 rats. The value reported for each experimental substance is the mean number of dying neurons expressed as a percentage of the mean number of dying neurons associated with contralateral saline injection sites (see Figure 5.2).

Human Aβ injection sites had only 79±17% (mean±SE) of the number of dying neurons that were present at saline injection sites, although these values were not significantly different from each other by 2-tailed paired t-test ($t(7)=1.922$, $p=0.096$). In contrast, rat Aβ injection sites (63±6%) had significantly fewer dying neurons than saline injection sites ($t(7)=4.975$, $p=0.002$).

Co-injection of human Aβ with iron killed 1.5-fold more neurons than saline injections, although this difference was not significant by 2-tailed paired t-test ($t(7)=1.851$, $p=0.107$). Nonetheless, this was twice the percentage of neurons that were killed by pure human Aβ ($t(14)=2.653$, $p=0.019$). Co-injection of rat Aβ with iron killed 203±39% more cells than saline injections ($t(7)=2.599$, $p=0.035$), which was three times that killed by pure rat Aβ ($t(7.3)=3.533$, $p=0.009$).

The number of dying neurons at iron injection sites was 262±45% of the number at saline control injections ($t(7)=4.090$, $p=0.005$). Co-injection of iron with human Aβ killed significantly fewer neurons than iron injections ($t(14)=2.160$, $p=0.049$). However, co-injection of iron with rat Aβ killed a similar proportion of neurons as iron alone ($t(14)=0.989$, $p=0.339$).

5.4. Discussion.

In the AD brain, Aβ plaques contain an elevated concentration of iron. When bound to Aβ *in vitro*, iron increases the toxicity of the peptide. In Chapter 4 it was shown that

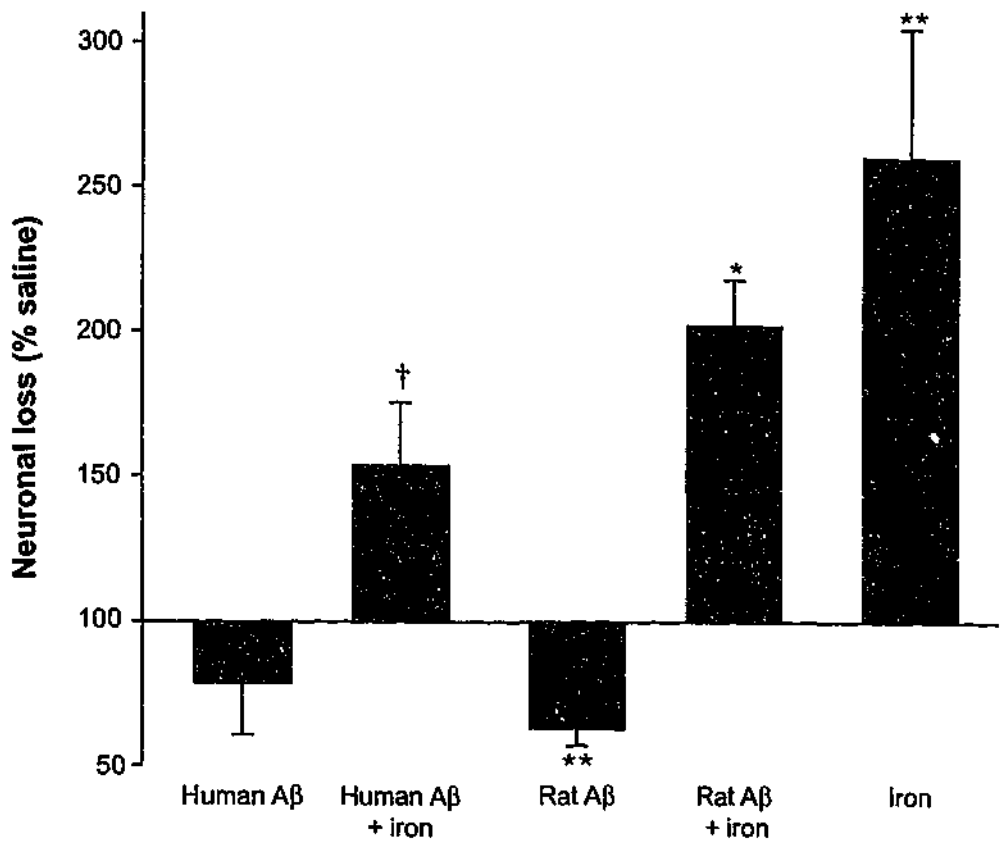

Figure 5.2. Relative toxicity of Aβ, iron or Aβ-iron complexes.
The neuronal loss for each experimental substance is expressed as a percentage of the neuronal loss caused by the saline vehicle (100%). Experimental substances that were significantly different from saline, *$p<0.05$, **$p<0.005$. † denotes a statistical difference from iron $p<0.05$. Human Aβ + iron produced significantly more neuronal loss than human Aβ, $p<0.05$. Similarly rat Aβ + iron killed significantly more neurons than rat Aβ, $p<0.005$.

intracortical injection of pure Aβ produces less neuronal death than control injections of saline, while Chapter 3 showed that injection of iron produces significantly more neuronal loss. To determine whether Aβ-iron complexes are toxic *in vivo*, human or rat Aβ peptide have been co-injected with iron into rat cerebral cortex. The number of dying neurons associated with the Aβ-iron deposits have been compared to the number of dying neurons associated with deposits of pure Aβ.

5.4.1. Human Aβ is not neurotoxic, but Aβ-iron complexes are.

Human Aβ1-42 was not toxic when compared to the saline vehicle. This lack of toxicity of human Aβ to rat neurons is consistent with findings from several other *in vivo* studies (Games et al., 1992; Geula et al., 1998; Holcomb et al., 2000). In Chapter 4 it was reported that human Aβ1-42 injection sites were associated with significantly fewer dying neurons than saline injection sites, in this study however, the difference did not reach statistical significance. This discrepancy may be due to the utilization of a more rigorous pair-matched design in this study.

Co-injection of human Aβ with iron produced 1.5-fold more neuronal death than saline injections. Although this increase was not significantly different from saline injections, it was significantly greater than the percentage of neuronal death caused by injections of pure Aβ peptide. These data show that human Aβ-iron complexes are neurotoxic compared to pure Aβ. This result supports *in vitro* findings that the presence of iron enhances the neurotoxicity of Aβ (see introduction).

5.4.2. Human Aβ reduces some of the neurotoxicity of iron.

Intracortical injection of iron produced 2.6-fold more neuronal death than the saline vehicle, which is consistent with the findings reported in Chapter 3. However this study has shown that when iron is co-injected with human Aβ, the percentage of neuronal loss is significantly reduced. Although this ability of Aβ to reduce iron-mediated neurotoxicity has not been previously reported, it has been reported that Aβ decreases copper-induced oxidation of low-density lipoprotein (LDL) (Kontush et al., 2001). This is consistent with the finding that the numbers of Aβ plaques in AD are inversely correlated with markers of neuronal oxidation, indicating that oxidative stress is reduced after Aβ has deposited in the brain (Nunomura et al., 2001). These observations suggest

that one of the physiological roles of Aβ may be to bind and remove iron from the extracellular space.

In AD brains, the amounts of iron, copper and zinc in plaques are reported to be 1.3-fold higher than in the surrounding neuropil (Lovell et al., 1998). Aβ has a high binding affinity for metal ions (Atwood et al., 1998; Atwood et al., 2000), and binding of metals appears to promote peptide aggregation (Atwood et al., 1998; Atwood et al., 2000; Mantyh et al., 1993). This suggests that Aβ may bind the metals in plaques in order to reduce their neurotoxicity, and thus limit the oxidative stress that occurs in AD. While it has only been shown here that human Aβ can decrease the toxicity of ferric iron, the same experimental paradigm can be used in future to determine whether Aβ also decreases the toxicity of copper or zinc ions. This has been examined in the study reported in Chapter 6.

5.4.3. Rat Aβ interacts with iron differently to human Aβ.

Injections of rat Aβ1-42 killed 37% fewer neurons than saline injections. Although the number of dying neurons produced by rat Aβ was similar to the number produced by human Aβ, only rat Aβ produced significantly less neuronal death than saline. Previous qualitative investigations have reported that rat Aβ1-42 is not neurotoxic *in vivo* (Waite et al., 1992; Winkler et al., 1994), however this study is the first quantitative investigation. In Chapter 4, it was shown that injections of rat Aβ1-40 kill significantly fewer neurons than injections of saline, which supports the current findings with rat Aβ1-42.

Co-injection of rat Aβ with iron was significantly more toxic than saline and was as toxic as injections of iron. This result suggests that iron interacts differently with rat Aβ than it does with human Aβ. The reason for this difference may be related to the three amino acid substitutions within the rat peptide (Shivers et al., 1988). Histidine-modification of human Aβ abolishes iron-induced aggregation, indicating that the binding of iron to Aβ requires Fe^{3+}-histidine coordination (Atwood et al., 1998). Thus, the substitution of histidine at residue 13 in rat Aβ (Shivers et al., 1988) may reduce or abolish the binding of iron to the peptide. If iron is not strongly bound to rat Aβ when the mixture is injected, ferric ions are likely to dissociate and cause neuronal loss. Nonetheless, the fact that the concentration of iron in the neuropil doubles in AD

(Lovell et al., 1998), while the concentration of iron in rodent brain increases by only 25% with aging (Focht et al., 1997), indicates that rodents may have a reduced need for protection against iron-mediated neurotoxicity. Indeed, a histochemical study of iron in brain has shown that the level of iron in old rats is comparable to those in young primates, and substantially less than in old primates (Fox et al., 1999).

5.4.4. Conclusions.

This study has shown that pure Aβ is not toxic to rat cortical neurons *in vivo*. However when the peptide is combined with the concentration of iron found in plaques, Aβ-iron complexes are neurotoxic. This finding indicates that iron bound to Aβ may be in part responsible for the neurodegeneration that is associated with Aβ plaques.

The unexpected finding that human Aβ decreases the toxicity of ferric iron supports a new physiological role for the Aβ peptide. Aβ may bind iron to limit its neurotoxicity: at the same time promoting the aggregation of the peptide and the formation of Aβ plaques. Further studies are needed to determine whether Aβ also protects neurons against other metal ions. This has been examined in the study that is reported in Chapter 6.

CHAPTER 6:

The amyloid paradox: Aβ-metal complexes are both neurotoxic and neuroprotective.

6.1. Introduction.

It has been believed for some time that the Aβ in senile plaques is the main pathogenic factor in AD, however this has recently been questioned by a number of studies that have reported a lack of Aβ neurotoxicity. Nonetheless, it is clear that Aβ can be neurotoxic under some circumstances. Chapter 5 examined the interaction of Aβ with iron in an *in vivo* model and found that when Aβ is complexed with iron it is neurotoxic. This finding was supportive of previous *in vitro* studies that demonstrated that the toxicity of Aβ is increased when iron is present (Rottkamp et al., 2001; Schubert and Chevion, 1995). There are, however other metal ions present in plaques that may also contribute to the toxicity normally attributed to Aβ.

In AD, the concentration of iron, zinc and copper in senile plaques is 1.3-fold greater than in the surrounding neuropil (Lovell et al., 1998). This increase may be due to the high binding affinity of Aβ for metal ions (Atwood et al., 1998; Balakrishnan et al., 1998; Garzon-Rodriguez et al., 1999); indeed Aβ has an exceptionally high binding affinity for copper (Atwood et al., 2000). Similar to the interaction of Aβ with iron, the *in vitro* toxicity of Aβ has been reported to increase in the presence of copper (Huang et al., 1999a; Huang et al., 1999b; White et al., 2001). In fact, the interaction between copper and Aβ is remarkably similar to that with iron, since either metal enables Aβ to generate hydrogen peroxide (Huang et al., 1999a). High concentrations of zinc have also been reported to increase the *in vitro* toxicity of Aβ, although the mechanism behind this interaction is not clear (Lovell et al., 1999; Moreira et al., 2000). Thus it is pertinent to examine the interaction of Aβ with copper or zinc in an *in vivo* model, as was done with iron in Chapter 5, to ascertain whether Aβ-copper or Aβ-zinc complexes are neurotoxic *in vivo*. Furthermore, the simultaneous presence of iron, copper and zinc in Aβ plaques in AD makes it necessary to examine the combined interaction of all three metal ion species with Aβ.

Another consideration arises from the finding in Chapter 5 that Aβ significantly reduces the neurotoxicity of iron. While it was not demonstrated in a cellular model, Aβ has been reported to protect against copper-induced LDL oxidation (Kontush et al., 2001). Since it has been shown that copper is neurotoxic both *in vitro* (Horning et al., 2000; White et al., 1999; White et al., 2001) and *in vivo* (Armstrong et al., 2001), the possibility arises that Aβ may be able to protect against copper-mediated neurotoxicity.

This can be tested using the *in vivo* model of intracortical injection by comparing the neuronal loss caused by copper to that produced when copper is bound to Aβ. To date, no studies have reported that Aβ can protect against zinc-mediated toxicity. However, given that zinc is elevated in plaques and is neurotoxic both *in vitro* (Choi et al., 1988; Kim et al., 1999) and *in vivo* (Armstrong et al., 2001; Cuajungco and Lees, 1998; Lees et al., 1990), there is a need to investigate whether Aβ can reduce the neurotoxicity of zinc.

Current knowledge of the interactions between Aβ and the metal ions found in plaques has been derived from diverse research paradigms that are not directly comparable. Thus, there is a need to examine the interactions between Aβ and iron, copper and zinc under equivalent conditions *in vivo* so that the relative toxicity of each combination can be determined. These results will assist in the clarification of the paradox that has appeared in recent literature, suggesting that Aβ-metal complexes can be both neurotoxic and neuroprotective.

In this study, human Aβ1-42 was co-injected into rat cerebral cortex with iron, copper, zinc, or a mixture of iron+copper+zinc, and the tissue was examined 24hr after injection, similar to the protocol used in Chapter 5. The numbers of Fluoro-Jade-labelled dying neurons associated with each experimental injection site were counted and compared to those at saline injection sites within the same animal. The neuronal loss caused by co-injections was compared to that produced by injections of pure human Aβ1-42 to determine whether Aβ-metal complexes are toxic compared to deposits of pure Aβ. In addition, the neuronal loss caused by co-injections of Aβ and metal ions was compared to that produced by injections of pure metal ions to ascertain whether Aβ reduces the neurotoxicity of any of the metal ion species found within Aβ plaques.

6.2. Materials and methods.

6.2.1. Animals.

Female Wistar (n=72) rats aged 12-13 weeks were obtained from Monash University Animal Services.

6.2.2. Substances injected.

All substances were dissolved in sterile saline (0.9% NaCl, pH 4.5), and are outlined in Table 6.1. Human Aβ1-42 was prepared as described in section 2.2.2. Iron, copper, zinc, and iron+copper+zinc were prepared as described in section 2.2.3. Mixtures of iron, copper and zinc with Aβ1-42 were prepared as described in section 2.2.4.

6.2.3. Intracortical injection.

Rats were anaesthetised as described in section 2.3.1 and received intracortical injections as described in section 2.3.2. Each rat received three injections of sterile saline in one hemisphere and three injections of the experimental substance in the contralateral hemisphere. After 24 hours, rats were euthanased and perfused as described in section 2.3.3. Injection sites were stained with Fluoro-Jade to detect dying neurons.

6.2.4. Detection of dying neurons.

Injection sites were labelled with Fluoro-Jade as described in section 2.6.2.

6.2.5. Microscopic analysis.

Fluoro-Jade-labelled neurons were counted as described in section 2.7.4.2.

6.2.6. Statistical analysis.

Eight animals were obtained for each experimental substance. Box-plot analysis was used to find extreme outliers, which were excluded from further statistical analysis. This resulted in the copper and iron+copper+zinc experimental groups having n=7; all other groups had n=8. Statistical analysis was performed as described in section 2.8.2.

6.2.7. Reuse of data.

The study in this chapter was begun in Chapter 5. Rather than repeat some of the experiments and unnecessarily kill additional animals, this chapter includes data from rats that were injected with human Aβ1-42, iron, or human Aβ1-42 + iron. Thus, the values reported in the results section below for these experimental groups are the same values that were reported in section 5.3.3. These results were restated in this chapter and

Table 6.1. Concentration of Aβ or metal ions injected for each experimental group.

Experimental Group	Human Aβ1-42	Ferric ammonium citrate	Cupric acetate	Zinc acetate
Human Aβ	1.0mM	-	-	-
Aβ + iron	1.0mM	1.0mM	-	-
Aβ + copper	1.0mM	-	0.4mM	-
Aβ + zinc	1.0mM	-	-	1.0mM
Aβ + iron+copper+zinc	1.0mM	1.0mM	0.4mM	1.0mM
Iron	-	1.0mM	-	-
Copper	-	-	0.4mM	-
Zinc	-	-	-	1.0mM
Iron+copper+zinc	-	1.0mM	0.4mM	1.0mM

graphed with the new results to allow direct comparison with the other experimental groups, and to highlight differences in the interactions between Aβ and the three metal ion species found in plaques.

6.3. Results.

The quantitative data and statistical analysis presented in this chapter are summarised in Appendix 5.

6.3.1. Neuronal loss at Aβ injection sites.

The number of Fluoro-Jade-labelled dying neurons associated with each experimental injection site was expressed as a percentage of the number of Fluoro-Jade-labelled neurons associated with control saline injection sites. More than 141,000 neurons were counted from a total of 72 brains. The value reported for each experimental substance is the mean number of dying neurons expressed as a percentage of the mean number of dying neurons associated with contralateral saline injection sites (see Figure 6.1).

Injection sites containing pure Aβ were associated with only 79±17% (mean±SE) of the number of dying neurons present at saline injection sites, but this was not significantly different from saline by 2-tailed paired-samples t-test ($t(7)=1.922$, $p=0.096$).

6.3.2. Comparative toxicity of pure Aβ and Aβ-metal complexes.

Co-injection of iron with Aβ killed 154±22% more neurons than injections of saline, but while this was not significantly different from saline by 2-tailed paired t-test ($t(7)=1.851$, $p=0.107$), it was significantly higher than the number killed by injections of pure Aβ ($t(14)=2.653$, $p=0.019$). In contrast, co-injection of copper with Aβ killed a similar number of neurons to injections of pure Aβ (77±13%). Co-injection of zinc with Aβ killed 159±22% more neurons than saline injections. The neuronal loss produced by co-injection of zinc plus Aβ was not significantly different from saline by 2-tailed paired t-test ($t(7)=3.012$, $p=0.169$), nor did it reach significance when compared to the neuronal loss produced by injections of pure Aβ ($t(14)=1.998$, $p=0.066$). Co-injection of iron+copper+zinc with Aβ killed 242±30% more neurons than saline injections ($t(7)=4.114$, $p=0.004$), which was significantly higher than injections of pure Aβ ($t(14)=4.683$, $p=0.001$).

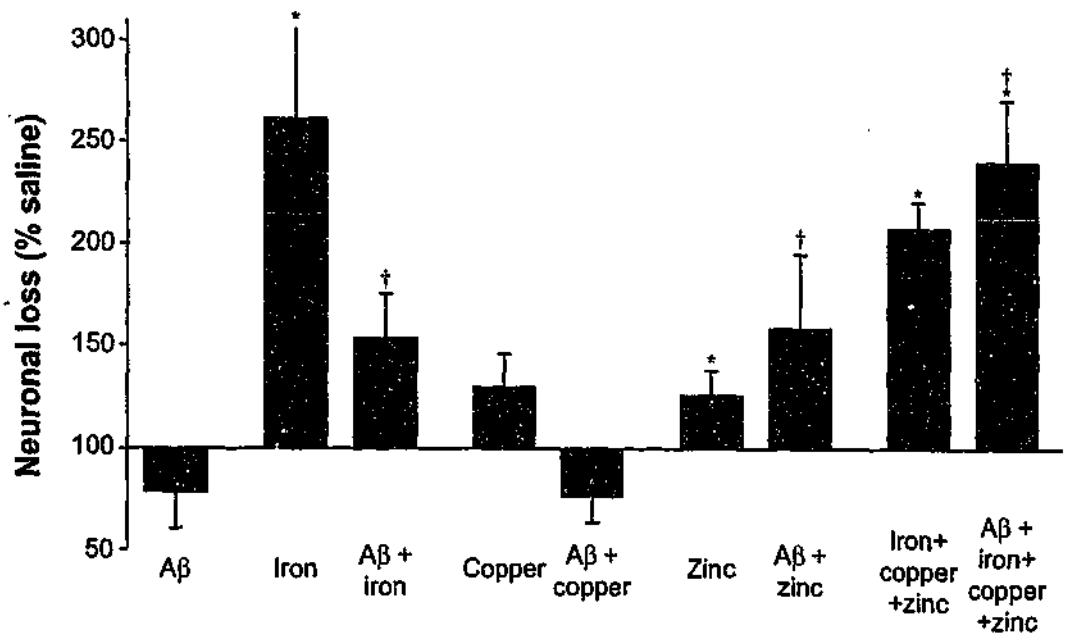

Figure 6.1. Relative toxicity of Aβ, iron, copper and zinc.
The value for each experimental substance is the mean number of dying neurons expressed as a percentage of the mean number of dying neurons associated with contralateral saline injection sites. Significant neuronal loss compared to saline *p<0.05 (paired-samples t-test), or compared to Aβ †p<0.05 (independent-samples t-test). Co-injection of Aβ+iron produced significantly less neuronal loss than injections of iron, and co-injection of Aβ+copper produced significantly less neuronal loss than injections of copper, p<0.05 (independent-samples t-test).

6.3.3. Comparative toxicity of metal ions and Aβ-metal complexes.

Injections of iron killed 262±45% more neurons than saline injections ($t(7)=4.090$, $p=0.005$), however co-injection with Aβ significantly reduced this percentage by two-thirds ($t(14)=2.160$, $p=0.049$). Copper injections killed 130±16% more neurons than saline injections, but this was not significantly greater than the number killed by saline by 2-tailed paired t-test ($t(6)=1.830$, $p=0.117$). Nonetheless, co-injection of Aβ with copper completely eliminated neuronal loss due to copper ($t(13)=2.576$, $p=0.023$). Injections of zinc killed 126±12% more neurons than saline injections ($t(7)=3.012$, $p=0.020$), and the percentage tended to increase when mixed with Aβ ($t(8.4)=0.864$, $p=0.412$). Similarly, co-injection of Aβ with iron+copper+zinc tended to increase ($t(9.6)=0.937$, $p=0.366$) the neuronal loss produced by injections of iron+copper+zinc, which killed 209±13% more neurons than saline injections ($t(6)=7.005$, $p=0.001$).

6.4. Discussion.

Senile plaques in the AD brain are primarily composed of the Aβ peptide and contain substantially elevated levels of iron, copper and zinc. These metals bind to Aβ, and increase the toxicity of Aβ to cultured neurons. Conversely, several reports indicate that Aβ can reduce the toxicity of metal ions, suggesting that the interaction can be protective. In order to investigate this seemingly paradoxical situation, human Aβ1-42 was co-injected with iron, copper and/or zinc, and the numbers of dying neurons associated with the injection sites were counted. The resulting neuronal death caused by each Aβ-metal complex was compared to that produced by human Aβ1-42 alone, or to injections of each of the metal ions alone.

6.4.1. Aβ-metal complexes containing iron or zinc, but not copper, are neurotoxic.

Injections of pure Aβ did not kill more neurons than injections of saline, which is consistent with the findings of several other *in vivo* studies (e.g. Geula et al., 1998; Holcomb et al., 2000) (discussed in sections 4.4.4 and 5.4.1). While pure Aβ was not neurotoxic, Aβ-iron, Aβ-zinc or Aβ-iron+copper+zinc complexes were found to be neurotoxic. These findings support *in vitro* reports that the presence of iron is required for Aβ-induced neurodegeneration (Schubert and Chevion, 1995), and that contamination of Aβ with iron may be the cause of its toxicity (Monji et al., 2001;

Rottkamp et al., 2001). They also confirm that high concentrations of zinc enhance Aβ-induced neuronal death (Lovell et al., 1999; Moreira et al., 2000).

The finding that Aβ-copper complexes produce no more neuronal loss than pure Aβ is in contrast to *in vitro* studies that have reported that when copper is present in culture media, the neurotoxicity of Aβ is increased (Huang et al., 1999b; White et al., 2001). It has been demonstrated in a cell-free system that copper facilitates the production of hydrogen peroxide by Aβ (Huang et al., 1999a). This finding is particularly relevant considering that the *in vitro* models that have examined the neurotoxicity of Aβ normally use primary neuronal cultures, which contain relatively few astrocytes. In these models, there is little defence against hydrogen peroxide toxicity, since neurons have a less efficient glutathione system for the detoxification of peroxides than astrocytes (Dringen et al., 1999). Furthermore, astrocytes strongly protect cultured neurons from hydrogen peroxide toxicity (Desagher et al., 1996; Langeveld et al., 1995), presumably via the presence of both catalase and glutathione peroxidase in astrocytes (Dringen and Hamprecht, 1997). Thus, the endogenous protection afforded by astrocytes in the present *in vivo* model may ameliorate the toxicity of hydrogen peroxide generated by Aβ-copper complexes.

6.4.2. Aβ reduces the neurotoxicity of iron and copper.

Injections of iron or copper killed more neurons than saline injections. The neurotoxicity of iron has been discussed in Chapter 3, and it appears that copper produces neurodegeneration in a similar manner to iron. Copper is a redox-active transition metal, and unbound copper can produce ROS (Halliwell and Gutteridge, 1990) and lipid peroxidation (Zago and Oteiza, 2001). In fact, copper catalyses the Fenton reaction at an order of magnitude faster than iron (Halliwell and Gutteridge, 1990), suggesting that free copper could generate more hydroxyl radicals and cause more neuronal damage than an equivalent amount of free iron.

When Aβ was present, the neuronal loss produced by copper was completely ameliorated, and the neurotoxicity of iron was reduced by two-thirds. The ability of Aβ to decrease the neurotoxicity of iron and copper may be due to antioxidant actions of Aβ. This idea is supported by a recent study demonstrating inhibition of copper-induced

LDL oxidation by Aβ (Kontush et al., 2001), and a report that markers of oxidation in AD brains decrease after Aβ has deposited into plaques (Nunomura et al., 2001).

6.4.3. Aβ cannot protect against zinc toxicity.

In contrast to when mixed with iron or copper, Aβ did not reduce the neurotoxicity of zinc. This result suggests that zinc neurotoxicity may operate via a different mechanism to that of iron and copper. Zinc is a redox-inactive metal ion and is not able to directly promote redox reactions, and may even inhibit some redox reactions (Berg and Shi, 1996). While zinc toxicity has been linked to the production of ROS (Kim et al., 1999), it may do so indirectly by inhibiting glutathione peroxidase activity (Splittgerber and Tappel, 1979). High concentrations of zinc can also decrease Na^+/K^+-ATPase activity (Lovell et al., 1999), enhance kainate toxicity (Shiraishi et al., 1993), and enter cells via voltage-gated calcium channels (Snider et al., 2000). While it is not clear how the interaction between Aβ and zinc increases the toxicity of zinc, it is clear that Aβ cannot protect against zinc toxicity.

The proportion of neuronal loss caused by zinc was increased by 33% compared to saline when zinc was co-injected with Aβ. It is noteworthy that the proportion of neuronal loss caused by injections of iron+copper+zinc was also increased by 33% when combined with Aβ. The consistency between the two treatments suggests that the interaction between zinc and Aβ may be primarily responsible for the increase in neuronal loss seen after co-injecting Aβ with iron+copper+zinc.

6.4.4. The Aβ-metal paradox: implications for the pathogenesis in AD.

The findings of this chapter show that while certain Aβ-metal complexes produce more neuronal loss than pure Aβ, this peptide reduces the neuronal loss produced by redox-active metal ions. This result does, to some degree, resolve the Aβ-metal paradox of neurotoxicity and neuroprotection that has appeared in recent literature. These results reconcile the apparently contradictory findings of studies that were performed on cell cultures and in cell-free systems. However, it raises the question of how the Aβ-metal paradox applies to AD.

In the human brain, Aβ is normally present in a soluble form within the interstitial fluid. Since Aβ is always present, it suggests that the peptide may have important physiological functions. Assuming that the results in this chapter are relevant to the human brain, Aβ may have a function in removing unbound iron, copper and zinc from the extracellular space. Since Aβ has a high binding affinity for metal ions, unbound iron and copper would readily bind to soluble Aβ, and the Aβ-metal complex would aggregate. Aggregated Aβ stimulates an inflammatory response in microglia, presumably by binding to C1q (Daly and Kotwal, 1998; Jiang et al., 1994; Rogers et al., 1992), which would promote rapid phagocytosis of the peptide. Thus, the binding of metals to Aβ may be a mechanism to remove metal ions from the extracellular space and to facilitate their clearance from the brain.

If an Aβ-metal complex is not cleared, it could form the nidus of a plaque, and over time, Aβ will continue to accrete, thereby seeding a plaque. The presence of the metal will cause the normally harmless Aβ to become neurotoxic, and in the region surrounding the plaque, there will be a disruption of neuronal function. While this situation may be detrimental to the immediate environment, the overall toxicity of the plaque will still be less than that caused if the highly redox-active metal ions, iron or copper, remained present in an unbound state.

It is not clear whether Aβ plaques always contain iron, copper, zinc or other metal ions. While it has been shown that high concentrations of these metal ions can be present simultaneously within plaques (Lovell et al., 1998), there may be plaques that contain only one or two of these metal ions. The present study suggests that plaques containing zinc would be a little more toxic than the metal ion alone, while plaques containing only iron and/or copper would be less toxic than if the metal ions remained unbound. Thus, depending on the proportions and concentrations of metals bound to Aβ, some plaques may be neurotoxic, while others may be neuroprotective.

Recent advances have produced a number of ways to remove Aβ from the brain. These anti-amyloidogenic therapies include immunisation against Aβ (Schenk et al., 1999), or inhibition of the enzymes β-secretase (Luo et al., 2001) or γ-secretase (Petit et al., 2001) to prevent the generation of Aβ from its precursor. If Aβ is neurotoxic, albeit only when combined with metal ions, then removal of Aβ by these methods will be beneficial.

However, if Aβ also has neuroprotective actions in the human brain, then removal of Aβ will reduce the protection that is normally afforded by Aβ. This will lead to an increase in the neurotoxicity of unbound metal ions. To this end, the application of anti-amyloidogenic therapies may benefit from combination with chelation therapies so that the unbound metal ions can be simultaneously removed from the brain.

6.4.5. Conclusions.

This chapter has shown that the interaction between Aβ and metal ions has both neurotoxic and neuroprotective outcomes. These findings suggest that a physiological role of Aβ may be to bind metal ions in order to reduce their neurotoxicity and facilitate their clearance from the neuropil. Thus, while the metal ions bound to plaques may cause localised neuronal injury, this may limit the damage caused by these redox-active metals elsewhere in the neuropil. When considered from this perspective, anti-amyloidogenic agents may reduce the protection of the AD brain from metal-induced peroxidation. In order to be effective, such treatments may need to be combined with chelation therapy.

CHAPTER 7:

Effect of the oestrous cycle on the neurotoxicity of Aβ-metal complexes.

7.1. Introduction.

In women the risk of developing AD after menopause is decreased with the use of oestrogen replacement therapy (Baldereschi et al., 1998; Manly et al., 2000; Paganini-Hill and Henderson, 1996; Waring et al., 1999). Moreover, AD patients who receive oestrogen replacement therapy exhibit better cognitive function than those who do not (Asthana et al., 2001; Henderson et al., 1994). The mechanism by which oestrogen is neuroprotective in AD is not clear. It may enhance cholinergic function or it may act on serotonin receptors to decrease the incidence of depression (for review see Garcia-Segura et al., 2001). Another potential mechanism of neuroprotection relates to the antioxidant properties of oestrogen (e.g. Behl et al., 1997; Behl et al., 1995; Sawada et al., 1998).

It is particularly relevant to AD pathology that oestrogen has been demonstrated to decrease Aβ-induced apoptosis of cultured neurons (Hosoda et al., 2001). This protection may be due to an enhanced expression of the anti-apoptotic protein Bcl-xL (Pike, 1999). Oestrogen has also been found to decrease Aβ-induced disruption of the peripheral vasculature and the associated inflammatory reaction (Thomas et al., 1999). It has been reported that oestrogen decreases the production of Aβ (Chang et al., 1997; Xu et al., 1998), possibly by promoting α-secretase cleavage of APP (Jaffe et al., 1994). The deposition of Aβ may also be decreased due to oestrogen's ability to decrease the expression of ApoE, a chaperone protein implicated in plaque formation (see Garcia-Segura et al., 2001). Thus, the protectiveness of oestrogen in AD appears to be mediated by a variety of mechanisms.

One of the most important mechanisms involved in reducing the *in vitro* toxicity of Aβ may be the antioxidant properties of oestrogen, since the toxicity of Aβ *in vitro* is enhanced by trace amounts of metal ions. In this context it is noteworthy that oestrogen has been reported to decrease iron-induced lipid peroxidation in rat and human brain homogenates (Vedder et al., 1999), and it decreases the rate of copper-induced oxidation of LDL isolated from human blood (Maziere et al., 1991; Schroder et al., 1996; Seeger et al., 1998). Oestrogen can also reduce the extent of iron-induced degeneration in neuronal cultures (Bae et al., 2000; Culmsee et al., 1999). Thus, by reducing the oxidative potential of metal ions bound to the peptide, oestrogen may reduce the *in vitro* toxicity of Aβ.

In female rats the level of plasma oestrogen is highest during proestrus, after which the levels decline, reaching their lowest point during the stages of metoestrus and early dioestrus (Everett, 1989; Jorgensen, 1972). The animals that were used in this project were female rats that had a normal oestrous cycle, and thus had cyclic changes in their plasma oestrogen levels. In Chapters 3 and 4 it was shown that even intracortical injections of saline produce some mechanical and pressure damage to the cortical tissue. Such neuronal disruption will inevitably cause some oxidative stress at the injection site. Since oestrogen can decrease oxidative stress, it is possible that when plasma oestrogen is high, the amount of neuronal loss produced by saline injections may be decreased compared to injections performed when plasma oestrogen levels are at their lowest. Similarly, the ability of oestrogen to decrease the toxicity of Aβ and metal ions *in vitro* suggests that high levels of plasma oestrogen may reduce the toxicity associated with injections of metal ions or Aβ-metal complexes. Thus, the toxicity of injected metal ions or Aβ-metal complexes may fluctuate during the oestrous cycle, as a function of oestrogen level.

An additional consideration is that the oestrous cycle has been demonstrated to produce fluctuations in the amount of iron in the serum, liver and substantia nigra (Hill, 1982). It is not known whether these fluctuations are due to cyclic changes in the level of oestrogen or to another gonadotropin such as follicle-stimulating hormone. Nonetheless, a fluctuation in endogenous brain iron could be of relevance when injecting Aβ complexes into the brain, since Aβ has a high binding affinity for iron. Thus if an Aβ-metal complex is not saturated at its metal-binding sites, there is potential for the endogenous iron to bind to the injected Aβ. If the level of endogenous cortical iron fluctuates with the oestrous cycle, then it is possible that during stages of the oestrous cycle when the level of iron is highest, the injected Aβ-metal complex could bind more iron and become more toxic. In view of these considerations, it was considered necessary to ascertain whether there are fluctuations in endogenous iron at different stages of the oestrous cycle in the regions of the cortex that receive intracortical injections in the current protocol.

In this study, the neuronal loss produced by saline injections was determined by counting the number of Fluoro-Jade-labelled dying neurons associated with intracortical injection sites. These numbers were correlated with the stage of the oestrous cycle by

performing a cervical smear at the time of injection. The neurotoxicity of metal ions and Aβ-metal complexes was correlated with the stage of the oestrous cycle to determine whether endogenous oestrogen levels affect the neurotoxicity of these substances. Furthermore, in the region of the cortex that received intracortical injections, the level of iron was determined histochemically with a modified Perl's technique and the intensity of the stain was correlated with the stage of the oestrous cycle.

7.2. Methods.

7.2.1. Animals.

Female Wistar rats (n=60) aged 10-14 weeks were obtained from Monash University Animal Services.

7.2.2. Staging of the oestrous cycle.

Staging of the oestrous cycle was determined by examining cervical smears obtained from a cervical lavage as described in section 2.3.4. Smears were viewed with bright-field microscopy and the relative proportion of each cell type was used to determine the stage of the oestrous cycle (see Fox and Laird, 1970; Waynforth and Flecknell, 1992). Three cell types can be found throughout the oestrous cycle (see Figure 7.1): nucleated epithelial cells, cornified epithelial cells and leukocytes. Oestrus smears primarily contain cornified epithelial cells (Figure 7.1A). Metoestrus smears contain numerous large nucleated epithelial cells and excessive numbers of smaller leukocytes (Figure 7.1B). Dioestrus smears contain very few cells of any type, but have occasional nucleated epithelial cells, cornified epithelial cells and leukocytes (Figure 7.1C). Proestrus smears primarily contain nucleated epithelial cells, and have very few cornified epithelial cells or leukocytes (Figure 7.1D).

7.2.3. Injections of saline, metal ions and Aβ-metal complexes.

Forty animals that contributed to data in Chapter 6 were also used to assess the neuronal loss associated with injections of saline, or the neurotoxicity of metal ions and Aβ-metal complexes at different stages of the oestrous cycle. These rats were anaesthetised and received intracortical injections of saline, metal ions or Aβ-metal complexes as described in section 6.2.3. At the end of the surgical procedure while the rats were still

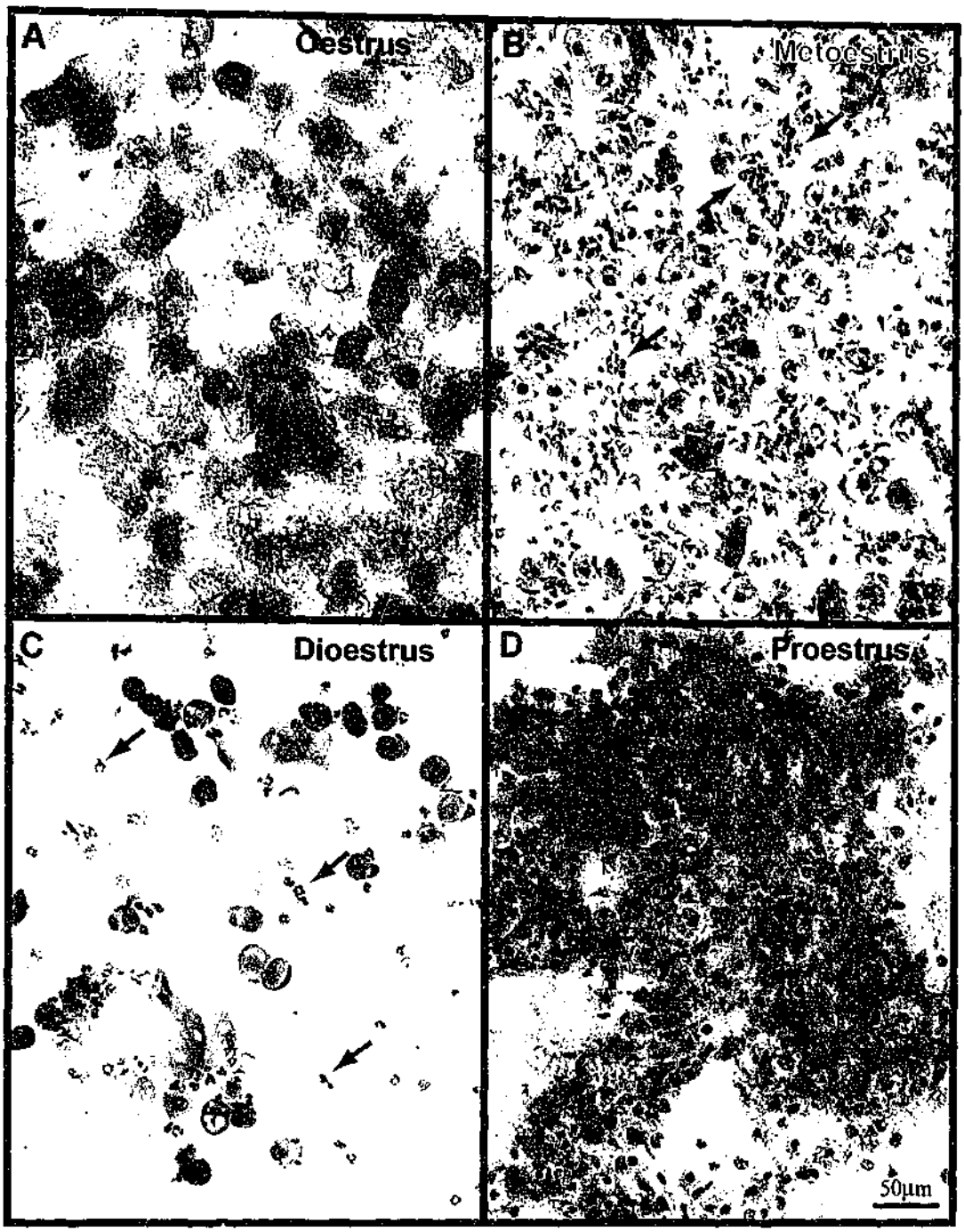

Figure 7.1. Staging of the oestrous cycle.
Three types of cells are present: nucleated epithelial cells (D), cornified epithelial cells (A) and polymorphonuclear leukocytes (arrows; B,C). Oestrus (A) is characterised by dense aggregates of cornified epithelial cells. Metoestrus (B) is characterised by large, nucleated epithelial cells and an abundance of leukocytes (arrows). Dioestrus (C) is characterised by the presence of few cells of all three types. Proestrus (D) is characterised by very large numbers of small, nucleated epithelial cells, which are often present in large sheets.

anaesthetised, a cervical lavage was performed. The rats were perfused the following day as described in section 6.2.3.

Injection sites were processed for Fluoro-Jade as described in section 2.6.2, and Fluoro-Jade-labelled neurons were counted as described in section 2.7.4.2. Every animal received injections of sterile saline in one hemisphere, and the mean number of Fluoro-Jade-labelled cells associated with saline injection sites in each animal was correlated with the stage of the oestrous cycle at the time of injection.

In Chapter 6, eight animals were injected with each experimental substance (e.g. Aβ+iron, Aβ+copper, etc; see Table 6.1), and the percentage of neuronal loss was compared to saline (% saline, see section 2.7.4.2). However, not all of these animals had received a cervical smear to determine their stage of oestrous. To overcome this limitation, the counts from the eight animals in each group were ranked on the basis of neurotoxicity (1 = lowest number of dying neurons expressed as a % saline; 8 = highest). For those animals in which the stage of the oestrous cycle was known, the rank assigned to them was recorded under the respective stage of oestrous. Subsequently all rank values were combined for each stage of oestrous, and the means and standard errors were calculated.

7.2.4. Detection of ferric iron.

To compare the amount of endogenous iron present in the cortex during different stages of the oestrous cycle, five rats were obtained for each of the four stages of the oestrous cycle. The entire oestrous cycle has a duration of 4-5 days and the duration of each stage varies considerably (Fox and Laird, 1970). To ensure that equal numbers of animals were obtained for each stage, cervical lavage (as described in section 2.3.4) was performed at approximately 9:00 am and 5:00 pm on each day until the desired stage was obtained. The rat was then euthanased and prepared for perfusion as described in section 2.3.3. When the rat was fully anaesthetised, another cervical lavage was performed, and this final smear was used for determination of the oestrous cycle stage of the animal. Immediately after cervical lavage, the rat was transcardially perfused and its brain was collected. The next day, the brain was sectioned and immediately processed with a modified Perl's stain to detect ferric iron, as described in section 2.4.2.

The intensity of iron label was determined as described in section 2.4.3. Six cortical sections from each animal were analysed, with half obtained from either hemisphere. For each animal, the mean luminosity of the six sections was determined. The cortices of five animals at each stage of the oestrous cycle were analysed, and the mean value for each stage obtained.

7.2.5. Statistical analysis.

To determine if there were differences between the four stages of the oestrous cycle with respect to the neuronal loss produced by saline injections, the toxicity ranking of metal ions and Aβ-metal complexes, or the average luminosity of iron staining, 2-tailed independent samples t-tests were performed with the level of significance set at α=0.05.

7.3. Results.

The quantitative data and statistical analysis presented in this chapter are summarised in Appendix 6.

7.3.1. Oestrus staging.

The numbers of rats obtained for each stage of the oestrous cycle were not equal. Data concerning the neuronal loss produced by injections of saline are based on 5 rats in proestrus, 14 in oestrus, 8 in metoestrus and 13 in dioestrus. The toxicity data for injections of metal ions and Aβ-metal complexes are based on 4 rats in proestrus, 14 in oestrus, 7 in metoestrus and 13 in dioestrus. This variability reflects the short duration of proestrus and metoestrus, which together occupy only 1 day of the 4-5 day cycle.

For the determination of the intensity of iron staining at different stages of the oestrous cycle, five rats were obtained for each stage. Since rats were given a cervical lavage twice a day, it was possible to ensure that equal numbers of animals were obtained for each stage of the oestrous cycle.

7.3.2. Neuronal loss produced by injection of saline.

The average number of Fluoro-Jade-labelled neurons associated with saline injection sites was: oestrus = 479±43 (mean±SE), metoestrus = 457±69, dioestrus = 436±36 and

proestrus = 386±58 (Figure 7.2A). When the different stages were compared with independent samples t-tests, no significant differences were found between the mean numbers of dying neurons produced by injection of saline at any stage of the oestrous cycle.

7.3.3. Neurotoxicity of metal ions and Aβ-metal complexes.

Injection sites of metal ions and Aβ-metal complexes were ranked from 1-8 for each experimental group in Chapter 6, where 1 is the least toxic, 8 is the most toxic, and the median is 4.5. The toxicity ranking varied greatly, and all stages of the cycle contained animals that were ranked at 2 or below as well as 7 or above. The average toxicity ranking for each stage of the oestrous cycle was (Figure 7.2B): oestrus = 3.57±0.67 (mean±SE), metoestrus = 4.86±0.74, dioestrus = 4.69±0.56 and proestrus = 4.25±1.60. Thus, all stages were close to the median toxicity ranking of 4.5, and no significant differences were found between any of the stages.

7.3.4. Iron staining of cortex.

Rat cerebral cortex contains low levels of histochemically detectable iron. During dioestrus, most of the label for iron is located in neurons within cortical layers 2-3 and 5 (Figure 7.3A). The distribution of iron label within neurons is not homogenous, but is granular and appears to be contained within small intracellular compartments. The iron label during proestrus was mostly present within blood vessels, and the label in neurons was very light (Figure 7.3B). During oestrus and metoestrus, the iron label in the cortex was present to some degree in both neurons and blood vessels, with the distribution appearing to be intermediate between dioestrus and proestrus. Occasionally, intense iron labelling was seen in microglial cells. Overall, the intensity of iron label was similar in each stage of the cycle, but with a subtle increase during proestrus.

The mean luminosity values for each stage have been graphed in Figure 7.2C: oestrus = 179±3.5 (mean±SE), metoestrus = 177±3.9, dioestrus = 181±2.0 and proestrus = 172±0.4. The iron label was significantly darker during proestrus than during dioestrus ($t(4.3)=4.668$, $p=0.008$), however there were no differences between other stages of the oestrous cycle.

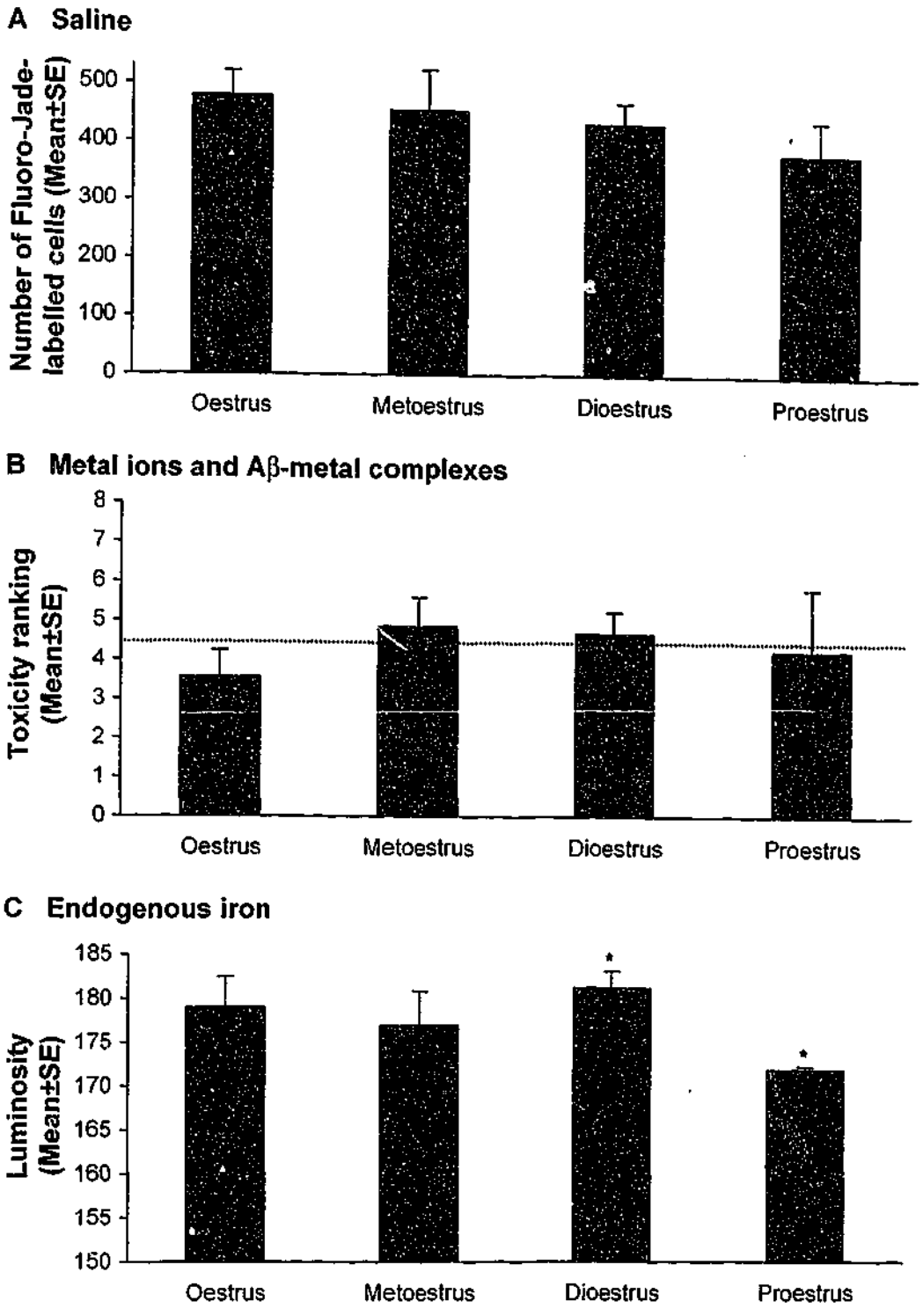

Figure 7.2. Quantitative analysis of neuronal loss and iron labelling during the oestrous cycle.

Mean neuronal loss produced by injection of saline at different stages of the oestrous cycle (A). Mean toxicity ranking of injections of metal ions or A β-metal complexes at different stages of the oestrous cycle (B). Mean intensity (luminosity) of iron staining in the rat cortex at different stages of the oestrous cycle (C). There is a significant difference in the intensity of iron staining between dioestrus and proestrus, * $p<0.05$.

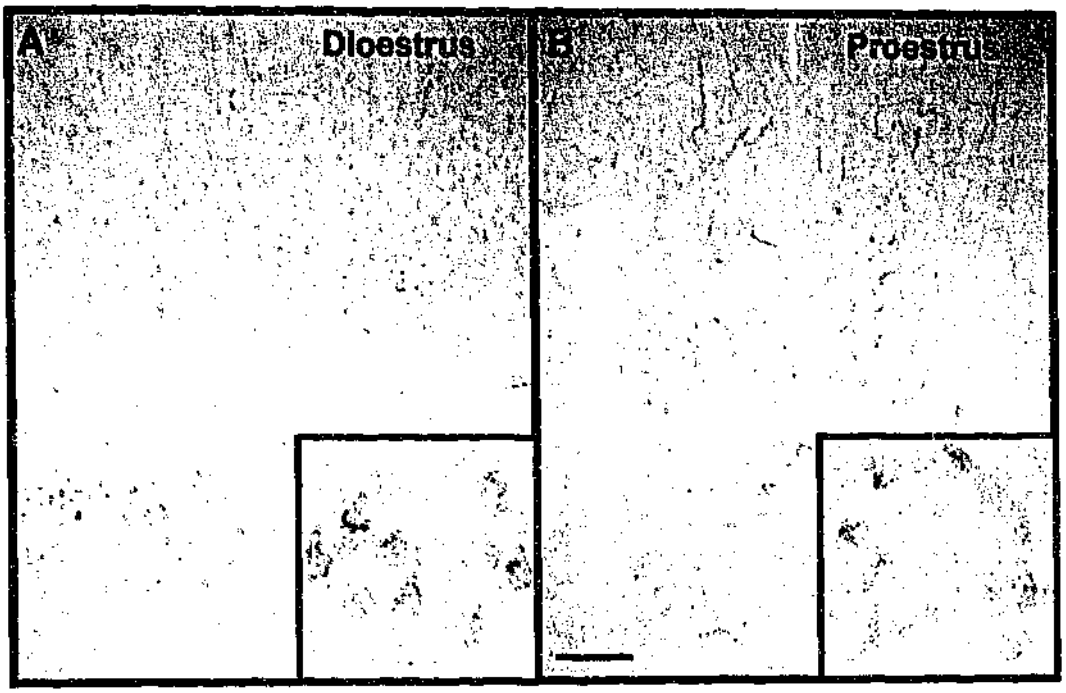

Figure 7.3. Detection of ferric iron in rat cortex.
Modified Perl's stain of rat cortex shows that during dioestrus the iron label is predominantly located in the neuronal somata in cortical layers 2-3 and 5 (A). In contrast, in the cortex from a rat in proestrus, iron label is predominantly located in blood vessels (B). Scale bar = 100μm; inset = 20μm.

7.4. Discussion.

Oestrogen has antioxidant actions *in vitro*. It was speculated therefore that in the stages of the oestrous cycle when plasma oestrogen levels are at their highest, neuronal loss resulting from oxidative damage may be decreased. To determine whether this happens, the numbers of Fluoro-Jade-labelled dying neurons associated with injection sites of saline, metal ions and Aβ-metal complexes were correlated with the stage of the oestrous cycle at the time of injection. It had previously been reported that endogenous iron levels fluctuate during the oestrous cycle. Given that Aβ has a high binding affinity for iron, it was considered possible that elevations of endogenous iron may enable Aβ-metal complexes to bind extra iron, increasing their toxicity. To examine this possibility, the relative level of cortical iron was compared at each stage of the oestrous cycle in the region of the cortex where injections are performed.

7.4.1. High endogenous oestrogen levels do not decrease neuronal loss.

Contrary to expectations, the mean number of Fluoro-Jade-labelled neurons associated with saline injection sites did not vary significantly across the stages of the oestrous cycle. Similarly, in each of the four stages of the oestrous cycle, the mean toxicity ranking of injection sites containing metal ions and Aβ-metal complexes was close to the median toxicity ranking of 4.5. In addition, each stage of the oestrous cycle contained injection sites at the upper and lower limits of the toxicity rankings. Together these data indicate that hormonal changes during the oestrous cycle of the rat do not increase or decrease the susceptibility of neurons to the oxidative damage produced by intracortical injections of saline, metal ions and Aβ-metal complexes.

Endogenous levels of oestrogen are highest during proestrus (Everett, 1989; Jorgensen, 1972). Numerous studies have reported that oestrogen can protect against neurotoxicity (e.g. Callier et al., 2001; Chen et al., 2001), and more specifically that oestrogen can protect against the neurotoxicity of Aβ or metal ions (Bae et al., 2000; Culmsee et al., 1999; Hosoda et al., 2001; Pike, 1999). However, since the amount of neuronal loss produced by intracortical injections was consistent throughout the oestrous cycle, it appears that endogenous levels of oestrogen are not sufficient to protect neurons from oxidative stress *in vivo*.

Endogenous plasma oestradiol levels in the cycling female rat range from 30-140pg/ml (Liao et al., 2001; Nequin et al., 1979) while in pre-menopausal women, the levels range from 50-180pg/ml (Santanam et al., 1998; Wuttke, 1989). In post-menopausal women, the level of plasma oestradiol is around 50pg/ml and oestrogen replacement therapy is used to increase plasma oestradiol to the middle of the pre-menopausal range (Buckler et al., 1995; Jarvinen et al., 2000). Thus, the levels in female rats are closely comparable to humans. It has been reported that physiological concentrations of oestrogen are not sufficiently high to provide antioxidant protection (Santanam et al., 1998), and the results of the present study are in agreement with this report. The present results make it unlikely that the cognitive improvement provided by oestrogen replacement therapy in AD is related to the antioxidant properties of oestrogen. It seems more likely that beneficial effects of oestrogen therapy are due to other effects of the hormone, such as its influence on the cholinergic and serotonergic systems (see Garcia-Segura et al., 2001).

7.4.2. Changes in endogenous cortical iron.

The intensity of iron label in the cortex was significantly higher during proestrus than during dioestrus. It should be noted however that the measurements acquired in the present study are relative measures, and the exact concentration of iron cannot be determined from the technique that was used here. Nonetheless, this finding of increased cortical iron content during proestrus in female rats is consistent with that reported for the substantia nigra (Hill, 1982). However, in that study, no difference was observed in the level of cortical iron at different stages of the oestrous cycle. This discrepancy may be due to regional differences in iron levels in the neocortex since Hill (1982) examined the rat cortex as a whole, but here only a restricted region of the cortex was examined. The difference that was detected in the intensity of the Perl's reaction between the stages of dioestrus and proestrus was subtle, suggesting that the overall amount of iron changed very little.

There was however, a dramatic shift in the distribution of iron label. Iron was predominantly located within neurons during dioestrus, whereas it was concentrated in vascular endothelial cells during proestrus. Such a shift in the cellular localisation of iron has not been reported before. This shift indicates that iron is transported out of neurons during proestrus and then back into neurons from blood vessels by dioestrus.

Such a dynamic process would require fluctuations in the expression of iron transport proteins in the brain during the oestrous cycle. Indeed there is evidence of such fluctuations in both iron-binding proteins and their receptors. For instance, endothelial cells in chick brain express hen oviduct transferrin receptor, which can bind transferrin, ferritin and lactoferrin (Fuernkranz et al., 1991; Poola, 1997; Poola and Kiang, 1994). It is noteworthy that expression of this receptor is induced by oestrogen (Fuernkranz et al., 1991), so its expression should be maximal during proestrus. Another iron transport protein that may be significant is lactoferrin. Both lactoferrin protein and mRNA expression in mouse genital tract are positively correlated with oestradiol levels (Walmer et al., 1992). It is conceivable that this protein may also be upregulated in the brain. Further research needs to be undertaken to elucidate the physiological significance and basis of the fluctuations in cellular iron localisation revealed by the present study. It should be noted however, that the present results establish that these cyclic changes in iron localisation do not potentiate the neurotoxicity of Aβ, or other injected agents. Therefore, the presence or absence of such changes are unlikely to contribute to the toxicity of Aβ in AD.

7.4.3. Conclusions.

This study demonstrates that the amount of neuronal loss produced by injections of saline, metal ions and Aβ-metal complexes is not affected by plasma oestrogen levels. This result suggests that the beneficial effects of oestrogen replacement therapy in AD are not related to its antioxidative properties.

CHAPTER 8:

General discussion.

8.1. Summary of the major findings.

The purpose of this thesis was to obtain data that would further our understanding of the relative contributions of Aβ peptide and metal ions to the pathogenesis of AD. Data were obtained from a series of studies that utilised an *in vivo* model involving the injection of Aβ into the cerebral cortices of adult rats. This model allowed the neurotoxicity of human Aβ variants to be determined, and an examination of whether the *in vivo* toxicity of Aβ is influenced by the presence of iron, copper or zinc. Human Aβ variants were compared to rat Aβ variants to determine whether their different amino acid sequences results in a different degree of toxicity, or whether it affects their interaction with iron. The influence of fluctuations in plasma oestrogen levels during the oestrous cycle on the neurotoxicity of Aβ-metal complexes was also determined.

The *in vivo* model used in this thesis to examine neurotoxicity was developed in the study reported in Chapter 3, where the neurotoxicity of iron was examined at time points varying from 1 to 7 days after injection. In this model, neuronal loss was examined with Fluoro-Jade, a marker that specifically labels dying neurons. With this model, Aβ peptide was injected into rat cerebral cortex, allowing examination of the neurotoxicity of the naturally occurring human Aβ variants, Aβ1-40 and Aβ1-42, and comparison to the 'endogenous' rat Aβ1-40. This study was reported in Chapter 4, and it was found that large deposits of Aβ peptide were present at the site of injection, and they were rapidly cleared from the extracellular space so that they were no longer present after 7 days. Examination of neurotoxicity demonstrated that injections of Aβ1-40 and Aβ1-42 produce less neuronal loss than injections of the saline vehicle, indicating that the peptides are not toxic to rat cortical neurons *in vivo* but instead tend to attenuate neuronal death. Similarly, injections of rat Aβ1-40 killed fewer neurons than saline injections. Together these findings suggest that Aβ is not solely responsible for the toxicity of plaques in AD, but that other factors present within plaques, such as metal ions, may be responsible for the associated neurodegeneration.

To determine whether iron, copper or zinc could mediate the neurotoxicity of Aβ in this *in vivo* model, each of the metal ions were mixed with Aβ and co-injected into rat cortex. Since it was found in Chapters 3 and 4 that the greatest amount of neuronal loss occurred 24hr after injection of Aβ or iron into rat cerebral cortex, further studies were limited to an investigation of neurotoxicity after this 24hr period. In Chapters 5 and 6 it

was reported that when iron or zinc were mixed with Aβ, a greater number of dying neurons were associated with the Aβ-metal complexes than were associated with deposits of pure Aβ. In contrast, the presence of copper in Aβ deposits did not increase the amount of neuronal loss. The combination of iron, copper and zinc in Aβ deposits also produced more neuronal loss than deposits of pure Aβ. An unexpected finding was that Aβ decreased the overall neurotoxicity of iron and completely eliminated copper neurotoxicity. By contrast, Aβ increased the neuronal loss caused by zinc. Moreover, it appeared that the presence of zinc prevented Aβ from protecting against the toxicity of iron and copper combined. These findings indicate that complex interactions occur between Aβ and metal ions, and these interactions can be both neurotoxic and neuroprotective.

The human and rat Aβ variants were compared in Chapter 5 to determine whether the amino acid differences between the peptides altered their interaction with iron. It was found that pure deposits of human or rat Aβ were associated with fewer dying neurons than injections of saline, and the amount of neuronal loss was similar for each of the variants. Moreover, the presence of iron increased the neuronal loss for both peptide variants. A difference was observed between the variants where the presence of iron increased the neuronal loss produced by rat Aβ to a greater extent than it did to human Aβ. Unlike human Aβ, the rat Aβ variant was unable to decrease the neurotoxicity of iron. Some of the amino acids within the Aβ peptide that are required for the binding of iron are substituted in the rat variant, suggesting that Aβ may need to bind iron in order to decrease its neurotoxicity.

Lastly, the study reported in Chapter 7 showed that fluctuations in endogenous oestradiol levels during the oestrous cycle do not influence the neurotoxicity of metal ions or Aβ-metal complexes. This finding demonstrates that even though oestrogen has been reported to protect against the neurotoxicity of Aβ and metal ions, the highest physiological levels of oestradiol in female rats cannot decrease the toxicity of Aβ-metal complexes. It had been suggested that the neuroprotection provided by oestrogen replacement therapy in AD is related to the antioxidant properties of the hormone, however the findings reported in Chapter 7 suggest that physiological levels of oestrogen will not provide this effect. Thus, other actions of oestrogen must be

responsible for the reduced risk of developing AD that is seen in patients receiving oestrogen replacement therapy.

8.2. A better model for studying Aβ neurotoxicity *in vivo.*

The model of intracortical injection employed in this thesis has a number of advantages over previous studies that have examined the *in vivo* neurotoxicity of Aβ. While the basic protocol used here is similar to that used in other studies that have injected Aβ into the cerebral cortices of rats, a number of additional factors were controlled for in order to reduce the experimental error and variability. These factors are detailed below.

1) Reduction of external damage produced by the injection procedure.

The animal was placed in a stereotaxic apparatus so that its head was firmly held in place, the burr holes were kept as small as possible, and intracortical injections were performed slowly to minimise pressure damage to the cerebral cortex. The damage caused in the present study was considerably smaller than that reported in other studies where the lesion produced by injections of vehicle solution had a diameter of up to 1.5mm (Games et al., 1992; Podlisny et al., 1992). Nonetheless, a small, unavoidable amount of mechanical and thermal damage did occur. Strict exclusion criteria (section 2.7.1) were used to ensure that this damage did not interfere with an accurate determination of the neurotoxicity of the injected substance.

2) Use of a physiological solvent to dissolve the experimental substances.

In this study, sterile saline was used to dissolve all of the substances that were injected. This ensured that the neurotoxicity was due to the substance that was being examined, rather than to potentiation by a nonphysiological solvent (refer to section 1.3.2.1).

3) Use of appropriate controls.

To ensure that the neurodegeneration associated with each injection site was due to the experimental substance, the extent of neuronal loss produced by each substance was compared to that produced by saline (the vehicle control). This ensured that the calculated toxicity of each experimental substance was not confounded by the injection procedure itself. This may seem an obvious precaution, however many studies have compared the toxicity of Aβ injections to healthy untreated tissue (Giordano et al., 1994; Giovannelli et al., 1998; Kowall et al., 1991; Kowall et al., 1992), or they have

made a comparison to saline injection sites rather than to the nonphysiological solvent that they used to dissolve the Aβ (Giovannelli et al., 1995; Giovannelli et al., 1998). In this study, the neurotoxicity of 'endogenous' rat Aβ variants were examined to ensure that the neuronal loss produced by deposits of human Aβ peptides was not solely due to the presence of an extracellular peptide deposit. This also provided an examination of the 'natural' situation within the rat brain, since sequence differences between human and rat variants may alter the actions of the peptides. To the best of my knowledge, only one other study has compared the toxicity of rat Aβ to human Aβ (Waite et al., 1992). Most studies prefer to examine peptide effects by injecting reverse or scrambled human Aβ variants (e.g. Games et al., 1992; Giovannelli et al., 1995; Kowall et al., 1992; Podlisny et al., 1992), and do not consider potential species differences in their model.

4) Direct assessment of neuronal death.

In this study, neurotoxicity was calculated on the basis of the number of dying neurons that were associated with the injection sites. Many previous studies have examined aspects of neurotoxicity but have not directly measured neuronal loss. For instance, counting the number of healthy neurons around an injection site is a common method of analysis (Giordano et al., 1994; Kowall et al., 1991; Kowall et al., 1992; Maurice et al., 1996). However, this is difficult to perform accurately (refer to section 1.3.2.1). Another commonly used method of analysis is to determine the size of the lesion caused by the injection (Emre et al., 1992; Rush et al., 1992; Sigurdsson et al., 1995; Smyth et al., 1994). In this case, researchers use a Nissl stain to view the injection site and find the 'area of neurodegeneration and gliosis' that was caused by the injection and determine the area of this lesion (e.g. Geula et al., 1998). However, measuring the area of the lesion does not take into account the number of dying cells within the lesion, since the density of dying neurons could differ according to the diffusion of the substance that was injected. With a Nissl stain, it is also difficult to determine whether a shrunken dying neuron is a glial cell, and thus some inaccuracy will result. Fluoro-Jade staining overcomes these problems because it is a selective marker for dying neurons and does not produce background labelling. Thus, counts of each Fluoro-Jade-labelled dying neuron associated with injection sites provide a precise determination of neurotoxicity. A few studies have determined the number of TUNEL-labelled profiles after Aβ deposition (Frautschy et al., 1998; Jen et al., 1998). While this is a valid measure of cell death by apoptosis, it may not detect cells dying through necrosis, and in any case is a more time consuming and costly methodology.

5) Appropriate statistical design.

The statistical analysis used in Chapters 3 and 4 differed from that used in Chapters 5 and 6. Initially, for each experimental substance, it was required that five injection sites were obtained from at least 3 different animals (see section 2.8.1). This meant that a single animal could have up to 3 different substances injected into its cortex, and that control injections were not necessarily performed in the same animal as the experimental injections. This minimised the number of animals that were required to obtain results. While similar experimental designs have been employed in other published studies (e.g. Frautschy et al., 1998; Geula et al., 1998; Weldon et al., 1998), a refinement of the present model was introduced so that the neuronal loss caused by an experimental substance could be directly compared to the neuronal loss caused by saline injections in the same animal. This new experimental design was used in Chapters 5 and 6 (see sections 2.7.4.2 and 2.8.2), where each animal received injections of saline in one hemisphere and injections of the experimental substance in the contralateral hemisphere. This innovation provided an internal control for each animal, so that the toxicity of the experimental substance could be expressed relative to the neuronal loss produced by injections of saline. This made the comparisons more conservative and increased the statistical power of the analysis.

8.3. Directions for future investigation.

8.3.1. Age and species differences.

Since age is the greatest risk factor for AD, it would be pertinent to examine the neurotoxicity of Aβ in old rats. The rats used in the present study were approximately 3 months old and had attained full reproductive maturity, yet it a rat can live for up to 3 years. This age difference does not appear to affect the toxicity of Aβ, since it has been reported that Aβ is not neurotoxic to either young or aged rats (Geula et al., 1998). That study however, used a semi-quantitative method to analyse neuronal death, and so may not have detected a difference that a quantitative method may observe. Using the model presented in this thesis, a preliminary study has been performed on a small number of aged rats (27-30 months) and these results were compared to those obtained in young rats (see Chapter 4). It was found that the neuroprotectiveness of human Aβ1-42 (as reported in Chapter 4) was decreased in the aged rats although it was still not toxic (Bishop and Robinson, 1999). However, this study had a small sample size and would

require a larger sample before firm conclusions could be drawn. The toxicity of Aβ-metal complexes have not been investigated in aged rat cortex, and this may well be a fruitful subject of investigation.

Another consideration arises due to the fact that rats do not spontaneously develop senile plaques in their brains, even when they are of considerable age. There are a number of reasons why this may be the case. Firstly, rats have a much shorter lifespan than humans do, and so they may not 'age' as much during this limited period. Secondly, there may be a decreased opportunity for Aβ deposits to form since rat Aβ differs from human Aβ by three amino acid substitutions (Shivers et al., 1988). This may confer physiological properties that are different to equivalent length human variants, however rat Aβ can still form amyloid fibrils similar to that of human Aβ (Fraser et al., 1992). Lastly, there is the possibility that senile plaques may not be present in rat brains if their phagocytic cells are more efficient at clearing Aβ as soon as it deposits in the neuropil. However, it appears that cultured rat microglial cells respond to Aβ in the same way as human microglial cells (Giulian et al., 1996), so this possibility is unlikely. Since the Aβ sequence of non-human primates is identical to that of humans (Podlisny et al., 1991), and as some of these animals spontaneously develop plaques (Selkoe et al., 1987), non-human primates may provide a better model for studying Aβ toxicity. Indeed, it has been reported that while Aβ is not toxic to young or old rats, or to young monkeys, it is toxic to aged monkey cortex (Geula et al., 1998). Thus, examination of the toxicity of Aβ-metal complexes in aged monkey brain may provide a model that more accurately reflects the neuronal loss that is seen in AD.

8.3.2. The absence of endogenous antioxidants in neuronal cultures.

It has been shown in a cell-free system that the interaction between Aβ and iron or copper generates hydrogen peroxide (Huang et al., 1999a). As discussed in section 6.4.1, astrocytes can protect neurons by detoxifying hydrogen peroxide with the endogenous enzyme glutathione peroxidase (Desagher et al., 1996; Langeveld et al., 1995). However, if Aβ toxicity is studied using an *in vitro* model of cultured neurons, the astrocyte-neuron ratio within the culture is far lower than that seen in the living brain, so the protection that would normally be provided by astrocytes in the brain will be greatly decreased. Indeed the lack of astrocytes may be the reason why Aβ neurotoxicity in cultures of clonal cell lines is observed at concentrations that are 3-4

orders of magnitude lower than that required to produce toxicity in primary neuronal cultures which do contain some astrocytes (see Iversen et al., 1995). Thus, it would be more accurate to use mixed cultures of neurons and astrocytes, where the ratio of cells is in proportion to that seen in the brain. Alternatively, addition of antioxidants to neuronal cultures would help to mimic the protection that would normally be provided if astrocytes were present. Critical consideration also needs to be given to the cell-free models that examine Aβ toxicity in test tubes. These *"in tubo"* models have often been used to shown that Aβ generates free radicals (e.g. Hensley et al., 1994; Huang et al., 1999a; Turnbull et al., 2001). However, the absence of cells and the use of a medium that lacks the physiological complement of antioxidants makes the interpretation of these findings very difficult. Results that have been generated using *in tubo* models represent an extremely simplistic situation, and before these findings can be applied to AD, they should be validated in more complex cellular systems where all types of brain cells are present.

8.3.3. Examination of AGE production by Aβ-metal complexes.

As noted in Chapter 1, AGEs are post-translational modifications to proteins, involving oxidation of sugar residues. AGEs are present in Aβ plaques (Sasaki et al., 1998; Smith et al., 1994; Takedo et al., 1996), and the presence of AGE-modified Aβ may increase the deposition of Aβ into plaques (Vitek et al., 1994). Iron and copper have been reported to accelerate the formation of AGEs on Aβ (Loske et al., 2000). This factor is relevant to the studies reported in Chapters 5 and 6, since the method used to prepare the Aβ-metal complexes for injection may have inadvertently created AGEs. Since AGEs are cytotoxic (Loske et al., 1998), the formation of AGEs by Aβ-metal complexes may be the ultimate cause of the neurotoxicity that was associated with the injected Aβ-metal deposits. This possibility could be examined in future by using antibodies raised against AGEs to determine whether these species are present in the injected Aβ-metal deposits. It would be expected that the Aβ-metal complexes that were associated with significant neuronal loss would contain AGEs, while those that were not neurotoxic would not be associated with significant amounts of AGE formation.

Another consideration arises from the ability of AGEs to activate phagocytic cells such as microglia and macrophages (Miyata et al., 1996; Neumann et al., 1999; Sugimoto et al., 1999). When microglia and macrophages are activated and primed for phagocytosis,

ferritin expression is induced within the cells (Grundke-Iqbal et al., 1990; Kaneko et al., 1989). In Chapter 4 it was reported that pure Aβ deposits did not induce the expression of ferritin in cells to a greater extent than saline injections, indicating that deposits of pure Aβ do not activate microglia and macrophages. The lack of phagocyte activation by pure Aβ deposits may indicate that AGEs are not present within these deposits. This suggestion is consistent with the additional finding in Chapter 4 that showed that these deposits were not neurotoxic compared to the saline vehicle, which also supports a lack of AGEs. If Aβ-metal complexes contain AGEs, then these deposits may be associated with activated phagocytes. Using the method reported in Chapter 4, Aβ-metal complexes could be injected into rat cerebral cortex and the injection sites immunolabelled with ferritin to determine whether these Aβ-metal deposits are associated with an induction of ferritin expression in activated phagocytic cells. If these deposits do contain AGEs, then it would be expected that ferritin-positive cells would be present in greater numbers around Aβ-metal deposits than around control injections of saline.

8.3.4. Investigation of the phagocytes that remove Aβ from the brain.

In Chapter 4 it was found that injected deposits of Aβ were rapidly removed from the brain, however the numbers of ferritin-rich cells associated with the deposits were not significantly different from the numbers associated with saline injections. Since Aβ was observed within small cells at the pial surface, it was suggested in section 4.4.3 that neutrophils may the phagocytic cells that are responsible for removing Aβ from the brain. To determine whether neutrophils infiltrate the injected Aβ deposits, injection sites could be immunolabelled for myeloperoxidase, which is the gold standard for detecting neutrophils (Barone et al., 1991; Schultz and Kaminker, 1962). Furthermore, double-immunolabelling of injection sites for Aβ and myeloperoxidase would determine whether Aβ is present within the neutrophils that are associated with the Aβ deposits.

8.3.5. Is zinc the real pathogenic agent in AD?

In recent years, the demonstration of an imbalance of iron metabolism in AD (Batton et al., 1997; Connor et al., 1992b; Pinero et al., 2000; Smith et al., 1998), along with the presence of oxidative stress (see Markesbery, 1997; Munch et al., 1998), has implicated

iron in the pathogenesis of AD. Alterations in copper metabolism have also become apparent (Lovell et al., 1998), and *in vitro* studies have supported the involvement of copper in AD pathogenesis (Atwood et al., 2000; Huang et al., 1999b). Indeed, considering that copper catalyses the Fenton reaction at an order of magnitude faster than iron (Halliwell and Gutteridge, 1990), it would be expected that copper would increase the toxicity of Aβ to a greater extent than iron. However, the findings in Chapter 6 cast doubt on the importance of copper as a contributor to neurodegeneration in AD.

The findings that Aβ cannot protect against zinc toxicity, and that Aβ tends to increase the toxicity of zinc (see Chapter 6), suggests that zinc may have a greater role in the pathogenesis of AD than was previously suspected. It was originally reported by Bush and colleagues that zinc binds to Aβ and promotes fibril formation (Bush et al., 1994b), and that zinc decreases the tryptic cleavage of Aβ at the secretase site (Bush et al., 1994a). These findings led to their suggestion that zinc may contribute to Aβ amyloidosis and thus have a role in the neuropathogenesis of AD. However this research group has recently reported that zinc "entombs" Aβ and prevents it from causing oxidative damage (Cuajungco et al., 2000), leading to their new suggestion that zinc has a protective role in AD. The results presented in Chapter 6 of this thesis suggest that Bush's original hypothesis has more relevance for *in vivo* systems. Nonetheless, further study is required before we can be sure that an interaction between Aβ and zinc promotes neurodegeneration, in addition to the aggregation of the peptide. Such studies will help to elucidate the involvement of zinc in the pathogenesis of AD.

8.3.6. The formation of plaques and the physiological role of Aβ.

The amyloid hypothesis of AD proposes that an aberrant production of Aβ leads to the deposition of the peptide into plaques, and that Aβ is responsible for the neurodegeneration that is associated with senile plaques (see section 1.2.5). The results presented in this thesis are inconsistent with the view that Aβ is the primary cause of neurotoxicity in AD. Indeed, the results show that Aβ itself is not neurotoxic, which is consistent with the view that Aβ may serve a physiological role. The results described in Chapters 5 and 6 suggest that a potential physiological role of Aβ may be to chelate excess redox-active metal ions in order to reduce oxidative stress.

Pathological stimuli such as inflammation or oxidative stress stimulate the production of KPI-APP (Abe et al., 1991; Banati et al., 1995; Brugg et al., 1995; Gray and Patel, 1993; Kim et al., 1998), which can be cleaved to produce the Aβ peptide. Both inflammation and oxidative stress are associated with an elevation of metal ions, and Aβ will bind these metal ions, promoting the aggregation of the peptide. The aggregated Aβ-metal complex will precipitate and promote an inflammatory reaction so that phagocytes are stimulated to remove the deposit from the brain. The ability of Aβ to decrease the toxicity of redox-active metal ions suggests that the formation of Aβ plaques may be a neuroprotective mechanism that is designed to remove toxic metals from the extracellular fluid of the brain. It is important to note however, that Aβ-metal complexes will cause some neurotoxicity, although this toxicity will be less than what would occur if the metals were not removed from the extracellular fluid. If the amount of metals present is excessive, then Aβ may not be sufficient to neutralise the toxic stimulus, and as a result, neuronal death will occur. Alternatively, if the Aβ-metal plaques are not removed from the brain, neurodegeneration will occur. The brain can tolerate some neurodegeneration without having a significant loss of function, however when the amount of neurodegeneration exceeds this level of tolerance, the loss of functions associated with AD will result.

Even very small occurrences of oxidative stress or inflammation may be enough to release small amounts of metals that can stimulate Aβ to bind and neutralise the metals, and form a senile plaque in the process. The presence of numerous senile plaques in the brains of non-demented aged humans may indicate that these people have undergone many episodes of such stimuli, and given enough time they may have developed a clinical presentation of AD. A more specific example of such pathological stimuli is seen in cases of traumatic brain injury, where there can be numerous plaques within the brain (e.g. Roberts et al., 1994). These patients also have an increase in the level of cortical iron (Bouras et al., 1997), thus in these people, Aβ plaques may have formed in an attempt to neutralise the excess iron present within their brains.

The possibility that Aβ may function as a chelator of excess metal ions within the brain is widely accepted. It may be possible that Aβ serves not only as a metal chelator, but as a general chelator and bioflocculant of toxic substances that are present within the brain, as we have hypothesised elsewhere (Robinson and Bishop, in press). If Aβ does in fact have such a beneficial role, then removal of the peptide from the brain by anti-

amyloidogenic agents will remove the protection that is normally afforded by Aβ. If these agents are administered to animals, and the animal undergoes episodes of oxidative stress of inflammation, then it would be predicted that the removal of Aβ will result in more rapid neurodegeneration. Similarly in humans, the removal of Aβ from the brain may decrease the number of Aβ deposits, but would hasten the rate of neurodegenerative decline in AD.

8.4. Conclusion.

The results presented in this thesis have provided valuable information regarding the *in vivo* neurotoxicity of Aβ and the potentiation of this neurotoxicity by the metal ions that are normally present in plaques in AD. The increased neurotoxicity of some Aβ-metal complexes indicates that the presence of metal ions within plaques may contribute to the neurodegeneration seen in AD brains. These findings have implications for the treatment of AD, since they indicate that for anti-amyloidogenic agents to be successful, they must be combined with chelation therapy.

This thesis has also reported an unexpected finding that Aβ can protect against the neurotoxicity of redox-active metal ions, which suggests a physiological role of Aβ may be to neutralise toxic metals. This novel finding suggests that plaques may form in order to reduce the neurotoxicity of elevated metal ions in the brain, and it provides an alternative explanation for the involvement of Aβ in the pathogenesis of AD.

References

Abe K., Tanzi R.E. and Kogure K. (1991) Selective induction of Kunitz-type protease inhibitor domain-containing amyloid precursor protein mRNA after persistent focal ischemia in rat cerebral cortex, Neurosci. Lett. 125:172-174.

Abraham C.R., Selkoe D.J. and Potter H. (1988) Immunochemical identification of the serine protease inhibitor α_1-antichymotrypsin in the brain amyloid deposits of Alzheimer's disease, Cell 52:487-501.

Aksenov M., Aksenova M.V., Harris M.E., Hensley K., Butterfield D.A. and Carney J.M. (1995) Enhancement of β-amyloid peptide Aβ(1-40)-mediated neurotoxicity by glutamine synthetase, J. Neurochem. 65:1899-1902.

Allen D.R., Wallis G.L. and McCay P.B. (1994) Catechol adrenergic agents enhance hydroxyl radical generation in xanthine oxidase systems containing ferritin: implications for ischemia/reperfusion, Arch. Biochem. Biophys. 315:235-243.

Anderson J.J., Holtz G., Baskin P.P., Wang R., Mazzarelli L., Wagner S.L. and Menzaghi F. (1999) Reduced cerebrospinal fluid levels of α-secretase-cleaved amyloid precursor protein in aged rats: correlation with spatial memory deficits, Neuroscience 93:1409-1420.

Arendash G.W., King D.L., Gordon M.N., Morgan D., Hatcher J.M., Hope C.E. and Diamond D.M. (2001) Progressive, age-related behavioral impairments in transgenic mice carrying both mutant amyloid precursor protein and presenilin-1 transgenes, Brain Res. 891:42-53.

Arispe N., Pollard H.B. and Rojas E. (1993a) Giant multilevel cation channels formed by Alzheimer disease amyloid β-protein [AβP-(1-40)] in bilayer membranes, Proc. Natl. Acad. Sci. U. S. A. 90:10573-10577.

Arispe N., Rojas E. and Pollard H.B. (1993b) Alzheimer disease amyloid β protein forms calcium channels in bilayer membranes: blockade by tromethamine and aluminum, Proc. Natl. Acad. Sci. U. S. A. 90:567-571.

Armstrong C., Leong W. and Lees G.J. (2001) Comparative effects of metal chelating agents on the neuronal cytotoxicity induced by copper (Cu^{+2}), iron (Fe^{+3}) and zinc in the hippocampus, Brain Res. 892:51-62.

Arnold S.E., Hyman B.T., Flory J., Damasio A.R. and Van Hoesen G.W. (1991) The topographical and neuroanatomical distribution of neurofibrillary tangles and neuritic plaques in the cerebral cortex of patients with Alzheimer's dise..., Cereb. Cortex 1:103-116.

Arriagada P.V., Growdon J.H., Hedley-Whyte E.T. and Hyman B.T. (1992) Neurofibrillary tangles but not senile plaques parallel duration and severity of Alzheimer's disease, Neurology 42:631-639.

Asthana S., Baker L.D., Craft S., Stanczyk F.Z., Veith R.C., Raskind M.A. and Plymate S.R. (2001) High-dose estradiol improves cognition for women with AD: results of a randomized study, Neurology 57:605-612.

Atwood C.S., Moir R.D., Huang X., Scarpa R.C , Bacarra N.M., Romano D.M., Hartshorn M.A., Tanzi R.E. and Bush A.I. (1998) Dramatic aggregation of Alzheimer Aβ by Cu(II) is induced by conditions representing physiological acidosis, J. Biol. Chem. 273:12817-12826.

Atwood C.S., Scarpa R.C., Huang X., Moir R.D., Jones W.D., Fairlie D.P., Tanzi R.E. and Bush A.I. (2000) Characterization of copper interactions with Alzheimer amyloid β peptides: identification of an attomolar-affinity copper binding site on amyloid β1-42, J. Neurochem. 75:1219-1233.

Axelman K., Basun H., Winblad B. and Lannfelt L. (1994) A large Swedish family with Alzheimer's disease with a codon 670/671 amyloid precursor protein mutation, Arch. Neurol. 51:1193-1197.

Bae Y.H., Hwang J.Y., Kim Y.H. and Koh J.Y. (2000) Anti-oxidative neuroprotection by estrogens in mouse cortical cultures. J. Korean Med. Sci. 15:327-336.

Balakrishnan R., Parthasarathy R. and Sulkowski E. (1998) Alzheimer's β-amyloid peptide: affinity for metal chelates, J. Pept. Res. 51:91-95.

Baldereschi M., Di Carlo A., Lepore V., Bracco L., Maggi S., Grigoletto F., Scarlato G. and Amaducci L. (1998) Estrogen-replacement therapy and Alzheimer's disease in the Italian Longitudinal Study on Aging, Neurology 50:996-1002.

Bales K.R., Verina T., Cummins D.J., Du Y., Dodel R.C., Saura J., Fishman C.E., DeLong C.A., Piccardo P., Petegnief V., Ghetti B. and Paul S.M. (1999) Apolipoprotein E is essential for amyloid deposition in the APP^{V717F} transgenic mouse model of Alzheimer's disease, Proc. Natl. Acad. Sci. U. S. A. 96:15233-15238.

Banati R.B., Gehrmann J., Wiessner C., Hossmann K.A. and Kreutzberg G.W. (1995) Glial expression of the β-amyloid precursor protein (APP) in global ischemia, J. Cereb. Blood Flow Metab. 15:647-654.

Barone F.C., Hillegass L.M., Price W.J., White R.F., Lee E.V., Feuerstein G.Z., Sarau H.M., Clark R.K. and Griswold D.E. (1991) Polymorphonuclear leukocyte

infiltration into cerebral focal ischemic tissue: myeloperoxidase activity assay and histologic verification, J. Neurosci. Res. 29:336-345.

Barrow C.J. and Zagorski M.G. (1991) Solution structures of β peptide and its constituent fragments: relation to amyloid deposition, Science 253:179-182.

Batton C.I., O'Dowd B.S., Noone D.F., Kril J. and Robinson S.R. (1997) Ferritin-rich microglia are concentrated within β-amyloid plaques, Alzheimer's Res. 3:23-28.

Behl C., Davis J., Cole G.M. and Schubert D. (1992) Vitamin E protects nerve cells from amyloid β protein toxicity, Biochem. Biophys. Res. Commun. 186:944-950.

Behl C., Davis J.B., Lesley R. and Schubert D. (1994) Hydrogen peroxide mediates amyloid β protein toxicity, Cell 77:817-827.

Behl C., Skutella T., Lezoualc'h F., Post A., Widmann M., Newton C.J. and Holsboer F. (1997) Neuroprotection against oxidative stress by estrogens: structure- activity relationsl ip, Mol. Pharmacol. 51:535-541.

Behl C., Widmann M., Trapp T. and Holsboer F. (1995) 17-β estradiol protects neurons from oxidative stress-induced cell death *in vitro*, Biochem. Biophys. Res. Commun. 216:473-482.

Ben-Shachar D. and Youdim M.B. (1991) Intranigral iron injection induces behavioral and biochemical "parkinsonism" in rats, J. Neurochem. 57:2133-2135.

Benkovic S.A. and Connor J.R. (1993) Ferritin, transferrin and iron in selected regions of adult and aged rat brain, J. Comp. Neurol. 338:97-113.

Berg J.M. and Shi Y. (1996) The galvanization of biology: a growing appreciation for the roles of zinc, Science 271:1081-1085.

Berg L. and Morris J.C. (1994) Diagnosis. In Terry R.D., Katzman R. and Bick K.L. (Eds.), *Alzheimer Disease*, 1st Edition edn., Raven Press, New York, pp. 9-25.

Bergamaschini L., Canziani S., Bottasso B., Cugno M., Braidotti P. and Agostoni A. (1999) Alzheimer's β-amyloid peptides can activate the early components of complement classical pathway in a C1q-independent manner, Clin. Exp. Immunol. 115:526-533.

Berr C., Hauw J.J., Delaere P., Duyckaerts C. and Amouyel P. (1994) Apolipoprotein E allele epsilon 4 is linked to increased deposition of the amyloid β-peptide (A-β) in cases with or without Alzheimer's disease, Neurosci. Lett. 178:221-224.

Beyreuther K., Pollwein P., Multhaup G., Monning U., Konig G., Dyrks T., Schubert W. and Masters C.L. (1993) Regulation and expression of the Alzheimer's β/A4

amyloid protein precursor in health, disease, and Down's syndrome, Ann. N. Y. Acad. Sci. 695:91-102.

Bianca V.D., Dusi S., Bianchini E., Dal Pra I. and Rossi F. (1999) β-amyloid activates the $O^{\cdot}_2$ forming NADPH oxidase in microglia, monocytes, and neutrophils. A possible inflammatory mechanism of neuronal damage in Alzheimer's disease, J. Biol. Chem. 274:15493-15499.

Biemond P., Swaak A.J., van Eijk H.G. and Koster J.F. (1988) Superoxide dependent iron release from ferritin in inflammatory diseases, Free Radic. Biol. Med. 4:185-198.

Bird T.D. (1994) Clinical genetics of familial Alzheimer disease. In Terry R.D., Katzman R. and Bick K.L. (Eds.), *Alzheimer Disease,* 1st Edition edn., Raven Press, New York, pp. 65-74.

Bishop G.M. and Robinson S.R. (1999) β-amyloid provides less neuroprotection in old rats, Proc. Aust. Neuroscience Soc. 10:212.

Bondy S.C., Guo-Ross S.X. and Truong A.T. (1998) Promotion of transition metal-induced reactive oxygen species formation by β-amyloid, Brain Res. 799:91-96.

Borchelt D.R., Ratovitski T., van Lare J., Lee M.K., Gonzales V., Jenkins N.A., Copeland N.G., Price D.L. and Sisodia S.S. (1997) Accelerated amyloid deposition in the brains of transgenic mice coexpressing mutant presenilin 1 and amyloid precursor proteins, Neuron 19:939-945.

Borchelt D.R., Thinakaran G., Eckman C.B., Lee M.K., Davenport F., Ratovitsky T., Prada C.M., Kim G., Seekins S., Yager D., Slunt H.H., Wang R., Seeger M., Levey A.I., Gandy S.E., Copeland N.G., Jenkins N.A., Price D.L., Younkin S.G. and Sisodia S.S. (1996) Familial Alzheimer's disease-linked presenilin 1 variants elevate Aβ1-42/1-40 ratio *in vitro* and *in vivo*, Neuron 17:1005-1013.

Bouras C., Giannakopoulos P., Good P.F., Hsu A., Hof P.R. and Perl D.P. (1997) A laser microprobe mass analysis of brain aluminum and iron in dementia pugilistica: comparison with Alzheimer's disease, Eur. Neurol. 38:53-58.

Braak H. and Braak E. (1991) Neuropathological stageing of Alzheimer-related changes, Acta Neuropathol. 82:239-259.

Bradt B.M., Kolb W.P. and Cooper N.R. (1998) Complement-dependent proinflammatory properties of the Alzheimer's disease β-peptide, J. Exp. Med. 188:431-438.

Bronfman F.C., Moechars D. and Van Leuven F. (2000) Acetylcholinesterase-positive fiber deafferentation and cell shrinkage in the septohippocampal pathway of

aged amyloid precursor protein London mutant transgenic mice, Neurobiol. Dis. 7:152-168.

Brousseau T., Legrain S., Berr C., Gourlet V., Vidal O. and Amouyel P. (1994) Confirmation of the ε4 allele of the apolipoprotein E gene as a risk factor for late-onset Alzheimer's disease, Neurology 44:342-344.

Brugg B., Dubreuil Y.L., Huber G., Wollman E.E., Delhaye-Bouchaud N. and Mariani J. (1995) Inflammatory processes induce β-amyloid precursor protein changes in mouse brain, Proc. Natl. Acad. Sci. U. S. A. 92:3032-3035.

Brumback R.A. and Lapham L.W. (1989) DNA synthesis in Alzheimer type II astrocytosis. The question of astrocytic proliferation and mitosis in experimentally induced hepatic encephalopathy, Arch. Neurol. 46:845-848.

Buckler H.M., Kalsi P.K., Cantrill J.A. and Anderson D.C. (1995) An audit of oestradiol levels and implant frequency in women undergoing subcutaneous implant therapy, Clin. Endocrinol. 42:445-450.

Burdick D., Soreghan B., Kwon M., Kosmoski J., Knauer M., Henschen A., Yates J., Cotman C. and Glabe C. (1992) Assembly and aggregation properties of synthetic Alzheimer's A4/β amyloid peptide analogs, J. Biol. Chem. 267:546-554.

Bush A.I., Pettingell W.H., Jr., Paradis M.D. and Tanzi R.E. (1994a) Modulation of Aβ adhesiveness and secretase site cleavage by zinc, J. Biol. Chem. 269:12152-12158.

Bush A.I., Pettingell W.H., Multhaup G., d Paradis M., Vonsattel J.P., Gusella J.F., Beyreuther K., Masters C.L. and Tanzi R.E. (1994b) Rapid induction of Alzheimer Aβ amyloid formation by zinc, Science 265:1464-1467.

Butterfield D.A., Hensley K., Harris M., Mattson M. and Carney J. (1994) β-Amyloid peptide free radical fragments initiate synaptosomal lipoperoxidation in a sequence-specific fashion: implications to Alzheimer's disease, Biochem. Biophys. Res. Commun. 200:710-715.

Calhoun M.E., Wiederhold K.H., Abramowski D., Phinney A.L., Probst A., Sturchler-Pierrat C., Staufenbiel M., Sommer B. and Jucker M. (1998) Neuron loss in APP transgenic mice, Nature 395:755-756.

Callier S., Morissette M., Grandbois M., Pelaprat D. and Di Paolo T. (2001) Neuroprotective properties of 17β-estradiol, progesterone, and raloxifene in MPTP C57Bl/6 mice, Synapse 41:131-138.

Chang D., Kwan J. and Timiras P.S. (1997) Estrogens influence growth, maturation, and amyloid β-peptide production in neuroblastoma cells and in a β-APP transfected kidney 293 cell line, Adv. Exp. Med. Biol. 429:261-271.

Chartier-Harlin M.C., Crawford F., Houlden H., Warren A., Hughes D., Fidani L., Goate A., Rossor M., Roques P., Hardy J. and Mullan M. (1991) Early-onset Alzheimer's disease caused by mutations at codon 717 of the β-amyloid precursor protein gene, Nature 353:844-846.

Chartier-Harlin M.C., Parfitt M., Legrain S., Perez-Tur J., Brousseau T., Evans A., Berr C., Vidal O., Roques P., Gourlet V., Fruchart J.C., Delacourte A., Rossor M. and Amouyel P. (1994) Apolipoprotein E, ε4 allele as a major risk factor for sporadic early and late-onset forms of Alzheimer's disease: analysis of the 19q13.2 chromosomal region, Hum. Mol. Genet. 3:569-574.

Cheepsunthorn P., Palmer C., Menzies S., Roberts R.L. and Connor J.R. (2001) Hypoxic/ischemic insult alters ferritin expression and myelination in neonatal rat brains, J. Comp. Neurol. 431:382-396.

Chen G., Chen K.S., Knox J., Inglis J., Bernard A., Martin S.J., Justice A., McConlogue L., Games D., Freedman S.B. and Morris R.G. (2000) A learning deficit related to age and β-amyloid plaques in a mouse model of Alzheimer's disease, Nature 408:975-979.

Chen J., Lei T., Ritz M.F. and Mendelowitsch A. (2001) Effect of 17β-estradiol on the brain damage and metabolic changes in rats, J. Tongji Med. Univ. 21:62-64.

Choi D.W., Yokoyama M. and Koh J. (1988) Zinc neurotoxicity in cortical cell culture, Neuroscience 24:67-79.

Chui D.H., Tanahashi H., Ozawa K., Ikeda S., Checler F., Ueda O., Suzuki H., Araki W., Inoue H., Shirotani K., Takahashi K., Gallyas F. and Tabira T. (1999) Transgenic mice with Alzheimer presenilin 1 mutations show accelerated neurodegeneration without amyloid plaque formation, Nat. Med. 5:560-564.

Citron M., Teplow D.B. and Selkoe D.J. (1995) Generation of amyloid β protein from its precursor is sequence specific, Neuron 14:661-670.

Clemens J.A. and Stephenson D.T. (1992) Implants containing β-amyloid protein are not neurotoxic to young and old rat brain, Neurobiol. Aging 13:581-586.

Combs C.K., Johnson D.E., Karlo J.C., Cannady S.B. and Landreth G.E. (2000) Inflammatory mechanisms in Alzheimer's disease: inhibition of β-amyloid-stimulated proinflammatory responses and neurotoxicity by PPARγ agonists, J. Neurosci. 20:558-567.

Connor J.R., Menzies S.L., St Martin S.M. and Mufson E.J. (1992a) A histochemical study of iron, transferrin, and ferritin in Alzheimer's diseased brains, J. Neurosci. Res. 31:75-83.

Connor J.R., Snyder B.S., Beard J.F., Fine R.E. and Mufson E.J. (1992b) Regional distribution of iron and iron-regulatory proteins in the brain in aging and Alzheimer's disease, J. Neurosci. Res. 31:327-335.

Cotton F.A., Wilkinson G. and Gaus P.L. (1995) *Basic Inorganic Chemistry*, 3rd edn., John Wiley and Sons, Inc., New York.

Crystal H., Dickson D., Fuld P., Masur D., Scott R., Mehler M., Masdeu J., Kawas C., Aronson M. and Wolfson L. (1988) Clinico-pathologic studies in dementia: nondemented subjects with pathologically confirmed Alzheimer's disease, Neurology 38:1682-1687.

Cuajungco M.P., Goldstein L.E., Nunomura A., Smith M.A., Lim J.T., Atwood C.S., Huang X., Farrag Y.W., Perry G. and Bush A.I. (2000) Evidence that the β amyloid plaques of Alzheimer's disease represent the redox-silencing and entombment of Aβ by zinc, J. Biol. Chem. 275:19439-19442.

Cuajungco M.P. and Lees G.J. (1998) Diverse effects of metal chelating agents on the neuronal cytotoxicity of zinc in the hippocampus, Brain Res. 799:97-107.

Culmsee C., Vedder H., Ravati A., Junker V., Otto D., Ahlemeyer B., Krieg J.C. and Krieglstein J. (1999) Neuroprotection by estrogens in a mouse model of focal cerebral ischemia and in cultured neurons: evidence for a receptor-independent antioxidative mechanism, J. Cereb. Blood Flow Metab. 19:1263-1269.

Cummings B.J., Pike C.J., Shankle R. and Cotman C.W. (1996) β-amyloid deposition and other measures of neuropathology predict cognitive status in Alzheimer's disease, Neurobiol. Aging 17:1-27.

Czech C., Lesort M., Tremp G., Terro F., Blanchard V., Schombert B., Carpentier N., Dreisler S., Bonici B., Takashima A., Moussaoui S., Hugon J. and Pradier L. (1998) Characterization of human presenilin 1 transgenic rats: increased sensitivity to apoptosis in primary neuronal cultures, Neuroscience 87:325-336.

Daly J. and Kotwal G.J. (1998) Pro-inflammatory complement activation by the Aβ peptide of Alzheimer's disease is biologically significant and can be blocked by vaccinia virus complement control protein, Neurobiol. Aging 19:619-627.

Delaere P., Duyckaerts C., He Y., Piette F. and Hauw J.J. (1991) Subtypes and differential laminar distributions of βA4 deposits in Alzheimer's disease:

relationship with the intellectual status of 26 cases, Acta Neuropathol. 81:328-335.

Desagher S., Glowinski J. and Premont J. (1996) Astrocytes protect neurons from hydrogen peroxide toxicity, J. Neurosci. 16:2553-2562.

Dikalov S.I., Vitek M.P., Maples K.R. and Mason R.P. (1999) Amyloid β peptides do not form peptide-derived free radicals spontaneously, but can enhance metal-catalyzed oxidation of hydroxylamines to nitroxides, J. Biol. Chem. 274:9392-9399.

Dodart J.C., Mathis C., Bales K.R., Paul S.M. and Ungerer A. (1999a) Early regional cerebral glucose hypometabolism in transgenic mice overexpressing the V717F β-amyloid precursor protein, Neurosci. Lett. 277:49-52.

Dodart J.C., Mathis C., Saura J., Bales K.R., Paul S.M. and Ungerer A. (2000) Neuroanatomical abnormalities in behaviorally characterized APP^{V717F} transgenic mice, Neurobiol. Dis. 7:71-85.

Dodart J.C., Meziane H., Mathis C., Bales K.R., Paul S.M. and Ungerer A. (1999b) Behavioral disturbances in transgenic mice overexpressing the V717F β-amyloid precursor protein, Behav. Neurosci. 113:982-990.

Dornan W.A., Kang D.E., McCampbell A. and Kang E.E. (1993) Bilateral injections of βA(25-35) + IBO into the hippocampus disrupts acquisition of spatial learning in the rat, Neuroreport 5:165-168.

Dringen R. and Hamprecht B. (1997) Involvement of glutathione peroxidase and catalase in the disposal of exogenous hydrogen peroxide by cultured astroglial cells, Brain Res. 759:67-75.

Dringen R., Kussmaul L., Gutterer J.M., Hirrlinger J. and Hamprecht B. (1999) The glutathione system of peroxide detoxification is less efficient in neurons than in astroglial cells, J. Neurochem. 72:2523-2530.

Duff K., Eckman C., Zehr C., Yu X., Prada C.M., Perez-tur J., Hutton M., Buee L., Harigaya Y., Yager D., Morgan D., Gordon M.N., Holcomb L., Refolo L., Zenk B., Hardy J. and Younkin S. (1996) Increased amyloid-β42(43) in brains of mice expressing mutant presenilin 1, Nature 383:710-713.

Durell S.R., Guy H.R., Arispe N., Rojas E. and Pollard H.B. (1994) Theoretical models of the ion channel structure of amyloid β-protein, Biophys. J. 67:2137-2145.

Dyrks T., Dyrks E., Monning U., Urmoneit B., Turner J. and Beyreuther K. (1993) Generation of βA4 from the amyloid protein precursor and fragments thereof, FEBS Lett. 335:89-93.

Emre M., Geula C., Ransil B.J. and Mesulam M.M. (1992) The acute neurotoxicity and effects upon cholinergic axons of intracerebrally injected β-amyloid in the rat brain, Neurobiol. Aging 13:553-559.

Esler W.P. and Wolfe M.S. (2001) A portrait of Alzheimer secretases - new features and familiar faces, Science 293:1449-1454.

Everett J.W. (1989) Neurobiology of reproduction in the female rat. A fifty-year perspective, Monogr. Endocrinol. 32:1-133.

Farrer L.A., Cupples L.A., Haines J.L., Hyman B., Kukull W.A., Mayeux R., Myers R.H., Pericak-Vance M.A., Risch N. and van Duijn C.M. (1997) Effects of age, sex, and ethnicity on the association between apolipoprotein E genotype and Alzheimer disease. A meta-analysis, JAMA 278:1349-1356.

Focht S.J., Snyder B.S., Beard J.L., Van Gelder W., Williams L.R. and Connor J.R. (1997) Regional distribution of iron, transferrin, ferritin, and oxidatively-modified proteins in young and aged Fischer 344 rat brains, Neuroscience 79:255-261.

Folstein M.F. and Bylsma F.W. (1994) Noncognitive symptoms of Alzheimer disease. In Terry R.D., Katzman R. and Bick K.L. (Eds.), *Alzheimer Disease*, 1st Edition edn., Raven Press, New York, pp. 27-40.

Fox R.R. and Laird C.W. (1970) Sexual cycles. In Hafez E.S.E. (Ed.), *Reproduction and Breeding Techniques for Laboratory Animals*, Lea & Febiger, Philadelphia.

Fox S.R., Bishop G.M. and Robinson S.R. (1999) High levels of microglial iron in the cortices of old primates: implications for the neurotoxicity of β-amyloid, Proc. Aust. Neuroscience Soc. 10:213.

Fraser P.E., Nguyen J.T., Inouye H., Surewicz W.K., Selkoe D.J., Podlisny M.B. and Kirschner D.A. (1992) Fibril formation by primate, rodent, and Dutch-hemorrhagic analogues of Alzheimer amyloid β-protein, Biochemistry 31:10716-10723.

Fraser P.E., Nguyen J.T., Surewicz W.K. and Kirschner D.A. (1991) pH-dependent structural transitions of Alzheimer amyloid peptides, Biophys. J. 60:1190-1201.

Frautschy S.A., Baird A. and Cole G.M. (1991) Effects of injected Alzheimer β-amyloid cores in rat brain, Proc. Natl. Acad. Sci. U. S. A. 88:8362-8366.

Frautschy S.A., Horn D.L., Sigel J.J., Harris-White M.E., Mendoza J.J., Yang F., Saido T.C. and Cole G.M. (1998) Protease inhibitor coinfusion with amyloid β-protein results in enhanced deposition and toxicity in rat brain, J. Neurosci. 18:8311-8321.

Freeman J.J. and Hayes E.P. (1988) Microsomal metabolism of acetonitrile to cyanide. Effects of acetone and other compounds, Biochem. Pharmacol. 37:1153-1159.

Fuernkranz H.A., Schwob J.E. and Lucas J.J. (1991) Differential tissue localization of oviduct and erythroid transferrin receptors, Proc. Natl. Acad. Sci. U. S. A. 88:7505-7508.

Fukumoto H., Asami-Odaka A., Suzuki N. and Iwatsubo T. (1996) Association of Aβ40-positive senile plaques with microglial cells in the brains of patients with Alzheimer's disease and in non-demented aged individuals, Neurodegeneration 5:13-17.

Games D., Adams D., Alessandrini R., Barbour R., Berthelette P., Blackwell C., Carr T., Clemens J., Donaldson T., Gillespie F., Guido T., Hagoplan S., Johnson-Wood K., Khan K., Lee M., Leibowitz P., Lieberburg I., Little S., Masliah E., McConlogue L., Montoya-Zavala M., Mucke L., Paganini L., E. P., Power M., Schenk D., Seubert P., Snyder B., Soriano F., Tan H., Vitale J., Wadsworth S., Wolozin B. and Zhao J. (1995) Alzheimer-type neuropathology in transgenic mice overexpressing V717F β-amyloid precursor protein, Nature 373:523-527.

Games D., Khan K.M., Soriano F.G., Keim P.S., Davis D.L., Bryant K. and Lieberburg I. (1992) Lack of Alzheimer pathology after β-amyloid protein injections in rat brain, Neurobiol. Aging 13:569-576.

Garcia-Segura L.M., Azcoitia I. and DonCarlos L.L. (2001) Neuroprotection by estradiol, Prog. Neurobiol. 63:29-60.

Garzon-Rodriguez W., Yatsimirsky A.K. and Glabe C.G. (1999) Binding of Zn(II), Cu(II), and Fe(II) ions to Alzheimer's Aβ peptide studied by fluorescence, Bioorg. Med. Chem. Lett. 9:2243-2248.

Geula C., Wu C.K., Saroff D., Lorenzo A., Yuan M. and Yankner B.A. (1998) Aging renders the brain vulnerable to amyloid β-protein neurotoxicity, Nat. Med. 4:827-831.

Ghersi-Egea J.F., Gorevic P.D., Ghiso J., Frangione B., Patlak C.S. and Fenstermacher J.D. (1996) Fate of cerebrospinal fluid-borne amyloid β-peptide: rapid clearance into blood and appreciable accumulation by cerebral arteries, J. Neurochem. 67:880-883.

Giordano T., Pan J.B., Monteggia L.M., Holzman T.F., Snyder S.W., Krafft G., Ghanbari H. and Kowall N.W. (1994) Similarities between β amyloid peptides 1-40 and 40-1: effects on aggregation, toxicity *in vitro*, and injection in young and aged rats, Exp. Neurol. 125:175-182.

Giovannelli L., Casamenti F., Scali C., Bartolini L. and Pepeu G. (1995) Differential effects of amyloid peptides β-(1-40) and β-(25-35) injections into the rat nucleus basalis, Neuroscience 66:781-792.

Giovannelli L., Scali C., Faussone-Pellegrini M.S., Pepeu G. and Casamenti F (1998) Long-term changes in the aggregation state and toxic effects of β-amyloid injected into the rat brain, Neuroscience 87:349-357.

Giulian D., Haverkamp L.J., Li J., Karshin W.L., Yu J., Tom D., Li X. and Kirkpatrick J.B. (1995) Senile plaques stimulate microglia to release a neurotoxin found in Alzheimer brain, Neurochem. Int. 27:119-137.

Giulian D., Haverkamp L.J., Yu J.H., Karshin W., Tom D., Li J., Kirkpatrick J., Kuo L.M. and Roher A.E. (1996) Specific domains of β-amyloid from Alzheimer plaque elicit neuron killing in human microglia, J. Neurosci. 16:6021-6037.

Goldberg M.P., Weiss J.H., Pham P.C. and Choi D.W. (1987) N-methyl-D-aspartate receptors mediate hypoxic neuronal injury in cortical culture, J. Pharmacol. Exp. Ther. 243:784-791.

Goldgaber D., Lerman M.I., McBride O.W., Saffiotti U. and Gajdusek D.C. (1987) Characterization and chromosomal localization of a cDNA encoding brain amyloid of Alzheimer's disease, Science 235:877-880.

Gong C., Hoff J.T. and Keep R.F. (2000) Acute inflammatory reaction following experimental intracerebral hemorrhage in rat, Brain Res. 871:57-65.

Gray C.W. and Patel A.J. (1993) Regulation of β-amyloid precursor protein isoform mRNAs by transforming growth factor-β1 and interleukin-1β in astrocytes, Mol. Brain Res. 19:251-256.

Gray C.W. and Patel A.J. (1995) Neurodegeneration mediated by glutamate and β-amyloid peptide: a comparison and possible interaction, Brain Res. 691:169-179.

Grundke-Iqbal I., Fleming J., Tung Y.C., Lassmann H., Iqbal K. and Joshi J.G. (1990) Ferritin is a component of the neuritic (senile) plaque in Alzheimer dementia, Acta Neuropathol. 81:105-110.

Guenette S.Y. and Tanzi R.E. (1999) Progress toward valid transgenic mouse models for Alzheimer's disease, Neurobiol. Aging 20:201-211.

Haass C., Hung A.Y., Schlossmacher M.G., Teplow D.B. and Selkoe D.J. (1993) β-Amyloid peptide and a 3-kDa fragment are derived by distinct cellular mechanisms, J. Biol. Chem. 268:3021-3024.

Hallgren B. and Sourander P. (1958) The effect of age on the non-haemin iron in the human brain, J. Neurochem. 3:41-51.

Halliwell B. (1989) Protection against tissue damage *in vivo* by desferrioxamine: what is its mechanism of action?, Free Radic. Biol. Med. 7:645-651.

Halliwell B. and Gutteridge J.M. (1990) Role of free radicals and catalytic metal ions in human disease: an overview, Methods Enzymol. 186:1-85.

Halliwell B. and Gutteridge J.M.C. (1999) *Free Radicals in Biology and Medicine*, 3rd edn edn., Oxford University Press, Oxford.

Hardy J. and Higgins G.A. (1992) Alzheimer's disease: the amyloid cascade hypothesis, Science 256:184-185.

Harris M.E., Hensley K., Butterfield D.A., Leedle R.A. and Carney J.M. (1995) Direct evidence of oxidative injury produced by the Alzheimer's β-amyloid peptide (1-40) in cultured hippocampal neurons, Exp. Neurol. 131:193-202.

Henderson V.W., Paganini-Hill A., Emanuel C.K., Dunn M.E. and Buckwalt . J.G. (1994) Estrogen replacement therapy in older women. Comparisons between Alzheimer's disease cases and nondemented control subjects, Arch. Neurol. 51:896-900.

Hendriks L., van Duijn C.M., Cras P., Cruts M., Van Hul W., van Harskamp F., Warren A., McInnis M.G., Antonarakis S.E., Martin J.J., Hofman A. and Van Broeckhoven C. (1992) Presenile dementia and cerebral haemorrhage linked to a mutation at codon 692 of the β-amyloid precursor protein gene, Nat. Genet. 1:218-221.

Hensley K., Aksenova M., Carney J.M., Harris M. and Butterfield D.A. (1995) Amyloid β-peptide spin trapping. I: Peptide enzyme toxicity is related to free radical spin trap reactivity, Neuroreport 6:489-492.

Hensley K., Carney J.M., Mattson M.P., Aksenova M., Harris M., Wu J.F., Floyd R.A. and Butterfield D.A. (1994) A model for β-amyloid aggregation and neurotoxicity based on free radical generation by the peptide: relevance to Alzheimer disease, Proc. Natl. Acad. Sci. U. S. A. 91:3270-3274.

Hertz L., Dringen R., Schousboe A. and Robinson S.R. (1999) Astrocytes: glutamate producers for neurons, J. Neurosci. Res. 57:417-428.

Hilbich C., Kisters-Woike B., Reed J., Masters C.L. and Beyreuther K. (1991) Aggregation and secondary structure of synthetic amyloid βA4 peptides of Alzheimer's disease, J. Mol. Biol. 218:149-163.

Hill J.M. (1982) Brain iron: sex difference and changes during the estrous cycle and pregnancy. In Saltman P. and Hegenauer J. (Eds.), *The Biochemistry and Physiology of Iron*, Elsevier, North Holland, pp. 599-601.

Ho L., Fukuchi K. and Younkin S.G. (1996) The alternatively spliced Kunitz protease inhibitor domain alters amyloid β protein precursor processing and amyloid β protein production in cultured cells, J. Biol. Chem. 271:30929-30934.

Hof P.R. and Morrison J.H. (1994) The cellular basis of cortical disconnection in Alzheimer disease and related dementing conditions. In Terry R.D., Katzman R. and Bick K.L. (Eds.), *Alzheimer Disease*, 1st Edition edn., Raven Press, New York, pp. 197-229.

Holcomb L., Gordon M.N., McGowan E., Yu X., Benkovic S., Jantzen P., Wright K., Saad I., Mueller R., Morgan D., Sanders S., Zehr C., O'Campo K., Hardy J., Prada C.M., Eckman C., Younkin S., Hsiao K. and Duff K. (1998) Accelerated Alzheimer-type phenotype in transgenic mice carrying both mutant amyloid precursor protein and presenilin 1 transgenes, Nat. Med. 4:97-100.

Holcomb L.A., Gordon M.N., Benkovic S.A. and Morgan D.G. (2000) Aβ and perlecan in rat brain: glial activation, gradual clearance and limited neurotoxicity, Mech. Ageing Dev. 112:135-152.

Holtzman D.M., Bales K.R., Tenkova T., Fagan A.M., Parsadanian M., Sartorius L.J., Mackey B., Olney J., McKeel D., Wozniak D. and Paul S.M. (2000) Apolipoprotein E isoform-dependent amyloid deposition and neuritic degeneration in a mouse model of Alzheimer's disease, Proc. Natl. Acad. Sci. U. S. A. 97:2892-2897.

Horning M.S., Blakemore L.J. and Trombley P.Q. (2000) Endogenous mechanisms of neuroprotection: role of zinc, copper and carnosine, Brain Res. 852:56-61.

Hosoda T., Nakajima H. and Honjo H. (2001) Estrogen protects neuronal cells from amyloid β-induced apoptotic cell death, Neuroreport 12:1965-1970.

Hsia A.Y., Masliah E., McConlogue L., Yu G.Q., Tatsuno G., Hu K., Kholodenko D., Malenka R.C., Nicoll R.A. and Mucke L. (1999) Plaque-independent disruption of neural circuits in Alzheimer's disease mouse models, Proc. Natl. Acad. Sci. U. S. A. 96:3228-3233.

Hsiao K., Chapman P., Nilsen S., Eckman C., Harigaya Y., Younkin S., Yang F. and Cole G. (1996) Correlative memory deficits, Aβ elevation, and amyloid plaques in transgenic mice, Science 274:99-102.

Hu J., Akama K.T., Krafft G.A., Chromy B.A. and Van Eldik L.J. (1998) Amyloid-β peptide activates cultured astrocytes: morphological alterations, cytokine induction and nitric oxide release, Brain Res. 785:195-206.

Huang X., Atwood C.S., Hartshorn M.A., Multhaup G., Goldstein L.E., Scarpa R.C., Cuajungco M.P., Gray D.N., Lim J., Moir R.D., Tanzi R.E. and Bush A.I. (1999a) The Aβ peptide of Alzheimer's disease directly produces hydrogen peroxide through metal ion reduction, Biochemistry 38:7609-7616.

Huang X., Cuajungco M.P., Atwood C.S., Hartshorn M.A., Tyndall J.D., Hanson G.R., Stokes K.C., Leopold M., Multhaup G., Goldstein L.E., Scarpa R.C., Saunders A.J., Lim J., Moir R.D., Glabe C., Bowden E.F., Masters C.L., Fairlie D.P., Tanzi R.E. and Bush A.I. (1999b) Cu(II) potentiation of Alzheimer Aβ neurotoxicity. Correlation with cell-free hydrogen peroxide production and metal reduction, J. Biol. Chem. 274:37111-37116.

Hussain I., Powell D., Howlett D.R., Tew D.G., Meek T.D., Chapman C., Gloger I.S., Murphy K.E., Southan C.D., Ryan D.M., Smith T.S., Simmons D.L., Walsh F.S., Dingwall C. and Christie G. (1999) Identification of a novel aspartic protease (Asp 2) as β-secretase, Mol. Cell. Neurosci. 14:419-427.

Hutter-Paier B., Grygar E., Fruhwirth M., Temmel I. and Windisch M. (1998) Further evidence that Cerebrolysin protects cortical neurons from neurodegeneration *in vitro*, J. Neural Transm. Suppl. 53:363-372.

Hyman B.T., Marzloff K. and Arriagada P.V. (1993) The lack of accumulation of senile plaques or amyloid burden in Alzheimer's disease suggests a dynamic balance between amyloid deposition and resolution, J. Neuropathol. Exp. Neurol. 52:594-600.

Hyman B.T., Van Hoesen G.W., Kromer L.J. and Damasio A.R. (1986) Perforant pathway changes and the memory impairment of Alzheimer's disease, Ann. Neurol. 20:472-481.

Ichikawa H. and Sakata T. (1998) Stimulation of epithelial cell proliferation of isolated distal colon of rats by continuous colonic infusion of ammonia or short-chain fatty acids is nonadditive, J. Nutr. 128:843-847.

Irizarry M.C., McNamara M., Fedorchak K., Hsiao K. and Hyman B.T. (1997a) APPSw transgenic mice develop age-related Aβ deposits and neuropil abnormalities, but no neuronal loss in CA1, J. Neuropathol. Exp. Neurol. 56:965-973.

Irizarry M.C., Soriano F., McNamara M., Page K.J., Schenk D., Games D. and Hyman B.T. (1997b) Aβ deposition is associated with neuropil changes, but not with

overt neuronal loss in the human amyloid precursor protein V717F (PDAPP) transgenic mouse, J. Neurosci. 17:7053-7059.

Ishimaru H., Ishikawa K., Ohe Y., Takahashi A., Tatemoto K. and Maruyama Y. (1996) Activation of iron handling system within the gerbil hippocampus after cerebral ischemia, Brain Res. 726:23-30.

Iversen L.L., Mortishire-Smith R.J., Pollack S.J. and Shearman M.S. (1995) The toxicity *in vitro* of β-amyloid protein, Biochem. J. 311:1-16.

Iwatsubo T., Odaka A., Suzuki N., Mizusawa H., Nukina N. and Ihara Y. (1994) Visualization of Aβ42(43) and Aβ40 in senile plaques with end- specific Aβ monoclonals: evidence that an initially deposited species is Aβ42(43), Neuron 13:45-53.

Jaffe A.B., Toran-Allerand C.D., Greengard P. and Gandy S.E. (1994) Estrogen regulates metabolism of Alzheimer amyloid beta precursor protein, J. Biol. Chem. 269:13065-13068.

Jancso G., Domoki F., Santha P., Varga J., Fischer J., Orosz K., Penke B., Becskei A., Dux M. and Toth L. (1998) β-amyloid (1-42) peptide impairs blood-brain barrier function after intracarotid infusion in rats, Neurosci. Lett. 253:139-141.

Jarrett J.T., Berger E.P. and Lansbury P.T., Jr. (1993) The carboxy terminus of the β amyloid protein is critical for the seeding of amyloid formation: implications for the pathogenesis of Alzheimer's disease, Biochemistry 32:4693-4697.

Jarvinen A., Granander M., Laine T. and Viitanen A. (2000) Effect of dose on the absorption of estradiol from a transdermal gel, Maturitas 35:51-56.

Jellinger K., Paulus W., Grundke-Iqbal I., Riederer P. and Youdim M.B. (1990) Brain iron and ferritin in Parkinson's and Alzheimer's diseases, J. Neural. Transm. 2:327-340.

Jen L.S., Hart A.J., Jen A., Relvas J.B., Gentleman S.M., Garey L.J. and Patel A.J. (1998) Alzheimer's peptide kills cells of retina *in vivo*, Nature 392:140-141.

Jenner P. and Olanow C.W. (1998) Understanding cell death in Parkinson's disease, Ann. Neurol. 44:S72-S84.

Jiang H., Burdick D., Glabe C.G., Cotman C.W. and Tenner A.J. (1994) β-amyloid activates complement by binding to a specific region of the collagen-like domain of the C1q A chain, J. Immunol. 152:5050-5059.

Johnson-Wood K., Lee M., Motter R., Hu K., Gordon G., Barbour R., Khan K., Gordon M., Tan H., Games D., Lieberburg I., Schenk D., Seubert P. and McConlogue L. (1997) Amyloid precursor protein processing and Aβ42 deposition in a

transgenic mouse model of Alzheimer disease, Proc. Natl. Acad. Sci. U. S. A. 94:1550-1555.

Johnstone E.M., Chaney M.O., Norris F.H., Pascual R. and Little S.P. (1991) Conservation of the sequence of the Alzheimer's disease amyloid peptide in dog, polar bear and five other mammals by cross-species polymerase chain reaction analysis, Mol. Brain Res. 10:299-305.

Jorgensen C.B. (1972) Reproduction. In Gordon M.S. (Ed.), *Animal Physiology: Principles and Adaptations*, Macmillan Publishing Co., New York, pp. 636-678.

Kamino K., Orr H.T., Payami H., Wijsman E.M., Alonso M.E., Pulst S.M., Anderson L., O'Dahl S., Nemens E., White J.A., Sadovnick A.D., Ball M.J., Kaye J., Warren A., McInnis M., Antonarakis S.E., Korenberg J.R., Sharma V., Kukull W., Larson E., Heston L.L., Martin G.M., Bird T.D. and Schellenberg G.D. (1992) Linkage and mutational analysis of familial Alzheimer disease kindreds for the APP gene region, Am. J. Hum. Genet. 51:998-1014.

Kaneko Y., Kitamoto T., Tateishi J. and Yamaguchi K. (1989) Ferritin immunohistochemistry as a marker for microglia, Acta Neuropathol. 79:129-136.

Karwatowska-Prokopczuk E., Czarnowska E. and Beresewicz A. (1992) Iron availability and free radical induced injury in the isolated ischaemic/reperfused rat heart, Cardiovasc. Res. 26:58-66.

Kawahara M. and Kuroda Y. (2000) Molecular mechanism of neurodegeneration induced by Alzheimer's β-amyloid protein: channel formation and disruption of calcium homeostasis, Brain Res. Bull. 53:389-397.

Kim H.S., Lee S.H., Kim S.S., Kim Y.K., Jeong S.J., Ma J., Han D.H., Cho B.K. and Suh Y.H. (1998) Post-ischemic changes in the expression of Alzheimer's APP isoforms in rat cerebral cortex, Neuroreport 9:533-537.

Kim Y.H., Kim E.Y., Gwag B.J., Sohn S. and Koh J.Y. (1999) Zinc-induced cortical neuronal death with features of apoptosis and necrosis: mediation by free radicals, Neuroscience 89:175-182.

King C.E., Jacobs I., Dickson T.C. and Vickers J.C. (1997) Physical damage to rat cortical axons mimics early Alzheimer's neuronal pathology, Neuroreport 8:1663-1665.

Kirschner D.A., Abraham C. and Selkoe D.J. (1986) X-ray diffraction from intraneuronal paired helical filaments and extraneuronal amyloid fibers in

Alzheimer disease indicates cross-β conformation, Proc. Natl. Acad. Sci. U. S. A. 83:503-507.

Kitaguchi N., Takahashi Y., Tokushima Y., Shiojiri S. and Ito H. (1988) Novel precursor of Alzheimer's disease amyloid protein shows protease inhibitory activity, Nature 331:530-532.

Klegeris A. and McGeer P.L. (1997) β-amyloid protein enhances macrophage production of oxygen free radicals and glutamate, J. Neurosci. Res. 49:229-235.

Koeppen A.H., Dickson A.C. and McEvoy J.A. (1995) The cellular reactions to experimental intracerebral hemorrhage, J. Neurol. Sci. 134 Suppl:102-112.

Koh J.Y., Yang L.L. and Cotman C.W. (1990) β-amyloid protein increases the vulnerability of cultured cortical neurons to excitotoxic damage, Brain Res. 533:315-320.

Kondo Y., Ogawa N., Asanuma M., Ota Z. and Mori A. (1995) Regional differences in late-onset iron deposition, ferritin, transferrin, astrocyte proliferation, and microglial activation after transient forebrain ischemia in rat brain, J. Cereb. Blood Flow Metab. 15:216-226.

Kontush A., Berndt C., Weber W., Akopyan V., Arlt S., Schippling S. and Beisiegel U. (2001) Amyloid-β is an antioxidant for lipoproteins in cerebrospinal fluid and plasma, Free Radic. Biol. Med. 30:119-128.

Kowall N.W., Beal M.F., Busciglio J., Duffy L.K. and Yankner B.A. (1991) An *in vivo* model for the neurodegenerative effects of β amyloid and protection by substance P, Proc. Natl. Acad. Sci. U. S. A. 88:7247-7251.

Kowall N.W., McKee A.C., Yankner B.A. and Beal M.F. (1992) *In vivo* neurotoxicity of beta-amyloid [β(1-40)] and the β(25-35) fragment, Neurobiol. Aging 13:537-542.

Kunicki S., Richardson J., Mehta P.D., Kim K.S. and Zorychta E. (1998) The effects of age, apolipoprotein E phenotype and gender on the concentration of amyloid-β (Aβ) 40, Aβ42, apolipoprotein E and transthyretin in human cerebrospinal fluid, Clin. Biochem. 31:409-415.

Langeveld C.H., Jongenelen C.A., Schepens E., Stoof J.C., Bast A. and Drukarch B. (1995) Cultured rat striatal and cortical astrocytes protect mesencephalic dopaminergic neurons against hydrogen peroxide toxicity independent of their effect on neuronal development, Neurosci. Lett. 192:13-16.

Lees G.J., Lehmann A., Sandberg M. and Hamberger A. (1990) The neurotoxicity of zinc in the rat hippocampus, Neurosci. Lett. 120:155-158.

Leutner S., Czech C., Schindowski K., Touchet N., Eckert A. and Muller W.E. (2000) Reduced antioxidant enzyme activity in brains of mice transgenic for human presenilin-1 with single or multiple mutations, Neurosci. Lett. 292:87-90.

Li Y.M., Xu M., Lai M.T., Huang Q., Castro J.L., DiMuzio-Mower J., Harrison T., Lellis C., Nadin A., Neduvelil J.G., Register R.B., Sardana M.K., Shearman M.S., Smith A.L., Shi X.P., Yin K.C., Shafer J.A. and Gardell S.J. (2000) Photoactivated γ-secretase inhibitors directed to the active site covalently label presenilin 1, Nature 405:689-694.

Liao S., Chen W., Kuo J. and Chen C. (2001) Association of serum estrogen level and ischemic neuroprotection in female rats, Neurosci. Lett. 297:159-162.

Liu S.T., Howlett G. and Barrow C.J. (1999) Histidine-13 is a crucial residue in the zinc ion-induced aggregation of the Aβ peptide of Alzheimer's disease, Biochemistry 38:9373-9378.

Loske C., Gerdemann A., Schepl W., Wycislo M., Schinzel R., Palm D., Riederer P. and Munch G. (2000) Transition metal-mediated glycoxidation accelerates cross-linking of β-amyloid peptide, Eur. J. Biochem. 267:4171-4178.

Loske C., Neumann A., Cunningham A.M., Nichol K., Schinzel R., Riederer P. and Munch G. (1998) Cytotoxicity of advanced glycation endproducts is mediated by oxidative stress, J. Neural Transm. 105:1005-1015.

Lovell M.A., Robertson J.D., Teesdale W.J., Campbell J.L. and Markesbery W.R. (1998) Copper, iron and zinc in Alzheimer's disease senile plaques, J. Neurol. Sci. 158:47-52.

Lovell M.A., Xie C. and Markesbery W.R. (1999) Protection against amyloid beta peptide toxicity by zinc, Brain Res. 823:88-95.

Luo Y., Bolon B., Kahn S., Bennett B.D., Babu-Khan S., Denis P., Fan W., Kha H., Zhang J., Gong Y., Martin L., Louis J.C., Yan Q., Richards W.G., Citron M. and Vassar R. (2001) Mice deficient in BACE1, the Alzheimer's β-secretase, have normal phenotype and abolished β-amyloid generation, Nat. Neurosci. 4:231-232.

Manly J.J., Merchant C.A., Jacobs D.M., Small S.A., Bell K., Ferin M. and Mayeux R. (2000) Endogenous estrogen levels and Alzheimer's disease among postmenopausal women, Neurology 54:833-837.

Mann D.M., Yates P.O. and Marcyniuk B. (1984) Alzheimer's presenile dementia, senile dementia of Alzheimer type and Down's syndrome in middle age form an

age related continuum of pathological changes, Neuropathol. Appl. Neurobiol. 10:185-207.

Mann D.M., Yates P.O. and Marcyniuk B. (1985) Some morphometric observations on the cerebral cortex and hippocampus in presenile Alzheimer's disease, senile dementia of Alzheimer type and Down's syndrome in middle age, J. Neurol. Sci. 69:139-159.

Mann D.M., Yates P.O., Marcyniuk B. and Ravindra C.R. (1986) The topography of plaques and tangles in Down's syndrome patients of different ages, Neuropathol. Appl. Neurobiol. 12:447-457.

Mantyh P.W., Ghilardi J.R., Rogers S., DeMaster E., Allen C.J., Stimson E.R. and Maggio J.E. (1993) Aluminum, iron, and zinc ions promote aggregation of physiological concentrations of β-amyloid peptide, J. Neurochem. 61:1171-1174.

Margaill I., Parmentier S., Callebert J., Allix M., Boulu R.G. and Plotkine M. (1996) Short therapeutic window for MK-801 in transient focal cerebral ischemia in normotensive rats, J. Cereb. Blood Flow Metab. 16:107-113.

Markesbery W.R. (1997) Oxidative stress hypothesis in Alzheimer's disease, Free Radic. Biol. Med. 23:134-147.

Maruyama K., Kawamura Y., Asada H., Ishiura S. and Obata K. (1994) Cleavage at the N-terminal site of Alzheimer amyloid β/A4 protein is essential for its secretion, Biochem. Biophys. Res. Commun. 202:1517-1523.

Maruyama K., Tomita T., Shinozaki K., Kume H., Asada H., Saido T.C., Ishiura S., Iwatsubo T. and Obata K. (1996) Familial Alzheimer's disease-linked mutations at Val^{717} of amyloid precursor protein are specific for the increased secretion of Aβ42(43), Biochem. Biophys. Res. Commun. 227:730-735.

Masliah E., Sisk A., Mallory M. and Games D. (2001) Neurofibrillary pathology in transgenic mice overexpressing V717F β-amyloid precursor protein, J. Neuropathol. Exp. Neurol. 60:357-368.

Matsuoka Y., Picciano M., Malester B., LaFrancois J., Zehr C., Daeschner J.M., Olschowka J.A., Fonseca M.I., O'Banion M.K., Tenner A.J., Lemere C.A. and Duff K. (2001) Inflammatory responses to amyloidosis in a transgenic mouse model of Alzheimer's disease, Am. J. Pathol. 158:1345-1354.

Mattson M.P. (1994) Calcium and neuronal injury in Alzheimer's disease. Contributions of β-amyloid precursor protein mismetabolism, free radicals, and metabolic compromise, Ann. N. Y. Acad. Sci. 747:50-76.

Mattson M.P., Cheng B., Culwell A.R., Esch F.S., Lieberburg I. and Rydel R.E. (1993a) Evidence for excitoprotective and intraneuronal calcium-regulating roles for secreted forms of the β-amyloid precursor protein, Neuron 10:243-254.

Mattson M.P., Cheng B., Davis D., Bryant K., Lieberburg I. and Rydel R.E. (1992) β-Amyloid peptides destabilize calcium homeostasis and render human cortical neurons vulnerable to excitotoxicity, J. Neurosci. 12:376-389.

Mattson M.P., Mark R.J., Furukawa K. and Bruce A.J. (1997) Disruption of brain cell ion homeostasis in Alzheimer's disease by oxy radicals, and signaling pathways that protect therefrom, Chem. Res. Toxicol. 10:507-517.

Mattson M.P., Rydel R.E., Lieberburg I. and Smith-Swintosky V.L. (1993b) Altered calcium signaling and neuronal injury: stroke and Alzheimer's disease as examples, Ann. N. Y. Acad. Sci. 679:1-21.

Mattson M.P., Tomaselli K.J. and Rydel R.E. (1993c) Calcium-destabilizing and neurodegenerative effects of aggregated β-amyloid peptide are attenuated by basic FGF, Brain Res. 621:35-49.

Maurice T., Lockhart B.P. and Privat A. (1996) Amnesia induced in mice by centrally administered β-amyloid peptides involves cholinergic dysfunction, Brain Res. 706:181-193.

May P.C., Gitter B.D., Waters D.C., Simmons L.K., Becker G.W., Small J.S. and Robison P.M. (1992) β-Amyloid peptide *in vitro* toxicity: lot-to-lot variability, Neurobiol. Aging 13:605-607.

Maziere C., Auclair M., Ronveaux M.F., Salmon S., Santus R. and Maziere J.C. (1991) Estrogens inhibit copper and cell-mediated modification of low density lipoprotein, Atherosclerosis 89:175-182.

McDonald D.R., Brunden K.R. and Landreth G.E. (1997) Amyloid fibrils activate tyrosine kinase-dependent signaling and superoxide production in microglia, J. Neurosci. 17:2284-2294.

McGeer P.L. and McGeer E.G. (1995) The inflammatory response system of brain: implications for therapy of Alzheimer and other neurodegenerative diseases, Brain Res. Rev. 21:195-218.

McGowan E., Sanders S., Iwatsubo T., Takeuchi A., Saido T., Zehr C., Yu X., Uljon S., Wang R., Mann D., Dickson D. and Duff K. (1999) Amyloid phenotype characterization of transgenic mice overexpressing both mutant amyloid precursor protein and mutant presenilin 1 transgenes, Neurobiol. Dis. 6:231-244.

Meda L., Cassatella M.A., Szendrei G.I., Otvos L., Jr., Baron P., Villalba M., Ferrari D. and Rossi F. (1995) Activation of microglial cells by β-amyloid protein and interferon-γ, Nature 374:647-650.

Miyata T., Iida Y., Ueda Y., Shinzato T., Seo H., Monnier V.M., Maeda K. and Wada Y. (1996) Monocyte/macrophage response to beta 2-microglobulin modified with advanced glycation end products, Kidney Int. 49:538-550.

Moechars D., Dewachter I., Lorent K., Reverse D., Baekelandt V., Naidu A., Tesseur I., Spittaels K., Haute C.V., Checler F., Godaux E., Cordell B. and Van Leuven F. (1999) Early phenotypic changes in transgenic mice that overexpress different mutants of amyloid precursor protein in brain, J. Biol. Chem. 274:6483-6492.

Monji A., Utsumi H., Ueda T., Imoto T., Yoshida I., Hashioka S., Tashiro K. and Tashiro N. (2001) The relationship between the aggregational state of the amyloid-beta peptides and free radical generation by the peptides, J. Neurochem. 77:1425-1432.

Moos T. and Mollgard K. (1993) A sensitive post-DAB enhancement technique for demonstration of iron in the central nervous system, Histochemistry 99:471-475.

Moreira P., Pereira C., Santos M.S. and Oliveira C. (2000) Effect of zinc ions on the cytotoxicity induced by the amyloid beta-peptide, Antioxid. Redox Signal. 2:317-325.

Morimoto K., Yoshimi K., Tonohiro T., Yamada N., Oda T. and Kaneko I. (1998) Co-injection of β-amyloid with ibotenic acid induces synergistic loss of rat hippocampal neurons, Neuroscience 84:479-487.

Morris J.C., Heyman A., Mohs R.C., Hughes J.P., van Belle G., Fillenbaum G., Mellits E.D. and Clark C. (1989) The Consortium to Establish a Registry for Alzheimer's Disease (CERAD). Part I. Clinical and neuropsychological assessment of Alzheimer's disease, Neurology 39:1159-1165.

Motter R., Vigo-Pelfrey C., Kholodenko D., Barbour R., Johnson-Wood K., Galasko D., Chang L., Miller B., Clark C., Green R. and et al. (1995) Reduction of β-amyloid peptide42 in the cerebrospinal fluid of patients with Alzheimer's disease, Ann. Neurol. 38:643-648.

Mufson E.J., Chen E.Y., Cochran E.J., Beckett L.A., Bennett D.A. and Kordower J.H. (1999) Entorhinal cortex β-amyloid load in individuals with mild cognitive impairment, Exp. Neurol. 158:469-490.

Mullan M., Crawford F., Axelman K., Houlden H., Lilius L., Winblad B. and Lannfelt L. (1992) A pathogenic mutation for probable Alzheimer's disease in the APP gene at the N-terminus of β-amyloid, Nat. Genet. 1:345-347.

Munch G., Schinzel R., Loske C., Wong A., Durany N., Li J.J., Vlassara H., Smith M.A., Perry G. and Riederer P. (1998) Alzheimer's disease - synergistic effects of glucose deficit, oxidative stress and advanced glycation endproducts, J. Neural Transm. 105:439-461.

Munch G., Thome J., Foley P., Schinzel R. and Riederer P. (1997) Advanced glycation endproducts in ageing and Alzheimer's disease, Brain Res. Rev. 23:134-143.

Murphy G.M., Jr., Forno L.S., Higgins L., Scardina J.M., Eng L.F. and Cordell B. (1994) Development of a monoclonal antibody specific for the COOH-terminal of β-amyloid 1-42 and its immunohistochemical reactivity in Alzheimer's disease and related disorders, Am. J. Pathol. 144:1082-1088.

Murrell J., Farlow M., Ghetti B. and Benson M.D. (1991) A mutation in the amyloid precursor protein associated with hereditary Alzheimer's disease, Science 254:97-99.

Nakamura S., Nakayama H., Uetsuka K., Sasaki N., Uchida K. and Goto N. (1995) Senile plaques in an aged two-humped (Bactrian) camel (Camelus bactrianus), Acta Neuropathol. 90:415-418.

Nakamura S., Tamaoka A., Sawamura N., Kiatipattanasakul W., Nakayama H., Shoji S., Yoshikawa Y. and Doi K. (1997) Deposition of amyloid β protein (Aβ) subtypes [Aβ40 and Aβ42(43)] in canine senile plaques and cerebral amyloid angiopathy, Acta Neuropathol. 94:323-328.

Namba Y., Tomonaga M., Kawasaki H., Otomo E. and Ikeda K. (1991) Apolipoprotein E immunoreactivity in cerebral amyloid deposits and neurofibrillary tangles in Alzheimer's disease and kuru plaque amyloid in Creutzfeldt-Jakob disease, Brain Res. 541:163-166.

Nelson P.T. and Saper C.B. (1996) Injections of okadaic acid, but not β-amyloid peptide, induce Alz-50 immunoreactive dystrophic neurites in the cerebral cortex of sheep, Neurosci. Lett. 208:77-80.

Nequin L.G., Alvarez J. and Schwartz N.B. (1979) Measurement of serum steroid and gonadotropin levels and uterine and ovarian variables throughout 4 day and 5 day estrous cycles in the rat, Biol. Reprod. 20:659-670.

Neumann A., Schinzel R., Palm D., Riederer P. and Munch G. (1999) High molecular weight hyaluronic acid inhibits advanced glycation endproduct-induced NF-kappaB activation and cytokine expression, FEBS Lett. 453:283-287.

Nitta A., Fukuta T., Hasegawa T. and Nabeshima T. (1997) Continuous infusion of β-amyloid protein into the rat cerebral ventricle induces learning impairment and neuronal and morphological degeneration, Jpn J. Pharmacol. 73:51-57.

Nunomura A., Perry G., Aliev G., Hirai K., Takeda A., Balraj E.K., Jones P.K., Ghanbari H., Wataya T., Shimohama S., Chiba S., Atwood C.S., Petersen R.B. and Smith M.A. (2001) Oxidative damage is the earliest event in Alzheimer disease, J. Neuropathol. Exp. Neurol. 60:759-767.

Ohgami T., Kitamoto T., Shin R.W., Kaneko Y., Ogomori K. and Tateishi J. (1991) Increased senile plaques without microglia in Alzheimer's disease, Acta Neuropathol. 81:242-247.

Oubidar M., Boquillon M., Marie C., Schreiber L. and Bralet J. (1994) Ischemia-induced brain iron delocalization: effect of iron chelators, Free Radic. Biol. Med. 16:861-867.

Oyama F., Sawamura N., Kobayashi K., Morishima-Kawashima M., Kuramochi T., Ito M., Tomita T., Maruyama K., Saido T.C., Iwatsubo T., Capell A., Walter J., Grunberg J., Ueyama Y., Haass C. and Ihara Y. (1998) Mutant presenilin 2 transgenic mouse: effect on an age-dependent increase of amyloid β-protein 42 in the brain, J. Neurochem. 71:313-322.

Paganini-Hill A. and Henderson V.W. (1996) Estrogen replacement therapy and risk of Alzheimer disease, Arch. Intern. Med. 156:2213-2217.

Paller M.S. and Hedlund B.E. (1994) Extracellular iron chelators protect kidney cells from hypoxia/reoxygenation, Free Radic. Biol. Med. 17:597-603.

Palmer C., Menzies S.L., Roberts R.L., Pavlick G. and Connor J.R. (1999) Changes in iron histochemistry after hypoxic-ischemic brain injury in the neonatal rat, J. Neurosci. Res. 56:60-71.

Palmer C., Roberts R.L. and Bero C. (1994) Deferoxamine posttreatment reduces ischemic brain injury in neonatal rats, Stroke 25:1039-1045.

Palmert M.R., Siedlak S.L., Podlisny M.B., Greenberg B., Shelton E.R., Chan H.W., Usiak M., Selkoe D.J., Perry G. and Younkin S.G. (1989) Soluble derivatives of the β amyloid protein precursor of Alzheimer's disease are labeled by antisera to the β amyloid protein, Biochem. Biophys. Res. Commun. 165:182-188.

Paris D., Town T., Parker T.A., Humphrey J. and Mullan M. (1998) Isoform-specific vasoconstriction induced by apolipoprotein E and modulation of this effect by Alzheimer's β-amyloid peptide, Neurosci. Lett. 256:73-76.

Paris D., Town T., Parker T.A., Tan J., Humphrey J., Crawford F. and Mullan M. (1999) Inhibition of Alzheimer's β-amyloid induced vasoactivity and proinflammatory response in microglia by a cGMP-dependent mechanism, Exp. Neurol. 157:211-221.

Paxinos G. and Watson C. (1982) *The Rat Brain in Stereotaxic Coordinates*, Academic Press, Sydney.

Petit A., Bihel F., da Costa C.A., Pourquie O., Checler F. and Kraus J.L. (2001) New protease inhibitors prevent γ-secretase-mediated production of Aβ40/42 without affecting Notch cleavage, Nat. Cell Biol. 3:507-511.

Phinney A.L., Deller T., Stalder M., Calhoun M.E., Frotscher M., Sommer B., Staufenbiel M. and Jucker M. (1999) Cerebral amyloid induces aberrant axonal sprouting and ectopic terminal formation in amyloid precursor protein transgenic mice, J. Neurosci. 19:8552-8559.

Pike C.J. (1999) Estrogen modulates neuronal Bcl-xL expression and β-amyloid-induced apoptosis: relevance to Alzheimer's disease, J. Neurochem. 72:1552-1563.

Pike C.J., Burdick D., Walencewicz A.J., Glabe C.G. and Cotman C.W. (1993) Neurodegeneration induced by β-amyloid peptides *in vitro*: the role of peptide assembly state, J. Neurosci. 13:1676-1687.

Pike C.J., Cummings B.J. and Cotman C.W. (1992) β-amyloid induces neuritic dystrophy *in vitro*: similarities with Alzheimer pathology, Neuroreport 3:769-772.

Pike C.J., Cummings B.J., Monzavi R. and Cotman C.W. (1994) β-amyloid-induced changes in cultured astrocytes parallel reactive astrocytosis associated with senile plaques in Alzheimer's disease, Neuroscience 63:517-531.

Pike C.J., Ramezan-Arab N. and Cotman C.W. (1997) β-amyloid neurotoxicity *in vitro*: evidence of oxidative stress but not protection by antioxidants, J. Neurochem. 69:1601-1611.

Pike C.J., Walencewicz A.J., Glabe C.G. and Cotman C.W. (1991) *In vitro* aging of β-amyloid protein causes peptide aggregation and neurotoxicity, Brain Res. 563:311-314.

Pinero D.J., Hu J. and Connor J.R. (2000) Alterations in the interaction between iron regulatory proteins and their iron responsive element in normal and Alzheimer's diseased brains, Cell. Mol. Biol. (Noisy-le-grand) 46:761-776.

Plassman B.L. and Breitner J.C. (1996) Recent advances in the genetics of Alzheimer's disease and vascular dementia with an emphasis on gene-environment interactions, J. Am. Geriatr. Soc. 44:1242-1250.

Podlisny M.B., Stephenson D.T., Frosch M.P., Lieberburg I., Clemens J.A. and Selkoe D.J. (1992) Synthetic amyloid β-protein fails to produce specific neurotoxicity in monkey cerebral cortex, Neurobiol. Aging 13:561-567.

Podlisny M.B., Stephenson D.T., Frosch M.P., Tolan D.R., Lieberburg I., Clemens J.A. and Selkoe D.J. (1993) Microinjection of synthetic amyloid β-protein in monkey cerebral cortex fails to produce acute neurotoxicity, Am. J. Pathol. 142:17-24.

Podlisny M.B., Tolan D.R. and Selkoe D.J. (1991) Homology of the amyloid β protein precursor in monkey and human supports a primate model for β amyloidosis in Alzheimer's disease, Am. J. Pathol. 138:1423-1435.

Pollard H.B., Arispe N. and Rojas E. (1995) Ion channel hypothesis for Alzheimer amyloid peptide neurotoxicity, Cell. Mol. Neurobiol. 15:513-526.

Pollard H.B., Rojas E. and Arispe N. (1993) A new hypothesis for the mechanism of amyloid toxicity, based on the calcium channel activity of amyloid beta protein (AβP) in phospholipid bilayer membranes, Ann. N. Y. Acad. Sci. 695:165-168.

Ponte P., Gonzalez-DeWhitt P., Schilling J., Miller J., Hsu D., Greenberg B., Davis K., Wallace W., Lieberburg I. and Fuller F. (1988) A new A4 amyloid mRNA contains a domain homologous to serine proteinase inhibitors, Nature 331:525-527.

Poola I. (1997) An estrogen inducible 104 kDa chaperone glycoprotein binds ferric iron containing proteins: a possible role in intracellular iron trafficking, FEBS Lett. 41(139-142.

Poola I. and Kiang J.G. (1994) The estrogen-inducible transferrin receptor-like membrane glycoprotein is related to stress-regulated proteins, J. Biol. Chem. 269:21762-21769.

Qi Y., Jamindar T.M. and Dawson G. (1995) Hypoxia alters iron homeostasis and induces ferritin synthesis in oligodendrocytes, J. Neurochem. 64:2458-2464.

Rauhala P. and Chiueh C.C. (2000) Effects of atypical antioxidative agents, S-nitrosoglutathione and manganese, on brain lipid peroxidation induced by iron leaking from tissue disruption, Ann. N. Y. Acad. Sci. 899:238-254.

Rauhala P., Lin A.M. and Chiueh C.C. (1998) Neuroprotection by S-nitrosoglutathione of brain dopamine neurons from oxidative stress, FASEB J. 12:165-173.

Regan R.F. and Panter S.S. (1993) Neurotoxicity of hemoglobin in cortical cell culture, Neurosci. Lett. 153:219-222.

Richard F. and Amouyel P. (2001) Genetic susceptibility factors for Alzheimer's disease, Eur. J. Pharmacol. 412:1-12.

Richardson J.S., Zhou Y. and Kumar U. (1996) Free radicals in the neurotoxic actions of β-amyloid, Ann. N. Y. Acad. Sci. 777:362-367.

Roberts G.W., Gentleman S.M., Lynch A., Murray L., Landon M. and Graham D.I. (1994) β amyloid protein deposition in the brain after severe head injury: implications for the pathogenesis of Alzheimer's disease, J. Neurol. Neurosurg. Psychiatry 57:419-425.

Robinson S.R. (2000) Neuronal expression of glutamine synthetase in Alzheimer's disease indicates a profound impairment of metabolic interactions with astrocytes, Neurochem. Int. 36:471-482.

Robinson S.R. and Bishop G.M. (in press) Aβ as a bioflocculant: implications for the amyloid hypothesis of Alzheimer's disease, Neurobiol. Aging.

Robinson S.R., Noone D.F., Kril J. and Halliday G.M. (1995) Most amyloid plaques contain ferritin-rich cells, Alzheimer's Res. 1:191-196.

Rod M.R. and Auer R.N. (1989) Pre- and post-ischemic administration of dizocilpine (MK-801) reduces cerebral necrosis in the rat, Can. J. Neurol. Sci. 16:340-344.

Rogers J., Cooper N.R., Webster S., Schultz J., McGeer P.L., Styren S.D., Civin W.H., Brachova L., Bradt B., Ward P. and Lieberburg I. (1992) Complement activation by β-amyloid in Alzheimer disease, Proc. Natl. Acad. Sci. U. S. A. 89:10016-10020.

Roher A.E., Ball M.J., Bhave S.V. and Wakade A.R. (1991) β-amyloid from Alzheimer disease brains inhibits sprouting and survival of sympathetic neurons, Biochem. Biophys. Res. Commun. 174:572-579.

Rottkamp C.A., Raina A.K., Zhu X., Gaier E., Bush A.I., Atwood C.S., Chevion M., Perry G. and Smith M.A. (2001) Redox-active iron mediates amyloid-β toxicity, Free Radic. Biol. Med. 30:447-450.

Rozemuller J.M., Eikelenboom P., Stam F.C., Beyreuther K. and Masters C.L. (1989) A4 protein in Alzheimer's disease: primary and secondary cellular events in extracellular amyloid deposition, J. Neuropathol. Exp. Neurol. 48:674-691.

Rozemuller J.M., Stam F.C. and Eikelenboom P. (1990) Acute phase proteins are present in amorphous plaques in the cerebral but not in the cerebellar cortex of patients with Alzheimer's disease, Neurosci. Lett. 119:75-78.

Rubinsztein D.C. (1997) A review of the contribution of apo E genotypes to Alzheimer's disease risk and meta-analysis of apo E associations with other neuro-psychiatric disorders, Nutr. Metab. Cardiovasc. Dis. 7:267-275.

Rumble B., Retallack R., Hilbich C., Simms G., Multhaup G., Martins R., Hockey A., Montgomery P., Beyreuther K. and Masters C.L. (1989) Amyloid A4 protein and its precursor in Down's syndrome and Alzheimer's disease, N. Engl. J. Med. 320:1446-1452.

Rush D.K., Aschmies S. and Merriman M.C. (1992) Intracerebral β-amyloid(25-35) produces tissue damage: is it neurotoxic?, Neurobiol. Aging 13:591-594.

Saido T.C. (1998) Alzheimer's disease as proteolytic disorders: anabolism and catabolism of β-amyloid, Neurobiol. Aging 19:S69-S75.

Santanam N., Shern-Brewer R., McClatchey R., Castellano P.Z., Murphy A.A., Voelkel S. and Parthasarathy S. (1998) Estradiol as an antioxidant: incompatible with its physiological concentrations and function, J. Lipid Res. 39:2111-2118.

Sasaki N., Fukatsu R., Tsuzuki K., Hayashi Y., Yoshida T., Fujii N., Koike T., Wakayama I., Yanagihara R., Garruto R., Amano N. and Makita Z. (1998) Advanced glycation end products in Alzheimer's disease and other neurodegenerative diseases, Am. J. Pathol. 153:1149-1155.

Sawada H., Ibi M., Kihara T., Urushitani M., Akaike A. and Shimohama S. (1998) Estradiol protects mesencephalic dopaminergic neurons from oxidative stress-induced neuronal death, J. Neurosci. Res. 54:707-719.

Sayre L.M., Perry G., Harris P.L., Liu Y., Schubert K.A. and Smith M.A. (2000) In situ oxidative catalysis by neurofibrillary tangles and senile plaques in Alzheimer's disease: a central role for bound transition metals, J. Neurochem. 74:270-279.

Schenk D., Barbour R., Dunn W., Gordon G., Grajeda H., Guido T., Hu K., Huang J., Johnson-Wood K., Khan K., Kholodenko D., Lee M., Liao Z., Lieberburg I., Motter R., Mutter L., Soriano F., Shopp G., Vasquez N., Vandevert C., Walker S., Wogulis M., Yednock T., Games D. and Seubert P. (1999) Immunization with amyloid-β attenuates Alzheimer-disease-like pathology in the PDAPP mouse, Nature 400:173-177.

Scheuner D., Eckman C., Jensen M., Song X., Citron M., Suzuki N., Bird T.D., Hardy J., Hutton M., Kukull W., Larson E., Levy-Lahad E., Viitanen M., Peskind E.,

Poorkaj P., Schellenberg G., Tanzi R., Wasco W., Lannfelt L., Selkoe D. and Younkin S. (1996) Secreted amyloid β-protein similar to that in the senile plaques of Alzheimer's disease is increased *in vivo* by the presenilin 1 and 2 and APP mutations linked to familial Alzheimer's disease, Nat. Med. 2:864-870.

Schmechel D.E., Saunders A.M., Strittmatter W.J., Crain B.J., Hulette C.M., Joo S.H., Pericak-Vance M.A., Goldgaber D. and Roses A.D. (1993) Increased amyloid β-peptide deposition in cerebral cortex as a consequence of apolipoprotein E genotype in late-onset Alzheimer disease, Proc. Natl. Acad. Sci. U. S. A. 90:9649-9653.

Schmued L.C., Albertson C. and Slikker W., Jr. (1997) Fluoro-Jade: a novel fluorochrome for the sensitive and reliable histochemical localization of neuronal degeneration, Brain Res. 751:37-46.

Schroder J., Doren M., Schneider B. and Oettel M. (1996) Are the antioxidative effects of 17β-estradiol modified by concomitant administration of a progestin?, Maturitas 25:133-139.

Schubert D. and Chevion M. (1995) The role of iron in beta amyloid toxicity, Biochem. Biophys. Res. Commun. 216:702-707.

Schultz J. and Kaminker K. (1962) Myeloperoxidase of the leukocyte of normal human blood. I. Content and localization, Arch. Biochem. Biophys. 98:465-471.

Seeger H., Mueck A.O. and Lippert T.H. (1998) The inhibitory effect of endogenous estrogen metabolites on copper-mediated *in vitro* oxidation of LDL, Int. J. Clin. Pharmacol. Ther. 36:383-385.

Selkoe D.J. (2001) Alzheimer's disease: genes, proteins, and therapy, Physiol. Rev. 81:741-766.

Selkoe D.J., Abraham C.R., Podlisny M.B. and Duffy L.K. (1986) Isolation of low-molecular-weight proteins from amyloid plaque fibers in Alzheimer's disease, J. Neurochem. 46:1820-1834.

Selkoe D.J., Bell D.S., Podlisny M.B., Price D.L. and Cork L.C. (1987) Conservation of brain amyloid proteins in aged mammals and humans with Alzheimer's disease, Science 235:873-877.

Sengstock G.J., Olanow C.W., Dunn A.J. and Arendash G.W. (1992) Iron induces degeneration of nigrostriatal neurons, Brain Res. Bull. 28:645-649.

Sengstock G.J., Olanow C.W., Menzies R.A., Dunn A.J. and Arendash G.W. (1993) Infusion of iron into the rat substantia nigra: nigral pathology and dose-dependent loss of striatal dopaminergic markers, J. Neurosci. Res. 35:67-82.

Shinkai Y., Yoshimura M., Morishima-Kawashima M., Ito Y., Shimada H., Yanagisawa K. and Ihara Y. (1997) Amyloid β-protein deposition in the leptomeninges and cerebral cortex, Ann. Neurol. 42:899-908.

Shiraishi K., Nakazawa S. and Ito H. (1993) Zinc enhances kainate neurotoxicity in the rat brain, Neurol. Res. 15:113-116.

Shivers B.D., Hilbich C., Multhaup G., Salbaum M., Beyreuther K. and Seeburg P.H. (1988) Alzheimer's disease amyloidogenic glycoprotein: expression pattern in rat brain suggests a role in cell contact, EMBO J. 7:1365-1370.

Shoji M., Matsubara E., Kanai M., Watanabe M., Nakamura T., Tomidokoro Y., Shizuka M., Wakabayashi K., Igeta Y., Ikeda Y., Mizushima K., Amari M., Ishiguro K., Kawarabayashi T., Harigaya Y., Okamoto K. and Hirai S. (1998) Combination assay of CSF tau, Aβ1-40 and Aβ1-42(43) as a biochemical marker of Alzheimer's disease, J. Neurol. Sci. 158:134-140.

Sigurdsson E.M., Hejna M.J., Lee J.M. and Lorens S.A. (1995) β-Amyloid 25-35 and/or quinolinic acid injections into the basal forebrain of young male Fischer-344 rats: behavioral, neurochemical and histological effects, Behav. Brain Res. 72:141-156.

Sigurdsson E.M., Lee J.M., Dong X.W., Hejna M.J. and Lorens S.A. (1997a) Bilateral injections of amyloid-β 25-35 into the amygdala of young Fischer rats: behavioral, neurochemical, and time dependent histopathological effects, Neurobiol. Aging 18:591-608.

Sigurdsson E.M., Lee J.M., Dong X.W., Hejna M.J. and Lorens S.A. (1997b) Laterality in the histological effects of injections of amyloid-β 25- 35 into the amygdala of young Fischer rats, J. Neuropathol. Exp. Neurol. 56:714-725.

Sigurdsson E.M., Lorens S.A., Hejna M.J., Dong X.W. and Lee J.M. (1996) Local and distant histopathological effects of unilateral amyloid-β 25-35 injections into the amygdala of young F344 rats, Neurobiol. Aging 17:893-901.

Smith M.A., Harris P.L., Sayre L.M. and Perry G. (1997) Iron accumulation in Alzheimer disease is a source of redox-generated free radicals, Proc. Natl. Acad. Sci. U. S. A. 94:9866-9868.

Smith M.A., Taneda S., Richey P.L., Miyata S., Yan S.D., Stern D., Sayre L.M., Monnier V.M. and Perry G. (1994) Advanced Maillard reaction end products are associated with Alzheimer disease pathology, Proc. Natl. Acad. Sci. U. S. A. 91:5710-5714.

Smith M.A., Wehr K., Harris P.L., Siedlak S.L., Connor J.R. and Perry G. (1998) Abnormal localization of iron regulatory protein in Alzheimer's disease, Brain Res. 788:232-236.

Smyth M.D., Kesslak J.P., Cummings B.J. and Cotman C.W. (1994) Analysis of brain injury following intrahippocampal administration of β-amyloid in streptozotocin-treated rats, Neurobiol. Aging 15:153-159.

Snider B.J., Choi J., Turetsky D.M., Canzoniero L.M., Sensi S.L., Sheline C.T., Wang X., Yu S.P. and Choi D.W. (2000) Nitric oxide reduces $Ca^{(2+)}$ and $Zn^{(2+)}$ influx through voltage-gated $Ca^{(2+)}$ channels and reduces $Zn^{(2+)}$ neurotoxicity, Neuroscience 100:651-661.

Snow A.D., Sekiguchi R., Nochlin D., Fraser P., Kimata K., Mizutani A., Arai M., Schreier W.A. and Morgan D.G. (1994) An important role of heparan sulfate proteoglycan (Perlecan) in a model system for the deposition and persistence of fibrillar A β-amyloid in rat brain, Neuron 12:219-234.

Soto C., Sigurdsson E.M., Morelli L., Kumar R.A., Castano E.M. and Frangione B. (1998) β-sheet breaker peptides inhibit fibrillogenesis in a rat brain model of amyloidosis: implications for Alzheimer's therapy, Nat. Med. 4:822-826.

Splittgerber A.G. and Tappel A.L. (1979) Inhibition of glutathione peroxidase by cadmium and other metal ions, Arch. Biochem. Biophys. 197:534-542.

Stein-Behrens B., Adams K., Yeh M. and Sapolsky R. (1992) Failure of β-amyloid protein fragment 25-35 to cause hippocampal damage in the rat, Neurobiol. Aging 13:577-579.

Steinberg G.K., Panahian N., Perez-Pinzon M.A., Sun G.H., Modi M.W. and Sepinwall J. (1995) Narrow temporal therapeutic window for NMDA antagonist protection against focal cerebral ischaemia, Neurobiol. Dis. 2:109-118.

Stephenson D.T. and Clemens J.A. (1992) *In vivo* effects of β-amyloid implants in rodents: lack of potentiation of damage associated with transient global forebrain ischemia, Brain Res. 586:235-246.

Strazielle N., Ghersi-Egea J.F., Ghiso J., Dehouck M.P., Frangione B., Patlak C., Fenstermacher J. and Gorevic P. (2000) *In vitro* evidence that β-amyloid peptide 1-40 diffuses across the blood-brain barrier and affects its permeability, J. Neuropathol. Exp. Neurol. 59:29-38.

Strittmatter W.J., Saunders A.M., Schmechel D., Pericak-Vance M., Enghild J., Salvesen G.S. and Roses A.D. (1993) Apolipoprotein E: high-avidity binding to

β-amyloid and increased frequency of type 4 allele in late-onset familial Alzheimer disease, Proc. Natl. Acad. Sci. U. S. A. 90:1977-1981.

Sturchler-Pierrat C., Abramowski D., Duke M., Wiederhold K.H., Mistl C., Rothacher S., Ledermann B., Burki K., Frey P., Paganetti P.A., Waridel C., Calhoun M.E., Jucker M., Probst A., Staufenbiel M. and Sommer B. (1997) Two amyloid precursor protein transgenic mouse models with Alzheimer disease-like pathology, Proc. Natl. Acad. Sci. U. S. A. 94:13287-13292.

Su G.C., Arendash G.W., Kalaria R.N., Bjugstad K.B. and Mullan M. (1999) Intravascular infusions of soluble β-amyloid compromise the blood-brain barrier, activate CNS glial cells and induce peripheral hemorrhage, Brain Res. 818:105-117.

Sugimoto H., Shikata K., Wada J., Horiuchi S. and Makino H. (1999) Advanced glycation end products-cytokine-nitric oxide sequence pathway in the development of diabetic nephropathy: aminoguanidine ameliorates the overexpression of tumour necrosis factor-alpha and inducible nitric oxide synthase in diabetic rat glomeruli, Diabetologia 42:878-886.

Suo Z., Humphrey J., Kundtz A., Sethi F., Placzek A., Crawford F. and Mullan M. (1998) Soluble Alzheimers β-amyloid constricts the cerebral vasculature *in vivo*, Neurosci. Lett. 257:77-80.

Suzuki N., Cheung T.T., Cai X.D., Odaka A., Otvos L., Eckman C., Golde T.E. and Younkin S.G. (1994) An increased percentage of long amyloid β protein secreted by familial amyloid β protein precursor (βAPP_{717}) mutants, Science 264:1336-1340.

Swaiman K.F. and Machen V.L. (1985) Iron uptake by glial cells, Neurochem. Res. 10:1635-1644.

Swaiman K.F. and Machen V.L. (1990) Effect of ferric nitrilotriacetate on predominantly cortical glial cell cultures, Neurochem. Res. 15:501-505.

Sziraki I., Mohanakumar K.P., Rauhala P., Kim H.G., Yeh K.J. and Chiueh C.C. (1998) Manganese: a transition metal protects nigrostriatal neurons from oxidative stress in the iron-induced animal model of parkinsonism, Neuroscience 85:1101-1111.

Takedo A., Yasuda T., Miyata T., Mizuno K., Li M., Yoneyama S., Horie K., Maeda K. and Sobue G. (1996) Immunohistochemical study of advanced glycation end products in aging and Alzheimer's disease brain, Neurosci. Lett. 221:17-20.

Tamaoka A., Fukushima T., Sawamura N., Ishikawa K., Oguni E., Komatsuzaki Y. and Shoji S. (1996) Amyloid β protein in plasma from patients with sporadic Alzheimer's disease, J. Neurol. Sci. 141:65-68.

Tamaoka A., Odaka A., Ishibashi Y., Usami M., Sahara N., Suzuki N., Nukina N., Mizusawa H., Shoji S., Kanazawa I. and Mori H. (1994) APP717 missense mutation affects the ratio of amyloid β protein species (Aβ1-42/43 and Aβ1-40) in familial Alzheimer's disease brain, J. Biol. Chem. 269:32721-32724.

Tanzi R.E., Gusella J.F., Watkins P.C., Bruns G.A., St George-Hyslop P., Van Keuren M.L., Patterson D., Pagan S., Kurnit D.M. and Neve R.L. (1987) Amyloid β protein gene: cDNA, mRNA distribution, and genetic linkage near the Alzheimer locus, Science 235:880-884.

Tanzi R.E., McClatchey A.I., Lamperti E.D., Villa-Komaroff L., Gusella J.F. and Neve R.L. (1988) Protease inhibitor domain encoded by an amyloid protein precursor mRNA associated with Alzheimer's disease, Nature 331:528-530.

Teller J.K., Russo C., De Busk L.M., Angelini G., Zaccheo D., Dagna-Bricarelli F., Scartezzini P., Bertolini S., Mann D.M., Tabaton M. and Gambetti P. (1996) Presence of soluble amyloid β-peptide precedes amyloid plaque formation in Down's syndrome, Nat. Med. 2:93-95.

Thomas T., Rhodin J.A., Sutton E.T., Bryant M.W. and Price J.M. (1999) Estrogen protects peripheral and cerebral blood vessels from toxicity of Alzheimer peptide amyloid-β and inflammatory reaction, J. Submicrosc. Cytol. Pathol. 31:571-579.

Tokuda T., Fukushima T., Ikeda S., Sekijima Y., Shoji S., Yanagisawa N. and Tamaoka A. (1997) Plasma levels of amyloid β proteins Aβ1-40 and Aβ1-42(43) are elevated in Down's syndrome, Ann. Neurol. 41:271-273.

Tomidokoro Y., Harigaya Y., Matsubara E., Ikeda M., Kawarabayashi T., Okamoto K. and Shoji M. (2000) Impaired neurotransmitter systems by Aβ amyloidosis in APPsw transgenic mice overexpressing amyloid β protein precursor, Neurosci. Lett. 292:155-158.

Triggs W.J. and Willmore L.J. (1984) *In vivo* lipid peroxidation in rat brain following intracortical Fe^{2+} injection, J. Neurochem. 42:976-980.

Tsujii M., Kawano S., Tsuji S., Takei Y., Tamura K., Fusamoto H. and Kamada T. (1995) Mechanism for ammonia-induced promotion of gastric carcinogenesis in rats, Carcinogenesis 16:563-566.

Turnbull S., Tabner B.J., El-Agnaf O.M., Twyman L.J. and Allsop D. (2001) New evidence that the Alzheimer β-amyloid peptide does not spontaneously form free radicals: an ESR study using a series of spin-traps, Free Radic. Biol. Med. 30:1154-1162.

Turner C.P., Bergeron M., Matz P., Zegna A., Noble L.J., Panter S.S. and Sharp F.R. (1998) Heme oxygenase-1 is induced in glia throughout brain by subarachnoid hemoglobin, J. Cereb. Blood Flow Metab. 18:257-273.

Van Muiswinkel F.L., Raupp S.F., de Vos N.M., Smits H.A., Verhoef J., Eikelenboom P. and Nottet H.S. (1999) The amino-terminus of the amyloid-β protein is critical for the cellular binding and consequent activation of the respiratory burst of human macrophages, J. Neuroimmunol. 96:121-130.

Vassar R., Bennett B.D., Babu-Khan S., Kahn S., Mendiaz E.A., Denis P., Teplow D.B., Ross S., Amarante P., Loeloff R., Luo Y., Fisher S., Fuller J., Edenson S., Lile J., Jarosinski M.A., Biere A.L., Curran E., Burgess T., Louis J.C., Collins F., Treanor J., Rogers G. and Citron M. (1999) β-secretase cleavage of Alzheimer's amyloid precursor protein by the transmembrane aspartic protease BACE, Science 286:735-741.

Vaughan D.W. and Peters A. (1981) The structure of neuritic plaque in the cerebral cortex of aged rats, J. Neuropathol. Exp. Neurol. 40:472-487.

Vedder H., Anthes N., Stumm G., Wurz C., Behl C. and Krieg J.C. (1999) Estrogen hormones reduce lipid peroxidation in cells and tissues of the central nervous system, J. Neurochem. 72:2531-2538.

Vitek M.P., Bhattacharya K., Glendening J.M., Stopa E., Vlassara H., Bucala R., Manogue K. and Cerami A. (1994) Advanced glycation end products contribute to amyloidosis in Alzheimer disease, Proc. Natl. Acad. Sci. U. S. A. 91:4766-4770.

Vogt B.A., Crino P.B. and Vogt L.J. (1992) Reorganization of cingulate cortex in Alzheimer's disease: neuron loss, neuritic plaques, and muscarinic receptor binding, Cereb. Cortex 2:526-535.

Waite J., Cole G.M., Frautschy S.A., Connor D.J. and Thal L.J. (1992) Solvent effects on beta protein toxicity *in vivo*, Neurobiol. Aging 13:595-599.

Walmer D.K., Wrona M.A., Hughes C.L. and Nelson K.G. (1992) Lactoferrin expression in the mouse reproductive tract during the natural estrous cycle: correlation with circulating estradiol and progesterone, Endocrinology 131:1458-1466.

Wang C., Wurtman R.J. and Lee R.K. (2000) Amyloid precursor protein and membrane phospholipids in primary cortical neurons increase with development, or after exposure to nerve growth factor or Aβ1-40, Brain Res. 865:157-167.

Waring S.C., Rocca W.A., Petersen R.C., O'Brien P.C., Tangalos E.G. and Kokmen E. (1999) Postmenopausal estrogen replacement therapy and risk of AD: a population-based study, Neurology 52:965-970.

Waynforth H.B. and Flecknell P.A. (1992) *Experimental and Surgical Technique in the Rat*, 2nd edn., Academic Press, London.

Weldon D.T., Rogers S.D., Ghilardi J.R., Finke M.P., Cleary J.P., O'Hare E., Esler W.P., Maggio J.E. and Mantyh P.W. (1998) Fibrillar β-amyloid induces microglial phagocytosis, expression of inducible nitric oxide synthase, and loss of a select population of neurons in the rat CNS *in vivo*, J. Neurosci. 18:2161-2173.

Weller R.O., Massey A., Newman T.A., Hutchings M., Kuo Y.M. and Roher A.E. (1998) Cerebral amyloid angiopathy: amyloid β accumulates in putative interstitial fluid drainage pathways in Alzheimer's disease, Am. J. Pathol. 153:725-733.

West M.J., Coleman P.D., Flood D.G. and Troncoso J.C. (1994) Differences in the pattern of hippocampal neuronal loss in normal ageing and Alzheimer's disease, Lancet 344:769-772.

West M.J., Kawas C.H., Martin L.J. and Troncoso J.C. (2000) The CA1 region of the human hippocampus is a hot spot in Alzheimer's disease, Ann. N. Y. Acad. Sci. 908:255-259.

White A.R., Bush A.I., Beyreuther K., Masters C.L. and Cappai R. (1999) Exacerbation of copper toxicity in primary neuronal cultures depleted of cellular glutathione, J. Neurochem. 72:2092-2098.

White A.R., Huang X., Jobling M.F., Barrow C.J., Beyreuther K., Masters C.L., Bush A.I. and Cappai R. (2001) Homocysteine potentiates copper- and amyloid β peptide-mediated toxicity in primary neuronal cultures: possible risk factors in the Alzheimer's-type neurodegenerative pathways, J. Neurochem. 76:1509-1520.

Whitson J.S., Glabe C.G., Shintani E., Abcar A. and Cotman C.W. (1990) β-amyloid protein promotes neuritic branching in hippocampal cultures, Neurosci. Lett. 110:319-324.

Whitson J.S., Selkoe D.J. and Cotman C.W. (1989) Amyloid β protein enhances the survival of hippocampal neurons *in vitro*, Science 243:1488-1490.

Willmore L.J. and Rubin J.J. (1982) Formation of malonaldehyde and focal brain edema induced by subpial injection of $FeCl_2$ into rat isocortex, Brain Res. 246:113-119.

Winkler J., Connor D.J., Frautschy S.A., Behl C., Waite J.J., Cole G.M. and Thal L.J. (1994) Lack of long-term effects after β-amyloid protein injections in rat brain, Neurobiol. Aging 15:601-607.

Wisniewski H.M., Robe A., Zigman W. and Silverman W. (1989a) Neuropathological diagnosis of Alzheimer disease, J. Neuropathol. Exp. Neurol. 48:606-609.

Wisniewski H.M., Wegiel J., Wang K.C., Kujawa M. and Lach B. (1989b) Ultrastructural studies of the cells forming amyloid fibers in classical plaques, Can. J. Neurol. Sci. 16:535-542.

Wisniewski T. and Frangione B. (1992) Apolipoprotein E: a pathological chaperone protein in patients with cerebral and systemic amyloid, Neurosci. Lett. 135:235-238.

Wong T.P., Debeir T., Duff K. and Cuello A.C. (1999) Reorganization of cholinergic terminals in the cerebral cortex and hippocampus in transgenic mice carrying mutated presenilin-1 and amyloid precursor protein transgenes, J. Neurosci. 19:2706-2716.

Wujek J.R., Dority M.D., Frederickson R.C. and Brunden K.R. (1996) Deposits of Aβ fibrils are not toxic to cortical and hippocampal neurons *in vitro*, Neurobiol. Aging 17:107-113.

Wuttke W. (1989) Sexual Functions. In Schmidt R.F. and Thews G. (Eds.), *Human Physiology*, 2nd edn., Springer-Verlag, Berlin, pp. 774-784.

Xu H., Gouras G.K., Greenfield J.P., Vincent B., Naslund J., Mazzarelli L., Fried G., Jovanovic J.N., Seeger M., Relkin N.R., Liao F., Checler F., Buxbaum J.D., Chait B.T., Thinakaran G., Sisodia S.S., Wang R., Greengard P. and Gandy S. (1998) Estrogen reduces neuronal generation of Alzheimer β-amyloid peptides, Nat. Med. 4:447-451.

Yankner B.A., Caceres A. and Duffy L.K. (1990a) Nerve growth factor potentiates the neurotoxicity of β amyloid, Proc. Natl. Acad. Sci. U. S. A. 87:9020-9023.

Yankner B.A., Duffy L.K. and Kirschner D.A. (1990b) Neurotrophic and neurotoxic effects of amyloid β protein: reversal by tachykinin neuropeptides, Science 250:279-282.

Zabar Y. and Kawas C.H. (2000) Epidemiology and clinical genetics of Alzheimer's disease. In Clark C.M. and Trojanowski J.Q. (Eds.), *Neurodegenerative Dementias*, McGraw Hill, New York, pp. 79-95.

Zago M.P. and Oteiza P.I. (2001) The antioxidant properties of zinc: interactions with iron and antioxidants, Free Radic. Biol. Med. 31:266-274.

Zhang Y., Tatsuno T., Carney J.M. and Mattson M.P. (1993) Basic FGF, NGF, and IGFs protect hippocampal and cortical neurons against iron-induced degeneration, J. Cereb. Blood Flow Metab. 13:378-388.

Zhao J., Paganini L., Mucke L., Gordon M., Refolo L., Carman M., Sinha S., Oltersdorf T., Lieberburg I. and McConlogue L. (1996) β-secretase processing of the β-amyloid precursor protein in transgenic mice is efficient in neurons but inefficient in astrocytes, J. Biol. Chem. 271:31407-31411.

APPENDIX 1:

Reagents used in the study and their suppliers.

A1.1. Substances injected.

Product	Product No.	Lot No.	*MW*	Source	Conc. prepared
Sterile physiological saline	AHB1324			Baxter Healthcare	0.9% NaCl
Ammonium citrate	A-8170		226.2	Sigma	1.0mM
Ferric ammonium citrate	158040		488.0	ICN	1.0mM
Human Aβ1-40	20-06-06	10	4328	U.S. Peptide, Inc.	1.0mM
Human Aβ1-42	20-06-08	12	4515	U.S. Peptide, Inc.	1.0mM
Rat Aβ1-40	642-102	BB0395	4233	California Peptide Research, Inc.	1.0mM
Rat Aβ1-42	642-15	MF0218	4418	California Peptide Research, Inc.	1.0mM
Cupric acetate	C-5409		199.7	Sigma	0.4mM
Zinc acetate	Z-4540		219.5	Sigma	1.0mM

A1.2. Reagents for modified Perl's staining.

Product	Product No.	Source
Paraformaldehyde	44,124-4	Aldrich
Potassium ferrocyanide	152560	ICN
Hydrochloric acid (37%)	101256J	BDH
3',3'-diaminobenzidine (tetrahydrochloride)	D-5637	Sigma
Nickel sulfate	831	Ajax
H_2O_2 (30% w/v)	260	Ajax

A1.3. General reagents for immunocytochemistry.

Product	Product No.	Source
Paraformaldehyde	C007	ProSciTech
Heparin	H-9399	Sigma
Bovine serum albumin (BSA)	A-3425	Sigma Chemical Co.
98-100% Formic acid	101154E	BDH
Triton-X 100	1552	Ajax
Ethanolamine	26	Ajax
Sodium azide	S-2002	Sigma
3',3'-diaminobenzidine (tetrahydrochloride)	D-5637	Sigma
Nickel sulfate	831	Ajax
H_2O_2 (30% w/v)	260	Ajax
Streptavidin-biotinylated horseradish peroxidase complex	RPN1051	Amersham

A1.4. Specific antibodies used for immunocytochemistry.

A1.4.1. Antibody combinations.

Primary antibody	Secondary antibody	Antigen recognised	Used to detect
Rabbit anti-human L-chain ferritin	Anti-rabbit Ig, biotinylated antibody	L-chain ferritin	Activated microglia and macrophages
Mouse anti-human Aβ (Clone 6F/3D)	Anti-mouse Ig, biotinylated antibody	Human Aβ8-17	Human Aβ1-40, human Aβ1-42
Rabbit anti-human Aβ	Anti-rabbit Ig, biotinylated antibody	Human Aβ1-40	Rat Aβ1-40

A1.4.2. Source of antibodies.

Product	Product No.	Source
Rabbit anti-human L-chain ferritin	65-077	ICN Biomedicals
Mouse anti-human Aβ (Clone 6F/3D)	M0872	DAKO Corporation
Rabbit anti-human Aβ	A-8326	Sigma Immunochemicals
Anti-rabbit Ig, biotinylated antibody	RPN1004	Amersham
Anti-mouse Ig, biotinylated antibody	RPN1001	Amersham

A1.5. Reagents for Fluoro-Jade staining.

Product	Product No.	Source
Paraformaldehyde	44,124-4	Aldrich
Fluoro-Jade	1 FJ	Histo-Chem Inc.
Acetic acid	100015N 859004	BDH FSE
Potassium permanganate	414	Ajax

APPENDIX 2:

Summary of the quantitative data and statistical analysis presented in Chapter 3.

A2.1. Ferritin-positive cells at ferric ammonium citrate injection sites.

Values expressed as the mean number of ferritin-positive cells±SE (n=5).

Substance injected	1 day	3 days	5 days	7 days
Saline	79±9	306±36	317±21	384±43
Ammonium citrate	71±24	360±29	345±26	314±21
FAC	565±78	638±104	658±95	617±100

A2.1.1. Statistical analysis of ferritin-positive cells at ferric ammonium citrate injection sites.

Independent samples t-tests, 1-tailed.

Substance 1	Substance 2	Survival	t-value	d.f.	p-value	Significant
Saline	FAC	7 days	-2.148	8	0.032	Yes

A2.2. Fluoro-Jade-labelled cells at ferric ammonium citrate injection sites.

Values expressed as the mean number of Fluoro-Jade-labelled cells±SE (n=5).

Substance injected	1 day	3 days	5 days	7 days
Saline	271±29	62±17	4±3	0±0
Ammonium citrate	147±26	6±2	5±3	5±2
FAC	664±64	340±77	207±42	177±48

A2.2.1. Statistical analysis of Fluoro-Jade-labelled cells at ferric ammonium citrate injection sites.

Independent samples t-tests, 2-tailed.

Substance 1	Substance 2	Survival	t-value	d.f.	p-value	Significant
Saline	Ammonium citrate	1 day	3.217	8	0.012	Yes
Saline	Ammonium citrate	3 days	3.367	8	0.010	Yes

A2.3. Fluoro-Jade staining and H&E staining after 1 day survival.

Values expressed as the mean number of Fluoro-Jade-labelled cells±SE (n=5), or the mean number of H&E stained basophilic profiles±SE (n=5).

Substance injected	Fluoro-Jade staining	H&E staining
Saline	271±29	175±29
Ammonium citrate	147±26	135±15
FAC	664±64	534±110

A2.3.1. Statistical analysis of Fluoro-Jade and H&E staining after 1 day survival.

Paired samples t-tests, 2-tailed. Values for all substances are compared simultaneously.

Stain 1	Stain 2	Survival	t-value	d.f.	p-value	Significant
Fluoro-Jade	H&E	1 day	2.060	14	0.059	No

APPENDIX 3:

Summary of the quantitative data and statistical analysis presented in Chapter 4.

A.3.1. Total volume of injected Aβ deposits.

Values are expressed as the mean total volume of the Aβ deposit (μm^3) ±SE (n).

Substance injected	1 day	3 days	5 days	7 days
Rat Aβ1-40	26±2 $\times 10^6$ (7)	12±3 $\times 10^6$ (5)	5±1 $\times 10^6$ (6)	2±1 $\times 10^6$ (6)
Human Aβ1-40	19±5 $\times 10^6$ (4)	9±1 $\times 10^6$ (3)	0±0 (5)	2±2 $\times 10^5$ (5)
Human Aβ1-42	18±5 $\times 10^6$ (3)	5±1 $\times 10^6$ (5)	3±1 $\times 10^5$ (5)	1±1 $\times 10^5$ (6)

A3.2. Fluoro-Jade-labelled cells at Aβ injection sites.

Values expressed as the mean number of Fluoro-Jade-labelled cells±SE (n=5).

Substance injected	1 day	3 days	5 days	7 days
Saline	271±29	58±14	4±3	0±0
Rat Aβ1-40	97±18	18±14	2±1	0±0
Human Aβ1-40	193±27	42±19	5±2	1±1
Human Aβ1-42	104±28	14±4	0±0	6±6

A3.2.1. Statistical analysis of Fluoro-Jade-labelled cells at Aβ injection sites: Comparison between Aβ variants.

Independent samples t-tests, 2-tailed.

Substance 1	Substance 2	Survival	t-value	d.f.	p-value	Significant
Saline	Rat Aβ1-40	1 day	5.172	8	0.001	Yes
Saline	Human Aβ1-40	1 day	1.985	8	0.082	No
Saline	Human Aβ1-42	1 day	4.151	8	0.003	Yes
Rat Aβ1-40	Human Aβ1-40	1 day	-2.947	8	0.019	Yes
Human Aβ1-40	Human Aβ1-42	1 day	2.261	8	0.054	No
Saline	Rat Aβ1-40	3 days	2.038	8	0.076	No
Saline	Human Aβ1-42	3 days	2.984	4.819	0.032	Yes*

* Levene's test for equality of differences was significant.

A3.2.2. Statistical analysis of Fluoro-Jade-labeled cells at Aβ injection sites: Comparison between survival times.

Independent samples t-tests, 2-tailed.

Survival time 1	Survival time 2	Substance	t-value	d.f.	p-value	Significant
1 day	3 days	Saline	6.661	8	<0.001	Yes
1 day	3 days	Rat Aβ1-40	3.509	8	0.008	Yes
1 day	3 days	Human Aβ1-40	4.559	8	0.002	Yes
1 day	3 days	Human Aβ1-42	3.132	4.208	0.033	Yes*
3 days	5 days	Saline	3.791	4.255	0.017	Yes*
3 days	5 days	Rat Aβ1-40	1.113	8	0.298	No
3 days	5 days	Human Aβ1-40	1.935	8	0.089	No
3 days	5 days	Human Aβ1-42	3.016	4	0.039	Yes*

* Levene's test for equality of differences was significant.

A3.3. Ferritin-positive cells at Aβ injection sites.

Values expressed as the mean number of ferritin-positive cells±SE (n=5).

Substance injected	1 day	3 days	5 days	7 days
Saline	79±9	306±36	317±21	384±43
Rat Aβ1-40	135±23	401±29	315±26	420±23
Human Aβ1-40	144±41	455±41	406±48	397±32
Human Aβ1-42	148±34	320±39	349±31	392±34

A3.3.1. Statistical analysis of ferritin-positive cells at Aβ injection sites: Comparison between Aβ variants.

Independent samples t-tests, 2-tailed.

Substance 1	Substance 2	Survival	t-value	d.f.	p-value	Significant
Saline	Rat Aβ1-40	1 day	-2.274	8	0.053	No
Saline	Human Aβ1-40	1 day	-1.565	4.384	0.186	No*
Saline	Human Aβ1-42	1 day	-1.987	4.553	0.109	No*
Saline	Rat Aβ1-40	3 days	-2.057	8	0.074	No
Saline	Human Aβ1-40	3 days	-2.726	8	0.026	Yes
Human Aβ1-40	Human Aβ1-42	3 days	2.378	8	0.045	Yes
Saline	Human Aβ1-40	5 days	-1.726	8	0.123	No
Human Aβ1-40	Human Aβ1-42	5 days	1.013	8	0.341	No

* Levene's test for equality of differences was significant.

A3.3.2. Statistical analysis of ferritin positive cells at Aβ injection sites: Comparison between survival times.

Independent samples t-tests, 2-tailed.

Survival time 1	Survival time 2	Substance	t-value	d.f.	p-value	Significant
3 days	5 days	Rat Aβ1-40	2.218	8	0.057	No
5 days	7 days	Rat Aβ1-40	-3.044	8	0.016	Yes

APPENDIX 4:

Summary of the quantitative data and statistical analysis presented in Chapter 5.

A4.1. Fluoro-Jade-labelled cells at the injection site after 1 day.

Values expressed as a percentage of saline; mean±SE (n=8).

Substance injected	% Saline
Human Aβ	79±17%
Human Aβ + iron	154±22%
Rat Aβ	63±6%
Rat Aβ + iron	203±39%
Iron	262±45%

A4.1.1. Statistical analysis of Fluoro-Jade-labelled cells at the site of injection; Comparison to saline vehicle.

Paired-samples t-test, 2-tailed.

Substance	t-value	d.f.	p-value	Significant
Human Aβ	1.922	7	0.096	No
Human Aβ + iron	-1.851	7	0.107	No
Rat Aβ	4.975	7	0.002	Yes
Rat Aβ + iron	-2.599	7	0.035	Yes
Iron	-4.090	7	0.005	Yes

A4.1.2. Statistical analysis of Fluoro-Jade-labelled cells at the site of injection; Comparison between experimental substances.

Independent-samples *t*-tests, 2-tailed.

Substance 1	Substance 2	t-value	d.f.	p-value	Significant
Human Aβ	Human Aβ + iron	-2.653	14	0.019	Yes
Rat Aβ	Rat Aβ + iron	-3.533	7.334	0.009	Yes*
Iron	Human Aβ + iron	2.160	14	0.049	Yes
Iron	Rat Aβ + iron	0.989	14	0.339	No

* Levene's test for equality of differences was significant.

APPENDIX 5:

Summary of the quantitative data and statistical analysis presented in Chapter 6.

A5.1. Fluoro-Jade-labelled cells at the injection site after 1 day.

Values expressed as a percentage of saline; mean±SE (n).

Substance injected	% Saline
Aβ	79±17% (8)
Aβ + iron	154±22% (8)
Aβ + copper	77±13% (8)
Aβ + zinc	159±36% (8)
Aβ + iron+copper+zinc	242±30% (8)
Iron	262±45% (8)
Copper	130±16% (7)
Zinc	126±12% (8)
Iron+copper+zinc	209±13% (7)

A5.1.1. Statistical analysis of Fluoro-Jade-labelled cells at the site of injection; Comparison to saline vehicle.

Paired-samples t-test, 2-tailed.

Substance	t-value	d.f.	p-value	Significant
Aβ	1.922	7	0.096	No
Aβ + iron	-1.851	7	0.107	No
Aβ + copper	2.251	7	0.059	No
Aβ + zinc	-1.534	7	0.169	No
Aβ + iron+copper+zinc	-4.114	7	0.004	Yes
Iron	-4.090	7	0.005	Yes
Copper	-1.830	6	0.117	No
Zinc	-3.012	7	0.020	Yes
Iron+copper+zinc	-7.005	6	0.001	Yes

A5.1.2. Statistical analysis of Fluoro-Jade-labelled cells at the site of injection; Comparison between experimental substances.

Independent-samples t-tests, 2-tailed.

Substance 1	Substance 2	t-value	d.f.	p-value	Significant
Aβ	Aβ + iron	-2.653	14	0.019	Yes
Aβ	Aβ + copper	0.063	14	0.950	No
Aβ	Aβ + zinc	-1.998	14	0.066	No
Aβ	Aβ + iron+copper+zinc	-4.683	14	0.001	Yes
Iron	Aβ + iron	2.160	14	0.049	Yes
Copper	Aβ + copper	2.576	13	0.023	Yes
Zinc	Aβ + zinc	-0.864	8.426	0.412	No*
Iron+copper+zinc	Aβ + iron+copper+zinc	-0.937	9.623	0.366	No*

* Levene's test for equality of differences was significant.

APPENDIX 6:

Summary of the quantitative data and statistical analysis presented in Chapter 7.

A6.1. Neuronal loss produced by injection of saline.

Values expressed as the mean number of Fluoro-Jade-labelled cells ±SE (n).

Oestrus cycle	Number of dying neurons
Oestrus	479±43 (14)
Metoestrus	457±69 (8)
Dioestrus	436±36 (13)
Proestrus	386±58 (5)

A6.2. Neurotoxicity of metal ions or Aβ-metal complexes.

Values expressed as the mean toxicity ranking ±SE (n).

Oestrus cycle	Toxicity ranking
Oestrus	3.57±0.67 (14)
Metoestrus	4.86±0.74 (7)
Dioestrus	4.69±0.56 (13)
Proestrus	4.25±1.60 (4)

A6.3. Intensity of cortical iron staining.

Values expressed as mean luminosity ±SE (n=5)

Oestrus cycle	Mean luminosity
Oestrus	179.02±3.50
Metoestrus	177.02±3.86
Dioestrus	181.29±1.96
Proestrus	171.95±0.37

A6.3.1. Statistical analysis of the luminosity of iron staining: Comparison between stage of the oestrous cycle.

Stage 1	Stage 2	t-value	d.f.	p-value	Significant
Dioestrus	Proestrus	4.668	4.290	0.008	Yes*

* Levene's test for equality of differences was significant.